PSEG Public Service Electric and Gas Company

80 Park Pla a, Newark, NJ 07101 / 201 430-8217 MAILING ADDRESS / P.O. Box 570, Newark, NJ 07101

Robert L. Mittl General Manager
Nuclear Assurance and Regulation

February 17, 1984

Director of Nuclear Reactor Regulation
United States Nuclear Regulatory Commission
7920 Norfolk Avenue
Bethesda, Maryland 20014

Attention: Mr. Albert Schwencer, Chief
Licensing Branch 2
Division of Licensing

Gentlemen:

HOPE CREEK GENERATING STATION
DOCKET NO. 50-354
NRC REVIEW OF STRUCTURAL/GEOTECHNICAL TOPICS

Pursuant to the agreements reached at the meetings held on January 10, 11, and 12, 1984, to review HCGS structural/geotechnical topics with the NRC, attached is one (1) set of responses to those items denoted as Category II target date. A listing of the attached Category II target date items, broken down by date of meeting, is as follows:

Meeting of January 10, 1984:
Items A.1, A.2, A.3, A.4, A.6, A.11, A.12, A.15, and A.16
B.5, B.10, B.12, and B.13

Meeting of January 11, 1984:
Items A.2, A.3, A.4, A.6, A.8, A.9, A.12, and A.13

Meeting of January 12, 1984:
Items B.1, B.2, and B.3
(Item C.3 will be included as part of Amendment 6 to the FSAR)

In addition, please note that four (4) advance sets of these responses were transmitted to D. Wagner via Federal Express on February 16, 1984.

B024
1/1

Should you have any questions in this regard, do not hesitate to contact us.

Very truly yours,

RL Mittl/RPDouglas

R. L. Mittl
General Manager -
Nuclear Assurance and Regulation

DJD:db

Attachment: Resolution of NRC Comments on Structural/Geotechnical Topics

CC: D. H. Wagner (w/attach.)
USNRC Licensing Project Manager

OQ 14 01/02-C

Response to NRC Audit

Meeting Date: January 10, 1984

Question No.: A-1

Question: Describe two alternate methods used for establishing soil damping values.

Response: Different techniques are used for establishing soil damping values in the FLUSH and EDSGAP programs.

1) The FLUSH program uses element damping directly and implements it in the formulation of element complex shear moduli. Numerically, the FLUSH program uses the frequency domain and complex response method of analysis. All stiffness and boundary matrices in the complex equation of motion are formed using the element complex shear moduli

$$G^* = G(1 - 2\xi^2 + 2i\xi\sqrt{1-\xi^2}) \simeq G \cdot \exp(2i\xi)$$

where G and ξ are the shear modulus and the fraction of critical damping of the element, respectively. This complex formulation allows the necessary freedom to adjust damping ratios for each element. Typical element damping values used in a soil column are shown on page 1 of the attachment.

2) The EDSGAP program uses Rayleigh Damping (α - β) technique in the direct step-by-step integration time history method. This technique is described below:

If the system were uncoupled into normal modes, the relationship among the generalized damping, generalized mass, and generalized stiffness for the n^{th} mode would be:

$$C_n^* = \alpha M_n^* + \beta K_n^* \qquad (1)$$

Hence, from the relationships:

$$C_n^* = 2\xi_n(2\pi f_n)M_n^* \qquad (2)$$

and:

$$K_n^* = (2\pi f_n)^2 M_n^* \qquad (3)$$

in which ξ_n = proportion of critical damping in the n^{th} mode, and f_n = frequency of the n^{th} mode, it follows that any specified values of α and β imply damping in the n^{th} mode equal to:

$$\xi_n = \frac{\alpha}{4\pi f_n} + \beta\pi f_n \qquad (4)$$

Conversely, if the amount of critical damping is specified at two distinct frequencies, f_i and f_j, then the damping coefficients, α and β, are uniquely determined:

$$\alpha = (4\pi f_i f_j) \frac{f_j \xi_i - f_i \xi_j}{f_j^2 - f_i^2} \qquad (5)$$

$$\beta = \frac{1}{\pi} \frac{f_j \xi_j - f_i \xi_i}{f_j^2 - f_i^2} \qquad (6)$$

For practical analysis, corresponding values of f and ξ, which provide a reasonable approximation of damping over the frequency range of interest, should be selected and values of α and β determined using Equations 5 and 6.

For the soil-structure interaction analysis, the modal damping ratios are determined from the deconvolution soil column model which contains strain-compatible soil dampings. The damping factors α and β are then selected to best fit these damping values. For the Hope Creek site, the Rayleigh damping values were chosen such that the resultant α-β damping curve would predict conservative damping values compared to corresponding modal dampings of the soil column in the frequency range of interest. This is indicated in page 2 of the attachment.

Finally, it is noted that for the structural analyses of the buildings, Rayleigh Damping technique is not used. Modal dampings based on material dampings specified in Regulatory Guide 1.61 are used in mode superposition time history analyses.

ATTACHMENT TO RESPONSE A-1

MATERIAL PROPERTIES OBTAINED USING EFFECTIVE SHEAR STRAIN ESTIMATED IN FREQUENCY DOMAIN

LAYER	G-USED (KSF)	G-NEW (KSF)	DIF-G (PERCENT)	DAMP-USED (FRACTION)	DAMP-NEW (FRACTION)	DIF-DAMP (PERCENT)	VS-USED (FPS)	VS-NEW (FPS)	DIFF-VS (PERCENT)	VP-USED (FPS)
1	96.	96.	0.1	0.068	0.068	0.1	161.	161.	0.1	823.
2	148.	150.	0.8	0.055	0.055	0.8	222.	223.	0.4	1132.
3	72.	77.	9.8	0.094	0.089	5.8	154.	162.	5.0	787.
4	43.	47.	7.6	0.115	0.112	2.9	120.	125.	3.9	613.
5	24.	26.	4.9	0.136	0.134	1.5	89.	91.	2.5	452.
6	9.	9.	0.3	0.161	0.161	0.0	53.	53.	0.1	273.
7	8.	8.	0.3	0.161	0.161	0.0	52.	52.	0.1	267.
8	8.	8.	0.3	0.161	0.162	0.0	52.	52.	0.1	26[illegible].
9	785.	782.	0.4	0.075	0.075	0.2	446.	445.	0.2	1092.
10	845.	844.	0.2	0.078	0.078	0.1	468.	468.	0.1	1148.
11	2549.	2545.	0.2	0.037	0.037	0.2	884.	883.	0.1	2166.
12	2517.	2516.	0.1	0.043	0.043	0.1	843.	843.	0.0	2063.
13	2285.	2284.	0.0	0.047	0.047	0.0	822.	822.	0.0	2014.
14	1004.	1007.	0.2	0.087	0.087	0.1	513.	513.	0.1	1256.
15	1080.	1083.	0.3	0.087	0.087	0.2	532.	533.	0.2	1302.
16	1314.	1320.	0.4	0.084	0.084	0.2	604.	605.	0.2	1724.
17	1409.	1408.	0.1	0.083	0.083	0.0	626.	625.	0.1	1785.
18	1494.	1497.	0.2	0.083	0.083	0.1	644.	645.	0.1	1838.
19	1590.	1593.	0.2	0.082	0.082	0.1	664.	665.	0.1	1896.
20	1752.	1753.	0.1	0.081	0.081	0.0	697.	698.	0.0	1990.
21	1969.	1970.	0.0	0.079	0.079	0.0	739.	740.	0.0	2110.
22	2191.	2190.	0.1	0.077	0.078	0.0	780.	780.	0.0	2225.
23	2402.	2400.	0.1	0.076	0.076	0.0	816.	816.	0.0	2330.
24	2600.	2598.	0.1	0.076	0.076	0.0	850.	849.	0.0	2424.
25	2788.	2786.	0.1	0.075	0.075	0.0	880.	879.	0.0	2510.
26	2957.	2955.	0.1	0.075	0.075	0.0	906.	906.	0.0	2585.
27	3116.	3115.	0.1	0.075	0.075	0.0	930.	930.	0.0	2654.
28	3331.	3330.	0.0	0.075	0.075	0.0	962.	961.	0.0	2744.
29	3612.	3611.	0.0	0.075	0.075	0.0	1001.	1001.	0.0	2857.
30	3910.	3913.	0.0	0.074	0.074	0.0	1042.	1042.	0.0	2973.
31	4232.	4232.	0.0	0.074	0.074	0.0	1084.	1084.	0.0	3093.
32	4575.	4577.	0.0	0.073	0.073	0.0	1127.	1127.	0.0	3216.
33	4937.	4940.	0.1	0.073	0.073	0.0	1171.	1171.	0.0	3342.
34	5306.	5310.	0.1	0.072	0.072	0.0	1214.	1214.	0.0	3463.
35	5687.	5690.	0.0	0.071	0.071	0.0	1256.	1257.	0.0	3585.
36	6069.	6071.	0.0	0.071	0.071	0.0	1298.	1298.	0.0	3704.
37	6446.	6448.	0.0	0.070	0.070	0.0	1338.	1338.	0.0	3817.
38	5986.	5987.	0.0	0.072	0.072	0.0	1280.	1280.	0.0	3136.
39	5968.	5967.	0.0	0.072	0.072	0.0	1287.	1287.	0.0	3153.
40	6029.	6028.	0.0	0.072	0.072	0.0	1294.	1294.	0.0	3169.
41	6091.	6090.	0.0	0.073	0.073	0.0	1300.	1300.	0.0	3185.
42	6153.	6154.	0.0	0.073	0.073	0.0	1307.	1307.	0.0	3201.
43	6214.	6215.	0.0	0.073	0.073	0.0	1313.	1313.	0.0	3217.
44	6264.	6266.	0.0	0.073	0.073	0.0	1319.	1319.	0.0	3230.
45	6318.	6320.	0.0	0.074	0.074	0.0	1324.	1325.	0.0	3244.
46	6361.	6363.	0.0	0.074	0.074	0.0	1329.	1329.	0.0	3258.
47	6405.	6406.	0.0	0.074	0.074	0.0	1333.	1333.	0.0	3266.
48	6445.	6445.	0.0	0.074	0.074	0.0	1338.	1338.	0.0	3276.
49	6483.	6482.	0.0	0.074	0.074	0.0	1341.	1341.	0.0	3286.
50	6525.	6524.	0.0	0.075	0.075	0.0	1346.	1346.	0.0	3296.
51	6565.	6564.	0.0	0.075	0.075	0.0	1350.	1350.	0.0	3307.
52	6606.	6605.	0.0	0.075	0.075	0.0	1354.	1354.	0.0	3317.
53	6641.	6642.	0.0	0.075	0.075	0.0	1358.	1358.	0.0	3326.

Typical Element Damping Values used
in soil column analyses, OBE case

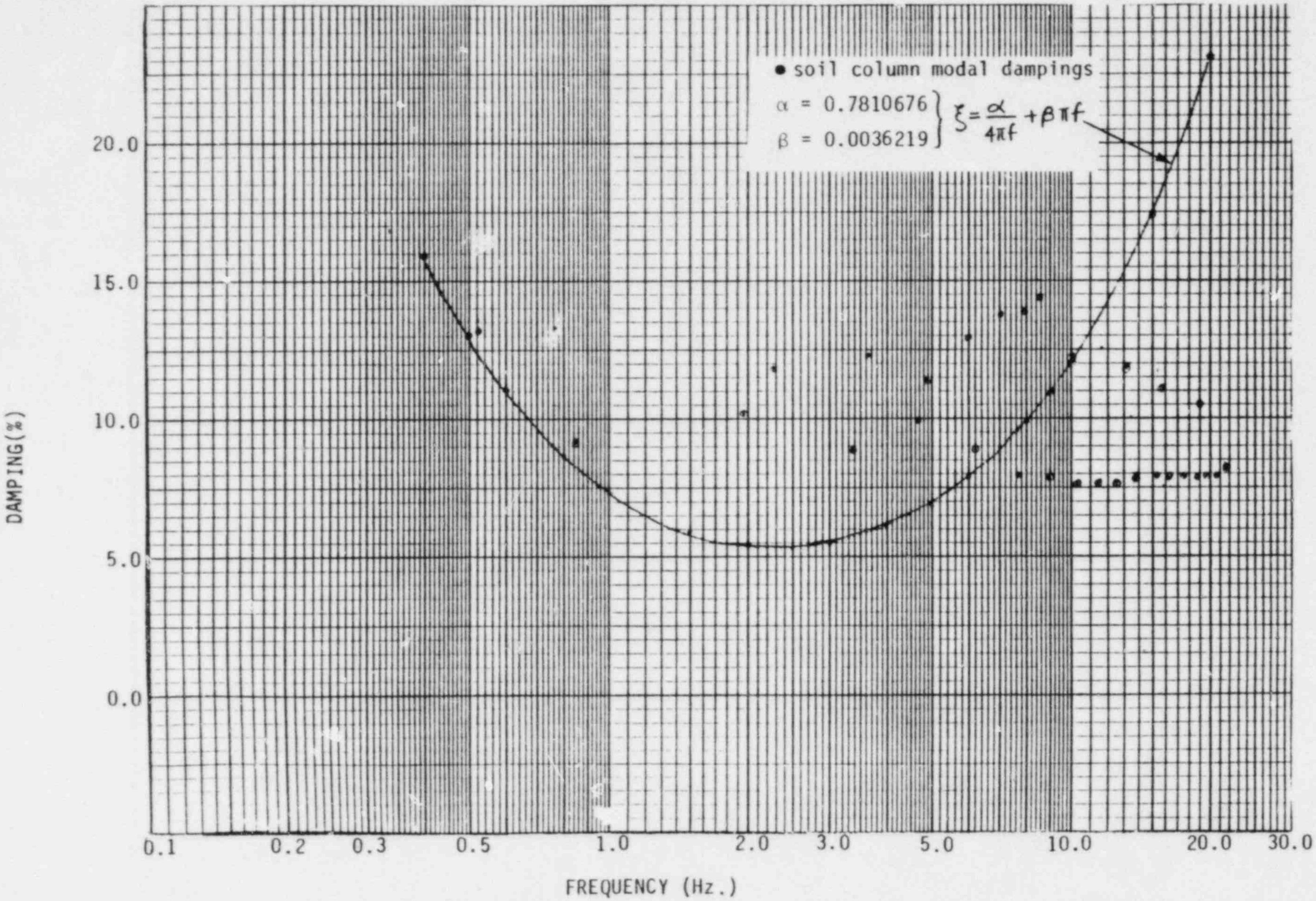

FIGURE 1: Plot of α-β versus modal damping for soil column, OBE case

Response to NRC Audit

Meeting Date: January 10, 1984

Question No.: A-2

<u>Question:</u> Provide comparison between foundation level response spectra for three soil depth models.

<u>Response:</u> The comparison between foundation level response spectra, as well as finite element representation of the three models in the N-S direction are given in the attachment for the power block area soil-structure interaction depth study. The lateral extent of all three models is approximately 1,000 feet from the edge of the building. A depth of 402 feet was utilized in developing the detailed SSI models for the design basis.

ATTACHMENT TO RESPONSE A-2 January 10/A2

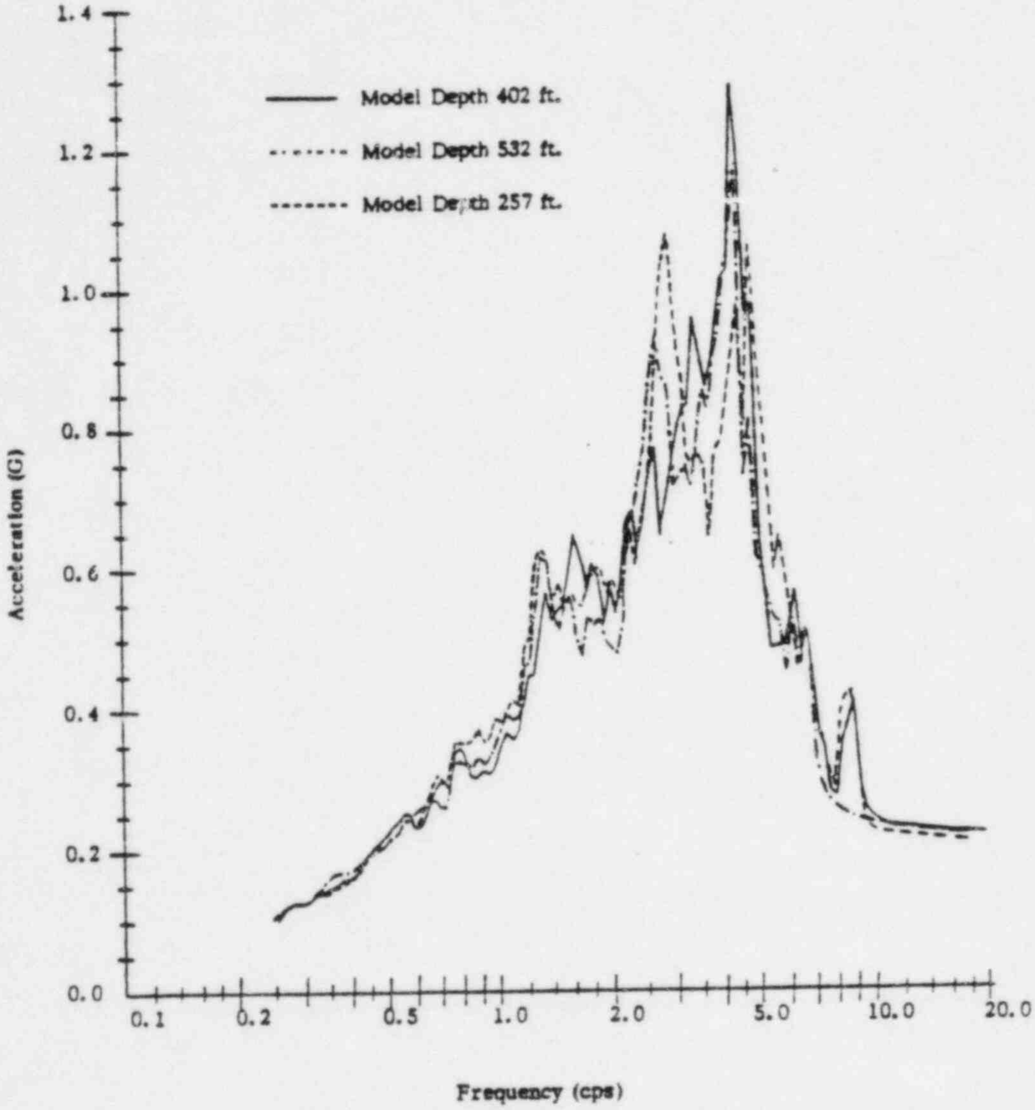

COMPARISON OF HORIZONTAL SPECTRA
AT FOUNDATION LEVEL FOR DETERMINING
SIGNIFICANT INTERACTION DEPTH
POWER BLOCK AREA, SSE CASE

FIGURE B-18

PUBLIC SERVICE ELECTRIC & GAS CO.	SEISMIC STRUCTURAL ANALYSES
HOPE CREEK PROJECT	

ATTACHMENT TO RESPONSE A-2

January 10/A2

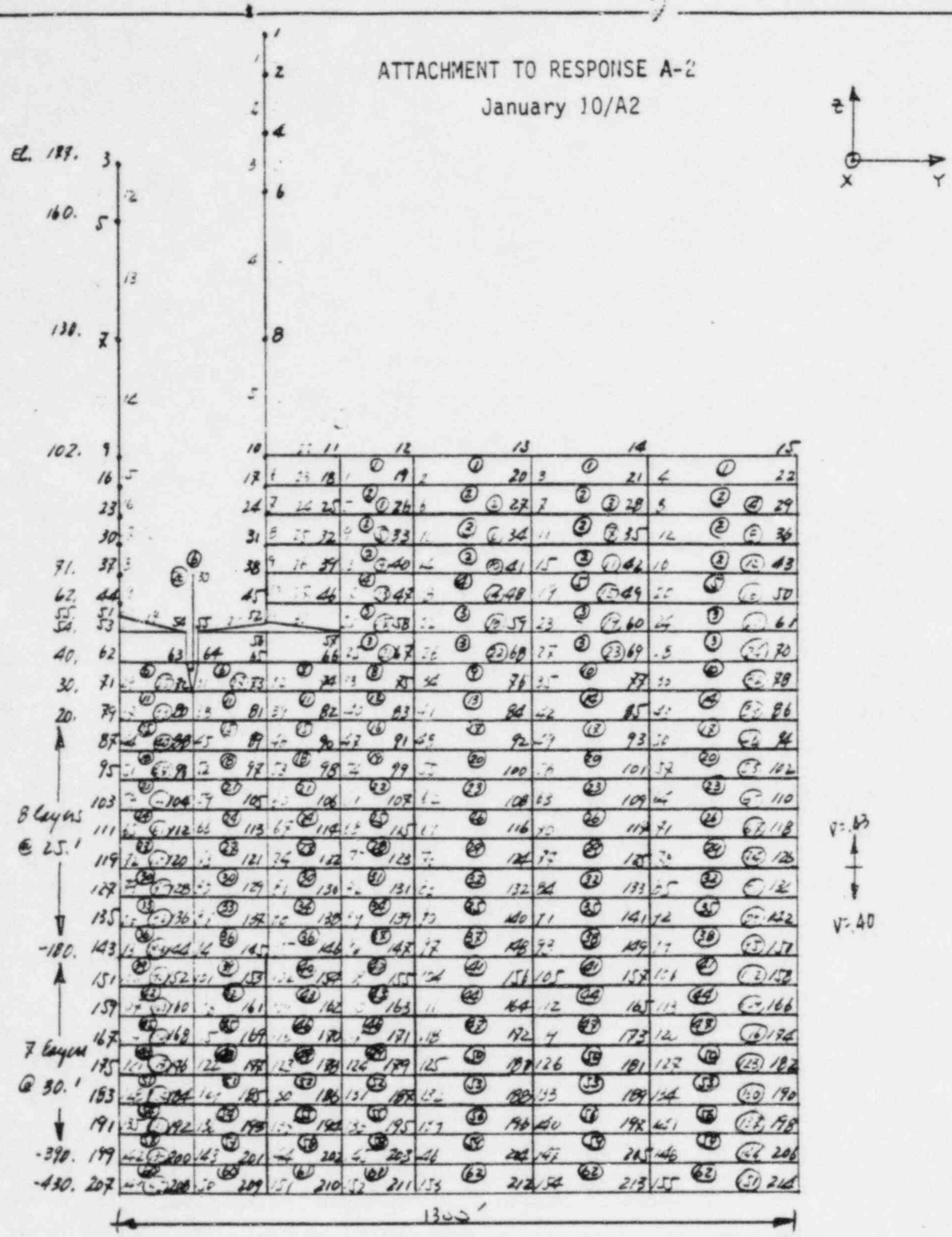

532' Model

ITEM	532' Simplified Interaction Model for Soil Sensitivity Studies	CLIENT	PSE & G
		PROJECT	Hope Creek
		JOB NO.	1400012
BY GH	DATE 18 AUG 77	CKD. HU	DATE	ITEM NO.	SHT. 1 OF

EDS NUCLEAR: 220 MONTGOMERY ST. • SAN FRANCISCO, CALIFORNIA 94104

EDS NUCLEAR: 220 MONTGOMERY ST. • SAN FRANCISCO, CALIFORNIA 94104

JOB NO. 1400012	CLIENT PSE&G	BY JJB	DATE 7/30/75
PROJECT HCNGS		CKD. GH	DATE 7/30/75
ITEM 402.0' Simplified Interaction Model for Soil Sensitivity Studies			SHT. 1 OF 1

ATTACHMENT TO RESPONSE A-2

January 10/A2

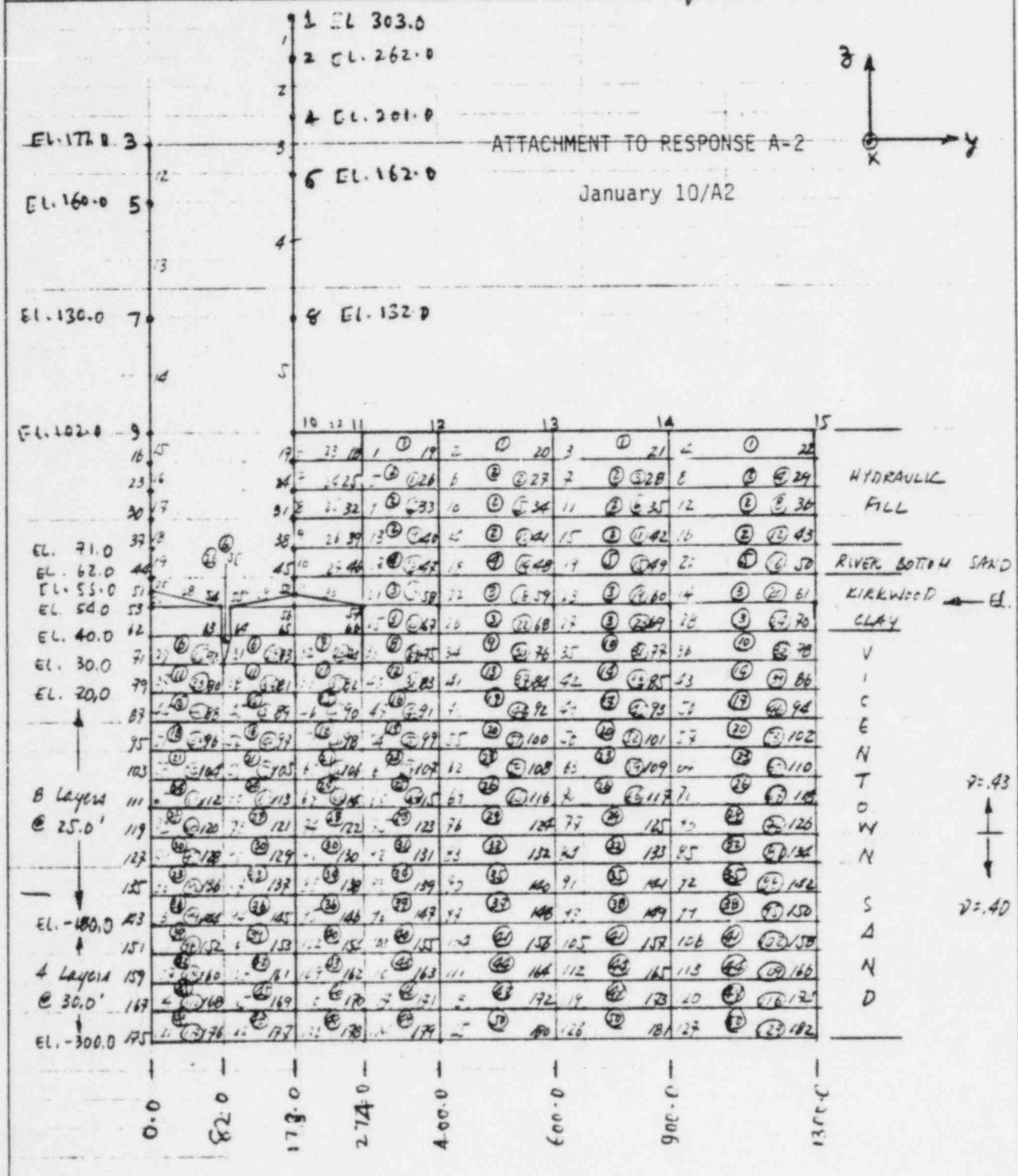

1 - Nodal points

① - HSL Numbering

1 - 2-D Elements

○ Fluid Elements

Beam Elements

geometric Numbering

402' Model

ATTACHMENT TO RESPONSE A-2
January 10/A2

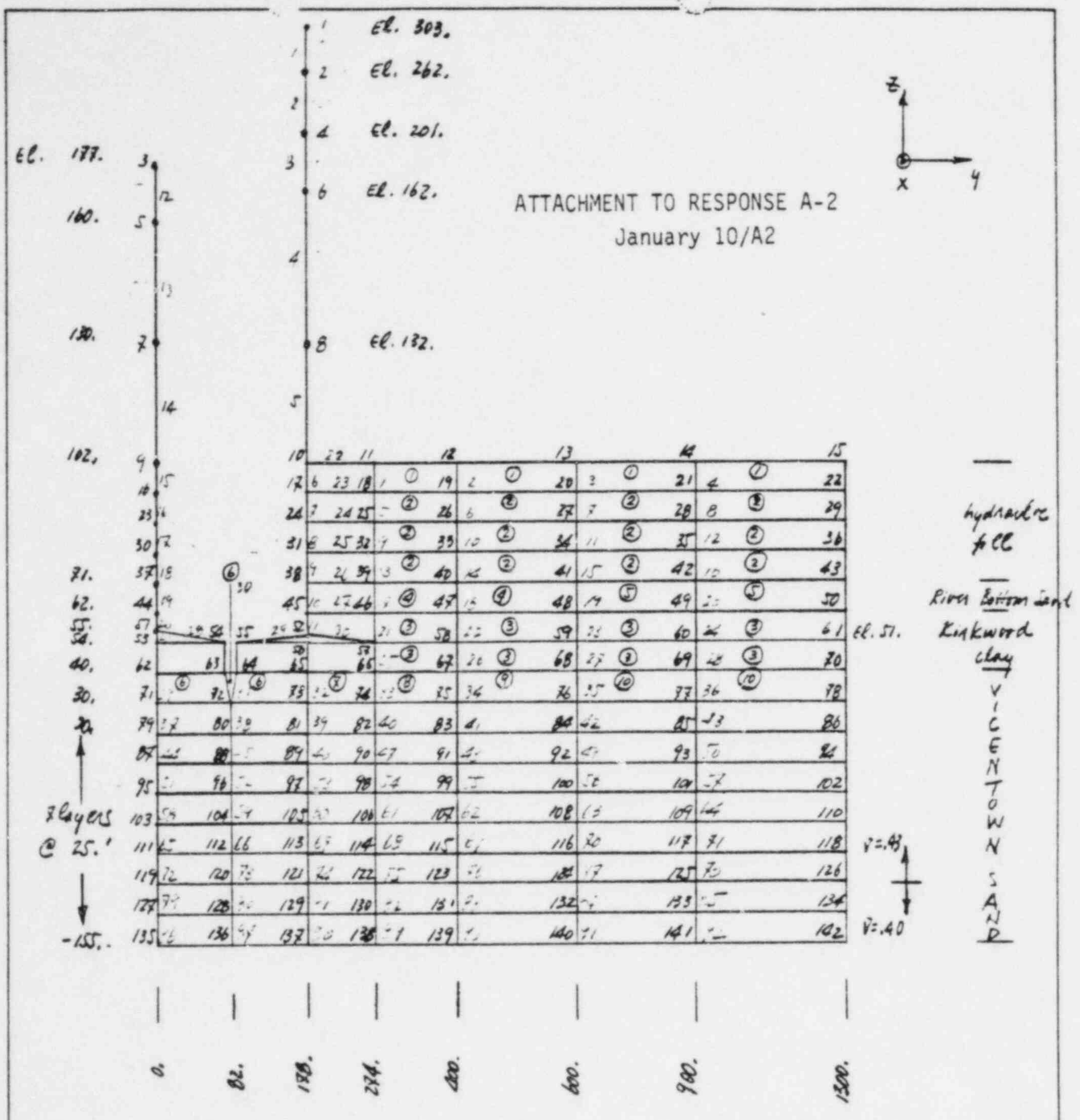

257' Model

ITEM 257' Simplified Interaction Model for Soil Sensitivity Studies	CLIENT PSE & G
	PROJECT Hope Creek
	JOB NO. 1400012
BY GH / DATE 15AUG75 / CKD. [illegible] / DATE	ITEM NO. / SHT. 1 OF

EDS NUCLEAR: 220 MONTGOMERY ST. • SAN FRANCISCO, CALIFORNIA 94104

Response to NRC Audit

Meeting Date: January 10, 1984

Question No.: A-3

Question: Provide comparison between basemat response spectra and regenerated response spectra at basemat.

Response: The attached two figures provide a comparison between basemat RG 1.60 response spectra and regenerated response spectra at basemat elevation for the horizontal North-South OBE and SSE earthquake soil column deconvolution analyses, respectively.

A 12 Hz cutoff frequency has been used in these analyses. As observed from the attached figures, the match between Reg. Guide 1.60 response spectra and the regenerated response spectra at basemat elevation is adequate below the 12 Hz cutoff frequency. The adequacy of the 12 Hz cutoff frequency is addressed in a separate response to question A-12 from the audit meeting on January 11, 1984.

ATTACHMENT TO RESPONSE A-3

January 10/A3

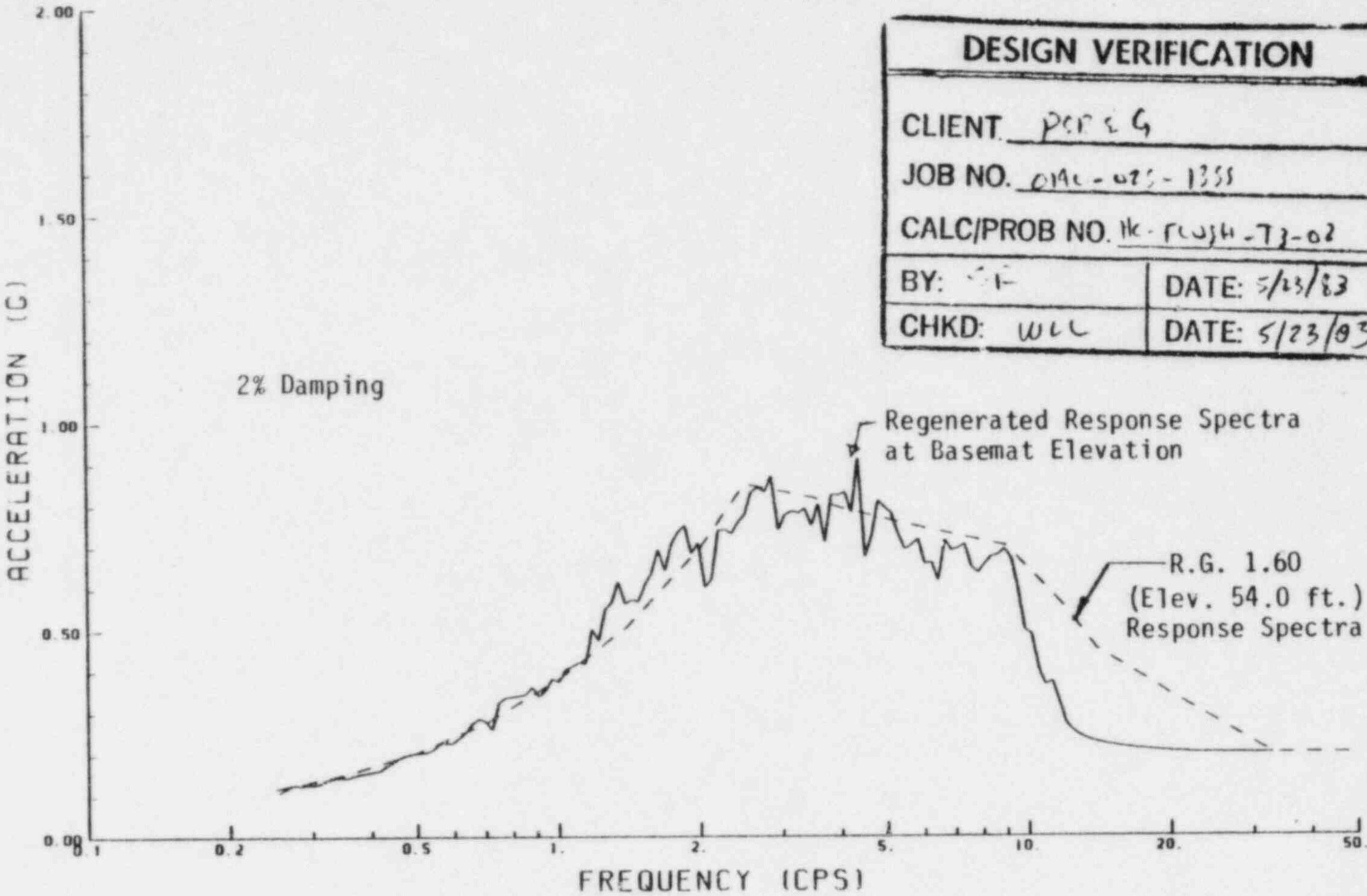

DESIGN VERIFICATION

CLIENT: PSE&G

JOB NO. 0146-025-1355

CALC/PROB NO. HC-FLUSH-T3-02

BY: SF	DATE: 5/23/83
CHKD: WLC	DATE: 5/23/83

NS-SSE FLUSH ANALYSIS
AVERAGE SOIL PROPERTIES
TOP OF LAYER 16. ELEV. 54.0 FT , FREE FIELD

HOPE CREEK
SOIL STRUCTURE INTERACTION

DESIGN VERIFICATION

CLIENT PSE & G
JOB NO. 0140-025-1355
CALC/PROB NO. HC-FLUSH-T3-04
BY: GF DATE: 5/23/83
CHKD: WLL DATE: 5/23/83

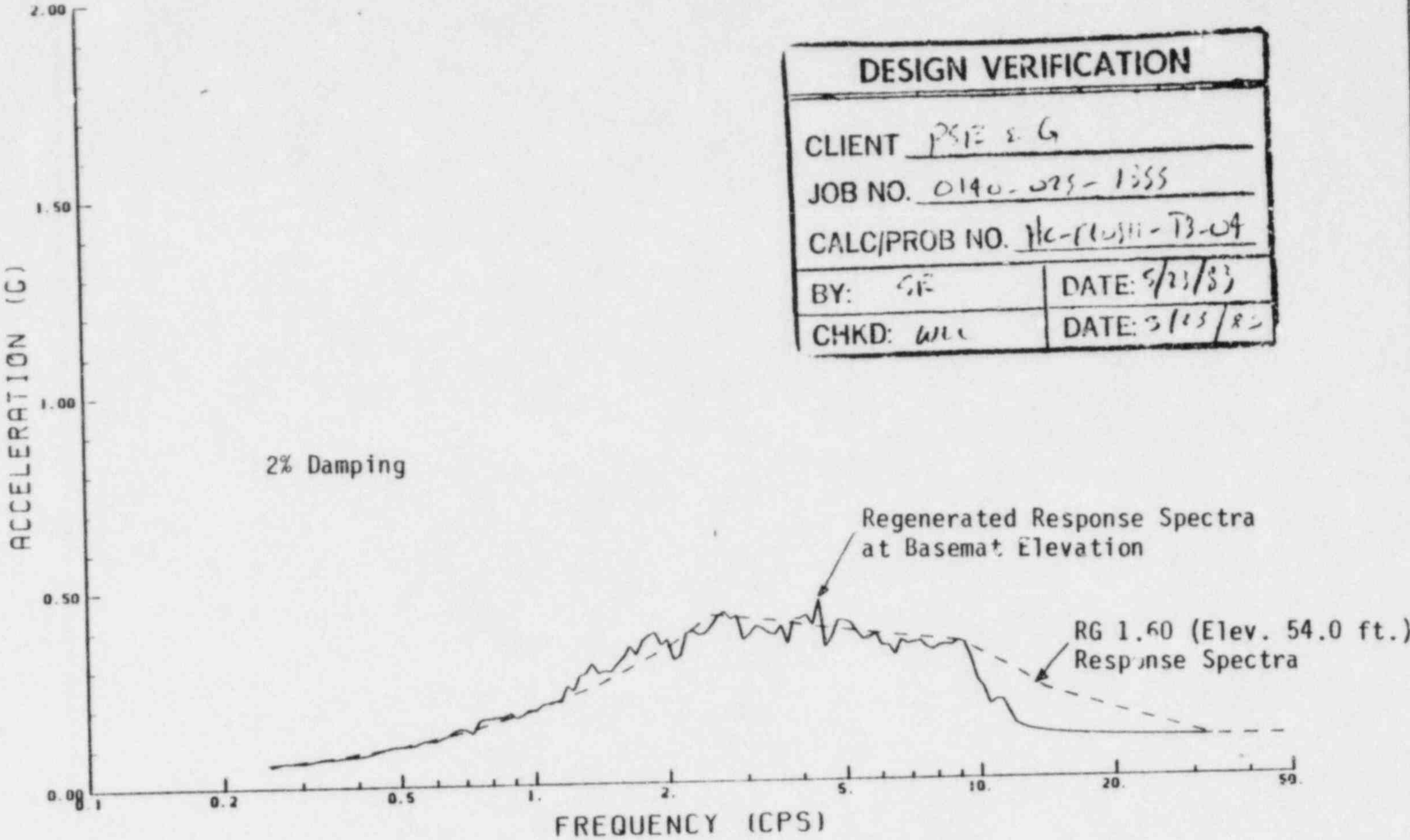

NS-OBE FLUSH ANALYSIS
AVERAGE SOIL PROPERTIES
TOP OF LAYER 16. ELEV. 54.0 FT . FREE FIELD

HOPE CREEK
SOIL STRUCTURE INTERACTION

Response to NRC Audit

Meeting Date: January 10, 1984

Question No.: A-4

<u>Question</u>: Describe method of establishing rocking time histories R(t).

<u>Response</u>: Rocking time histories are obtained directly from the SSI analysis in terms of rotation at the center of mass at each building basemat. They are input into the uncoupled building model as a moment time history applied to a very large rotational mass at the base of the model such that:

$$I_M \ \ddot{\Phi}(t) = M(t)$$

Large Rotational Mass Moment of Inertia | Rocking time History from SSI | Input to uncoupled building model

This is a common modelling technique and is used in codes where a fixed-base rotational time history cannot be input directly.

The large rotational mass moment of inertia is selected to be several orders of magnitude, a minimum of 5 orders for Hope Creek, higher than the total rotational mass moment of inertia of the building. In conjunction with this large rotational mass moment of inertia, a rotational spring constant is used to introduce a rocking mode with frequency f, where

$$f = \frac{1}{2\pi}\sqrt{\frac{K \longleftarrow \text{stiffness}}{I_M \longleftarrow \text{mass}}}$$

The spring constant, K, is selected such that f is considerably lower than the fundamental frequency of the system, a minimum of 3 orders for Hope Creek.

The attachment shows this modelling technique for the reactor building, where the resultant frequencies for the two rocking modes (about N-S and E-W axes) are 0.005 and 0.0067 Hz which are well uncoupled from the first true mode at 2.73 hz (first torsional mode of the building). Page 1 of the attachment shows the actual values of these large spring constants and rotational masses for the two directions of rocking about N-S and E-W respectively. Page 2 shows the resultant rocking mode frequencies computed by the program. These frequencies are verified by hand calculation as shown in page 3 of the attachment.

ATTACHMENT TO RESPONSE A-4

7	3							
107	270			1			3.867E10	.10
107	271			1			2.128E10	.10
107	272			1			3.[illegible]51E10	0.26
1		43.00	43.00	43.00	.012E6	.012E6	.024E6	
2		100.00	100.00	100.00	.118E6	.118E6	.236E6	
3		91.00	91.00	91.00	.210E6	.210E6	.420E6	
4		63.00	63.00	63.00	.193E6	.193E6	.386E6	
5		58.00	58.00	58.00	.198E6	.198E6	.396E6	
6		106.00	106.00	106.00	.373E6	.373E6	.746E6	
7		274.00	274.00	274.00	.856E6	.856E6	1.712E6	
8		350.00	350.00	350.00	.905E6	.958E6	1.863E6	
9		411.00	411.00	411.00	.216E6	.364E6	.580E6	
11		112.00	112.00	112.00	.091E6	.290E6	.382E6	
12		440.00	440.00	440.00	.169E6	.578E6	.747E6	
13		.56	.56	.56				
14		1.15	1.15	1.15				
15		1.27	1.27	1.27				
16		1.53	1.53	1.53				
17		168.00	168.00	168.00	.099E6	.218E6	.317E6	
21		2.63	2.63	2.63				
22		3.59	3.59	3.59				
23		3.19	3.19	3.19				
25		269.00	269.00	269.00	.832E6	.758E6	1.590E6	
26		428.00	428.00	428.00	.266E6	.534E6	.799E6	
27		1.85	1.89	1.89				
29		.65	.65	.65				
30		6.66	6.66	6.66				
31		231.00	231.00	231.00	.191E6	.516E6	.706E6	
35		.71	.71	.71				
36		8.40	8.40	8.40				
37		9.68	9.68	9.68				
40		156.00	156.00	156.00	.544E6	.191E6	.735E6	
41		254.00	254.00	254.00	.176E6	.206E6	.382E6	
42		1.10	1.10	1.10				
43		.81	.81	.81				
44		15.02	15.02	15.02				
46		293.00	293.00	293.00	.228E6	.617E6	.846E6	
50		2.11	2.11	2.11				
51		15.77	15.77	15.77				
52		7.12	7.12	7.12				
54		712.00	712.00	712.00	3.076E6	2.798E6	5.874E6	
55		384.00	384.00	384.00	.267E6	.408E6	.674E6	
56		5.20	5.20	5.20				
57		9.85	9.85	9.85				
58		8.72	8.72	8.72				
59		2.07	2.07	2.07				
60		3.34	3.34	3.34				
61		470.00	470.00	470.00	.519E6	1.158E6	1.677E6	
64		5.32	5.32	5.32				
65		7.33	7.33	7.33				
66		10.37	10.37	10.37				
67		6.09	6.09	6.09				
68		4.55	4.55	4.55				
72		17.75	17.75	17.75				
73		24.14	24.14	24.14				
75		.60	.60	.60				
76		12.20	12.20	12.20				
80		5.08	5.08	5.08				
82		7.11	7.11	7.11				
83		.16	.16	.16				
84		4.01	4.01	4.01				
85		1375.00	1375.00	1375.00	12.367E6	5.287E6	17.654E6	
86		332.00	332.00	332.00	.273E6	.360E6	.633E6	
87		13.16	13.16	13.16				
88		21.68	21.68	21.68				
89		3.42	3.42	3.42				
91		2.48	2.48	2.48				
92		445.00	445.00	445.00	.516E6	1.231E6	1.748E6	
93		950.00	950.00	950.00	6.681E6	4.270E6	10.551E6	
96		9.17	9.17	9.17				
97		2.12	2.12	2.12				
98		1.65	1.65	1.65				
99		.35	.35	.35				
103		13.90	13.90	13.90				
104		6.62	6.62	6.62				
105		3.44	3.44	3.44				
106		.12	.12	.12				
107					3.918E13	1.213E13	4.286E07	
109		426.00	426.00	426.00	.158E6	.158E6	.316E6	
110		8.17	8.17	8.17				
111		19.93	19.93	19.93				
112		1.03	1.03	1.03				
113		.12	.12	.12				
114		.42	.42	.42				
116		12.54	12.54	12.54				
117		.42	.42	.42				
118		1.03	1.03	1.03				

Large Rotational Spring Constants

Units are in kips, feet, seconds and radians

Large Rotational Mass Moment of Inertia

ATTACHMENT TO RESPONSE A-4

January 10/A-4

Frequencies of Rocking Modes about N-S & E-W Axes

MODE	FREQ.(RAD/SEC)	FREQ.(CPS)	PERIOD
1	.314162E-01	.500005E-02	199.997905
2	.418845E-01	.666613E-02	150.012044
3	.171578E+02	.273075E+01	.366200
4	.257620E+02	.410031E+01	.243884
5	.265532E+02	.422610E+01	.236625
6	.273077E+02	.434616E+01	.230088
7	.277367E+02	.441444E+01	.226529
8	.445608E+02	.709207E+01	.141003
9	.446275E+02	.710275E+01	.140791
10	.554215E+02	.882068E+01	.113370
11	.561265E+02	.893287E+01	.111946
12	.595675E+02	.948053E+01	.105479
13	.624632E+02	.994124E+01	.100590
14	.627874E+02	.999293E+01	.100071
15	.712713E+02	.113432E+02	.088159
16	.733325E+02	.116712E+02	.085681
17	.768402E+02	.122295E+02	.081769
18	.794821E+02	.126501E+02	.079050
19	.891050E+02	.141815E+02	.070514
20	.891182E+02	.141836E+02	.070504
21	.997349E+02	.158733E+02	.062999
22	.102866E+03	.163717E+02	.061081
23	.104000E+03	.165521E+02	.060415
24	.106675E+03	.169779E+02	.058900
25	.110265E+03	.175493E+02	.056982
26	.111154E+03	.176907E+02	.056527
27	.114807E+03	.182721E+02	.054728
28	.119873E+03	.190787E+02	.052414
29	.119918E+03	.190855E+02	.052396
30	.122174E+03	.194446E+02	.051428
31	.124924E+03	.198839E+02	.050292
32	.124948E+03	.198861E+02	.050286
33	.126869E+03	.201919E+02	.049525
34	.133452E+03	.212395E+02	.047082
35	.134754E+03	.214532E+02	.046613
36	.136889E+03	.217865E+02	.045900
37	.143055E+03	.227750E+02	.043908
38	.152072E+03	.242030E+02	.041317
39	.160132E+03	.254858E+02	.039238
40	.165112E+03	.262784E+02	.038054
41	.165255E+03	.263011E+02	.038021
42	.165672E+03	.263677E+02	.037925
43	.170411E+03	.271218E+02	.036871
44	.174328E+03	.277468E+02	.036040
45	.177437E+03	.282401E+02	.035411
46	.181965E+03	.289606E+02	.034530
47	.190781E+03	.303637E+02	.032934
48	.192773E+03	.306808E+02	.032594
49	.193092E+03	.307316E+02	.032540
50	.195614E+03	.311330E+02	.032120
51	.195615E+03	.311332E+02	.032120
52	.196647E+03	.312974E+02	.031952

ATTACHMENT TO RESPONSE A-4

$$F = \frac{1}{2\pi}\sqrt{\frac{K}{I_M}}$$

FREQUENCY OF ROCKING MODE ABOUT N-S AXIS

$$F_1 = \frac{1}{2\pi}\sqrt{\frac{3.867 \times 10^{10}}{3.918 \times 10^{13}}}$$

$$= 0.005 \quad HZ$$

FREQUENCY OF ROCKING MODE ABOUT E-W AXIS

$$F_2 = \frac{1}{2\pi}\sqrt{\frac{2.128 \times 10^{10}}{1.213 \times 10^{13}}}$$

$$= 0.0067 \quad HZ$$

UNITS ARE IN KIPS, FEET, SECONDS AND RADIANS

Response to NRC Audit

Meeting Date: January 10, 1984

Question No.: A-6

Question: Assess and justify that the random combination of soil layer properties is adequate and conservative.

Response: The soil property variation study was performed to establish criteria for broadening of spectral peak frequencies. To achieve the upper bound frequency shift of spectral peaks, all soil layer shear moduli were obtained from a set of upper bound soil property curves. Similary, to achieve the lower bound frequency shift, all soil layer shear moduli were obtained from a set of lower bound soil property curves. This particular combination of soil layer property variation would provide the largest possible range of spectral peak frequency shift.

Response to NRC Audit

Meeting Date: January 10, 1984

Question No.: A-11

Question: Justify why it is acceptable to use gross concrete section.

Response: In performing seismic analysis of concrete structures, properties based on gross concrete section are used. This procedure is consistent with ACI recommendations. Neglecting cracked concrete properties is frequently justified on the basis of discounting the transformed steel area of the reinforcing steel (Reference: "Vibration of Concrete Structures", Publication SP-60, American Concrete Institute, Paper SP 60-12).

In addition, a parametric evaluation was performed to assess whether cracking will occur during the postulated seismic event. The lower elevation (El. 54 ft.) of the Reactor Building was selected for this evaluation as the shear stress in this elevation was determined to be maximum.

This evaluation is based on the following:

- o In-situ average 90-day concrete strength is used. To be conservative, actual concrete strength, though higher, is not used.
- o ACI 349-76 code is used to establish the cracking strength of the concrete shear walls.

The calculated shear stresses (factored in accordance with the ACI code) are determined to be less than the nominal permissible shear stress allowed for concrete. Therefore, the concrete is not expected to crack during the postulated seismic event. Furthermore, for the strength evaluation of the concrete shear wall, the distance from the extreme compression fiber to the centroid of tension reinforcement is taken to the 80% of the horizontal length of concrete shear wall (Reference: Section 11.15.1 of ACI 349-76). Based on the above, it is determined that the use of gross concrete section is justified.

Response to NRC Audit

Meeting Date: January 10, 1984

Question No: A-12

Question: Pick one particular floor to define why particular modes were selected for development of vertical floor flexibility response spectra.

Response: All significant modes below 25.0 Hz were selected from the finite element model of the floor slab for development of vertical floor flexibility response spectra. In general, three to five modes were included with each mode representing a particular region of the floor slab.

For the Reactor Building floor slab at elevation 145.0 feet, five modes were used. Based on the mode shapes of these modes, these modes were determined to represent five different regions of the floor slab, as shown in Figure 1. These five modes were represented by five single-degree-of-freedom beam elements in the vertical floor flexibility model shown in Figure 2.

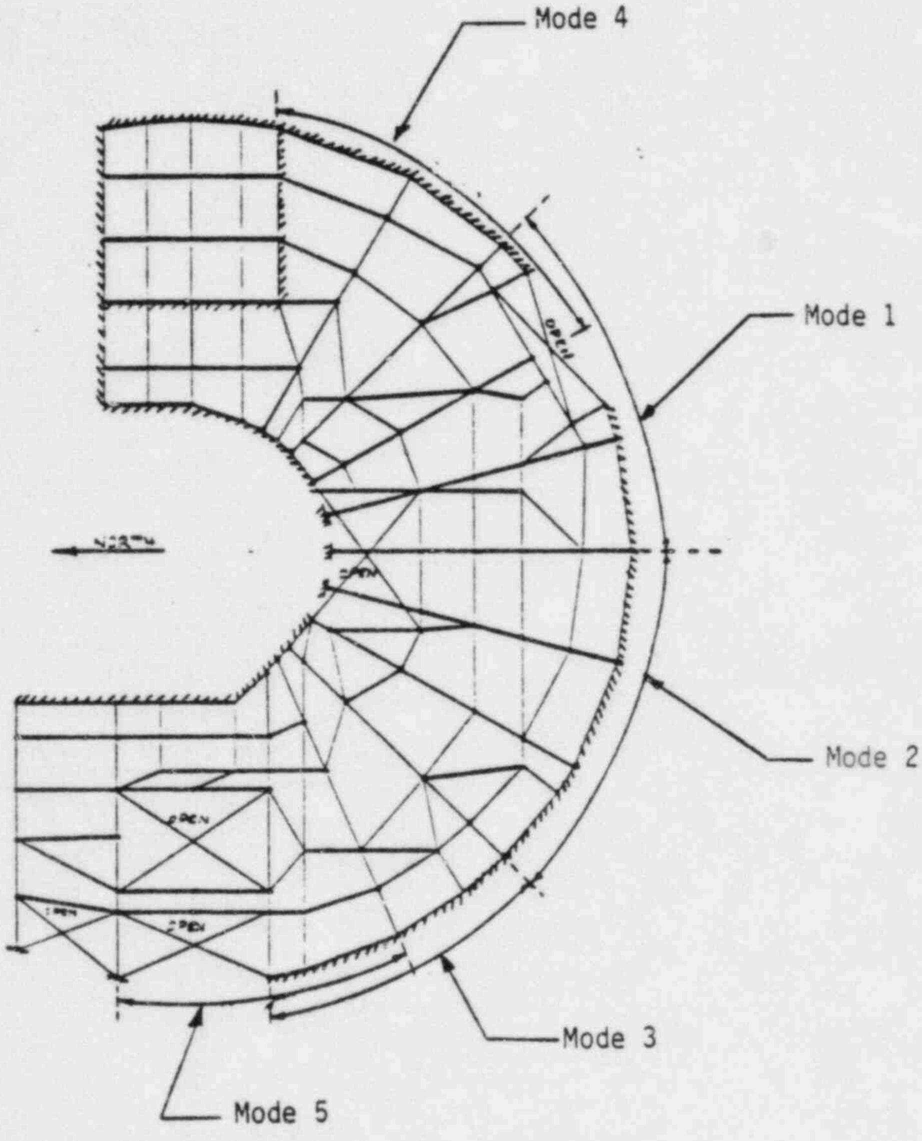

REACTOR BUILDING VERTICAL FLEXIBILITY ANALYSIS
FINITE ELEMENT PLATE AND BEAM MODEL
FLOOR ELEVATION 145.0 FT.

FIGURE 1

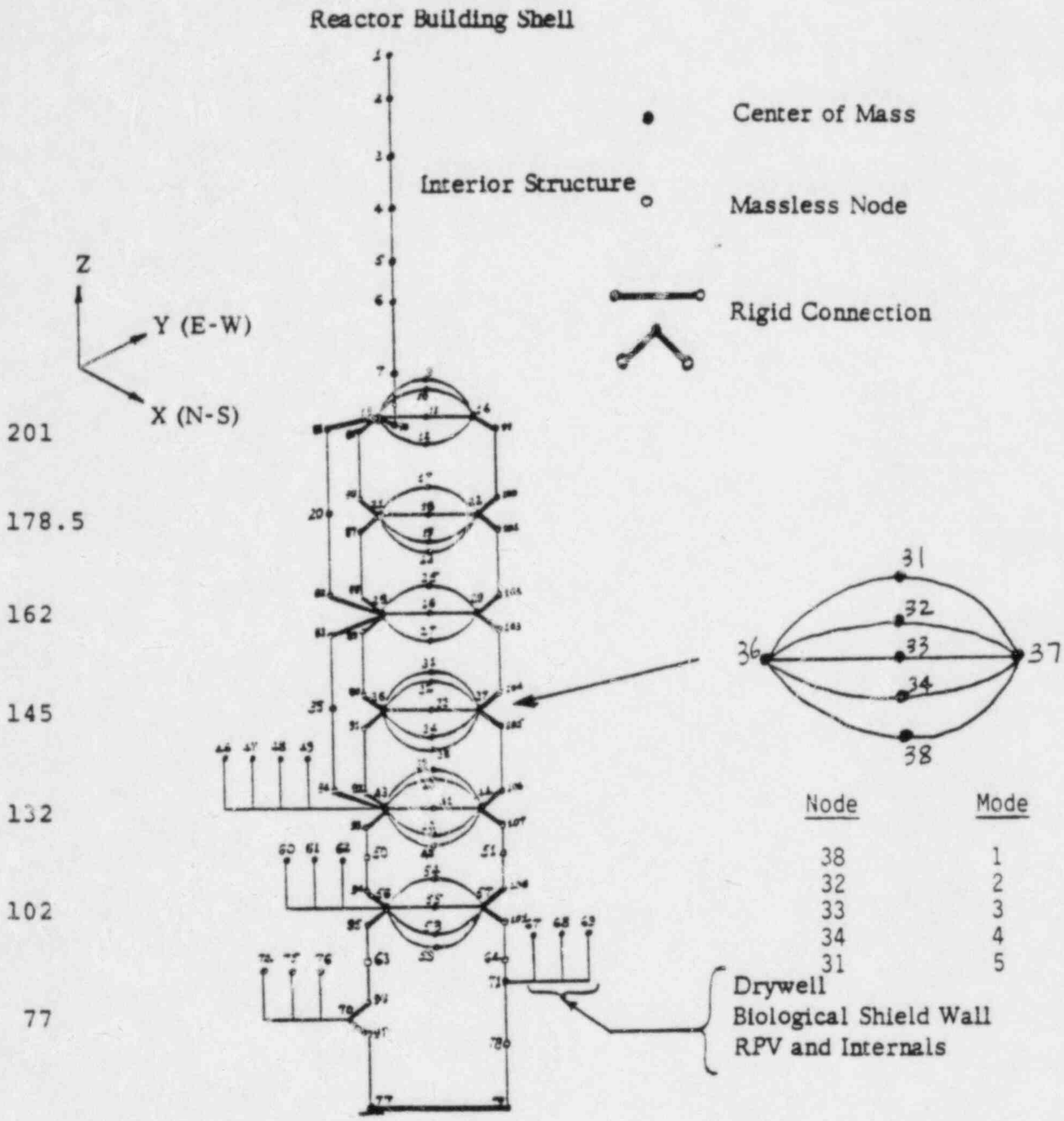

REACTOR BUILDING VERTICAL FLEXIBILITY ANALYSIS
MATHEMATICAL MODEL

FIGURE 2

Response to NRC Audit

Meeting Date: January 10, 1984

Question No.: A.15

QUESTION: Provide liquefaction analysis of river bottom sands using simplified Seed approach to determine induced shear stresses and compare dynamic shear strengths from laboratory tests.

RESPONSE: The liquefaction potential assessment of the river bottom sands has been previously performed based on one-dimensional shear wave propagation analyses, two-dimensional finite element analyses and dynamic cyclic triaxial tests as described in References 2.5-114 and 2.5-79, Part I.

In response to this action item, a simplified assessment based on the Seed and Idriss procedure has been performed. For this assessment, the cyclic strength of the saturated sandy soils was estimated from both dynamic laboratory tests and the average field SPT blowcount data. The calculations indicate that even with the various conservative assumptions made in the simplified analyses, the average factor of safety against liquefaction of the river bottom sands is well above unity. Calculations for the simplified analyses are attached.

Soil Profile and Vertical Stresses :

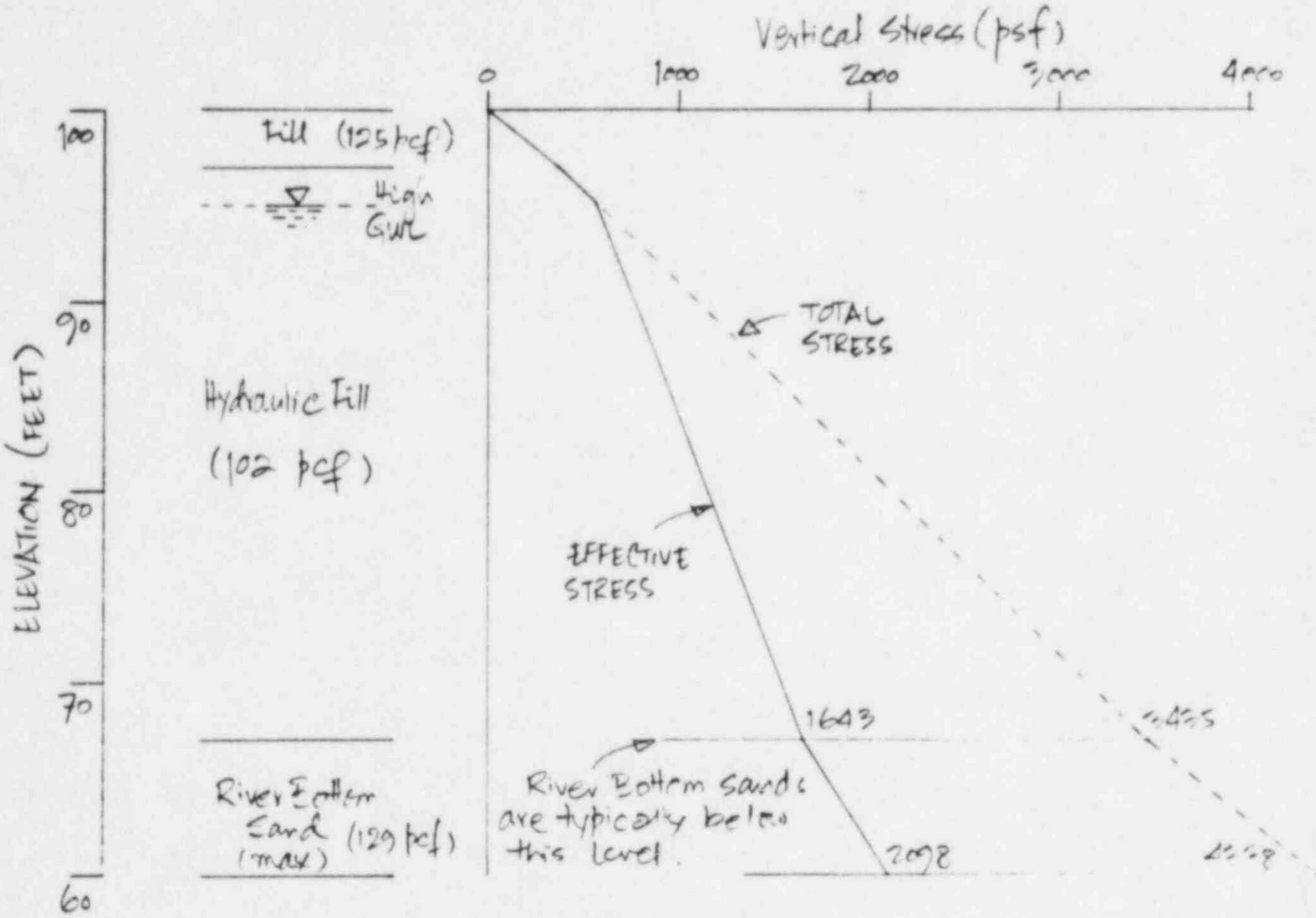

Seismic Induced Stress :

$\frac{(\sigma_0)_{total}}{(\sigma_0')_{effective}}$: at El. 67' $= \frac{3435}{1643} = 2.09$; at El. 60' $= \frac{4338}{2098} = 2.067$ } Use 2.1

r_d : Reduction factor from chart for depths of 33' to 40'

$= 0.9$

Seismic induced shear stress ratio : $\tau_{av}/\sigma_0' = 0.65 \times \frac{a_{max}}{g} \times \frac{\sigma_0}{\sigma_0'} \times r_d$

$= 0.65 \times 0.2 \times 2.1 \times 0.9$

$= \underline{0.25}$

REVISIONS
BY ____ DATE ____ TO EO ____
BY ____ DATE ____ TO EO ____

BY UKP DATE 2/1/84
CHECKED BY [illegible] DATE 2/3/84
COPY TO EO ____

FILE 2443.132.10 (5554)
SUBJECT River bottom sands - Liquef.
SHEET ___ OF ___

EVALUATION OF BLOWCOUNT DATA:

NOTES:

1) Little data is available along the service water pipeline primarily due to the very small thickness of river bottom sand along the pipeline. Available data is therefore reviewed in conjunction with data for the whole site.

2) Some of the lower blowcounts are misleading since part of the sample was in materials other than the River bottom sands which are underlain by Kirkwood clay and overlain by Hydraulic fill (mostly softer clayey material).

3) The D&M sample blowcounts are converted by using the Swantko & Roth correlation (1982), which is simply:

$$N_{spt} = N_{D\&M} \times \frac{\text{Weight of hammer (lbs)} \times \text{height of fall (ft)}}{6200}$$

This correlation is based on extensive data on actual field data. The Gibbs & Holtz correlation (1962) and Lacroix and Horn correlation (1973), based mostly on theoretical considerations tend to underestimate the resistance significantly.

4) (SPT) data on primarily cohesive materials, belonging to the "River bottom sands" group are ignored.

5) The simplified Seed and Idriss procedure, updated 1982 (Ground motions and Soil liquefaction during earthquakes - EERI), is used to normalize the penetration resistance (and for further analysis).

REVISIONS
BY ___ DATE ___ TO EO ___
BY ___ DATE ___ TO EO ___

BY LKP DATE 2/1/84
CHECKED BY HSG 2/6/84
COPY TO EO ___

DAMES & MOORE

FILE 2443-132-10 (5554)
SUBJECT River Bottom Sand... Liquefied
SHEET ___ OF ___

REVISIONS
BY ___ DATE ___ TO EO ___
BY ___ DATE ___ TO EO ___

BLOWCOUNTS (Converted to SPT, if not SPT)

SP/SW/GW/GP	SM/GM	ML	SC/MH/OL/CH etc.
23	24	32	8
72	24	23	7
55×4	35		12
56	30		17
26	48		24
85	67		10
43	17 ←		17
75	20		47
55	15		6
77	50		6
55	6 ←		8
38	14 ←		17
76	6 ←		19
36	31		4
19	30		9
45	20		56
20	30		
33	75		
25	average 30 18 values		
59			
11 ←			
39			
49			
average (mid-40's) 26 values			

* Arrow shows 'SPT' values less than 18.

BY UKP DATE 1/31/84
CHECKED BY HSG 2/6/84
COPY TO EO ___

DAMES & MOORE

945.1 (3-72) PRINTED IN U.S.A.

FILE 2443-132-10 (5554)
SUBJECT River Bottom Sands - Liquefaction
SHEET ___ OF ___

REVISIONS
BY ____ DATE ____ TO EO ____
BY ____ DATE ____ TO EO ____

LIQUEFACTION POTENTIAL

A) Using Cyclic Triaxial Test Data:

Figure A-19A of Ref. 2.5-96 shows the test data for river bottom sands.

For a Magnitude 6 earthquake (SSE) ≡ 5 cycles of (0.65 × Peak Acc) uniform cycles, the average shear stress ratio induced by the earthquake to cause ±2.5 % axial strain is 0.55.
(Note: ±2.5 % is conservative compared to ±5.0 % normal – both single amplitude)

Assuming normally consolidated conditions, use $C_r = 0.57$ for converting this ratio to field conditions.

$$\therefore \left(\frac{\tau_{av}}{\sigma_0'}\right)_{field} = \left(\frac{\tau_{av}}{\sigma_0'}\right)_{\substack{lab\\ triaxial}} \times 0.57$$

$$= 0.55 \times 0.57 = \underline{0.31}$$

Therefore, Factor of Safety against Liquefaction $= \dfrac{(\tau/\sigma_0')\ \text{to liquefy}}{(\tau/\sigma_0')\ \text{seismic induced}}$

$$= \frac{0.31}{0.25}$$

$$= \underline{1.24}$$

The margin of safety will be higher than 1.24 in general since:

1) Failure criterion of ±2.5 % axial strain is very conservative for overall stability
2) Test data used is for the relatively less dense sands – samples corresponding to SPT 24 to 35.

BY UKP DATE 1/31/84
CHECKED BY HSG 3/2/84
COPY TO EO ____

DAMES & MOORE

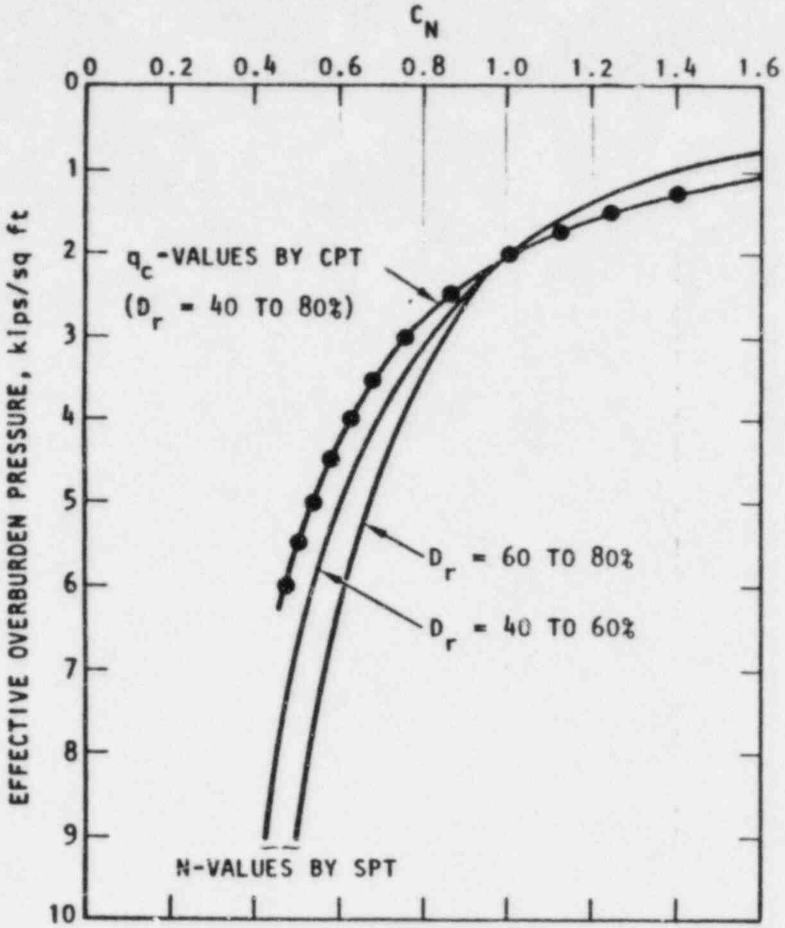

Chart for values of C_N.

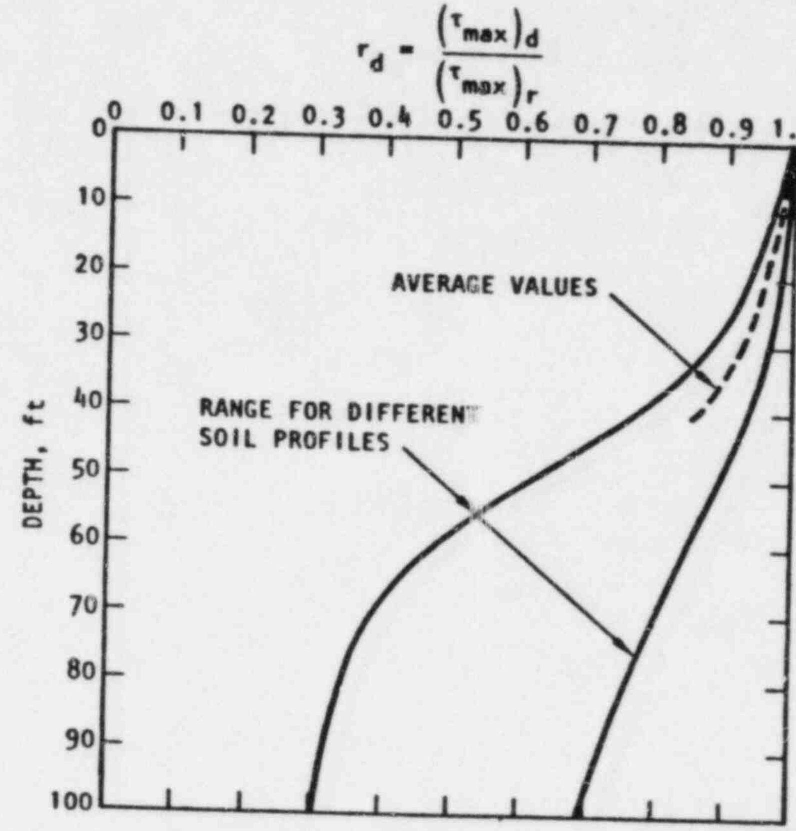

Range of values of r_d for different soil profiles.

FILE 2443-132-10 (5554)
SUBJECT River Bottom Sands - Liquefact
SHEET ___ OF ___

B) Using Seed & Idriss Curves for Cyclic Strength based on 'SPT' data:

Seed & Idriss Curve is attached
To backfigure required blowcount for a Factor of Safety against liquefaction = 1,
From the curve:
Modified penetration resistance, N_1 blows/ft
for $(\tau_{av}/\sigma_0') = 0.25$ (induced stress ratio)
= 18

Assuming $C_N \simeq 1.0$ (from the attached chart, it may vary between 1.0 & 1.1)
and no correction for amount of fines in sands (SPT can be increased by roughly 7.5 for silty sands and silts with $D_{50} < 0.15$. Although data along service water pipeline shows D_{50} is typically 0.25 mm, in many other places D_{50} is less).

This means an SPT of 18 represents a Factor of safety $\simeq 1.0$

The blowcount data on the next page shows that:

1) The sandy soils w/ little or no fines have only 1 blowcount lower than 18 (in 28 values). Average blowcount is in mid 40s, highs up to 85.
2) In silty sands/gravels, 4 values below 18 (out of 18) values. average 30. If correction for fines is made FS against liquefaction even in the 4 cases will be high.
3) Cohesive materials are not susceptible.

⇒ In general there is a fairly high margin of safety against liquefaction of R.B. sands

DAMES & MOORE

REVISIONS
BY ___ DATE ___ TO EO ___
BY ___ DATE ___ TO EO ___

BY UKP DATE 1/31/84
CHECKED BY HSG 2/6/84
COPY TO EO ___

945.1 (3-72) PRINTED IN U.S.A.

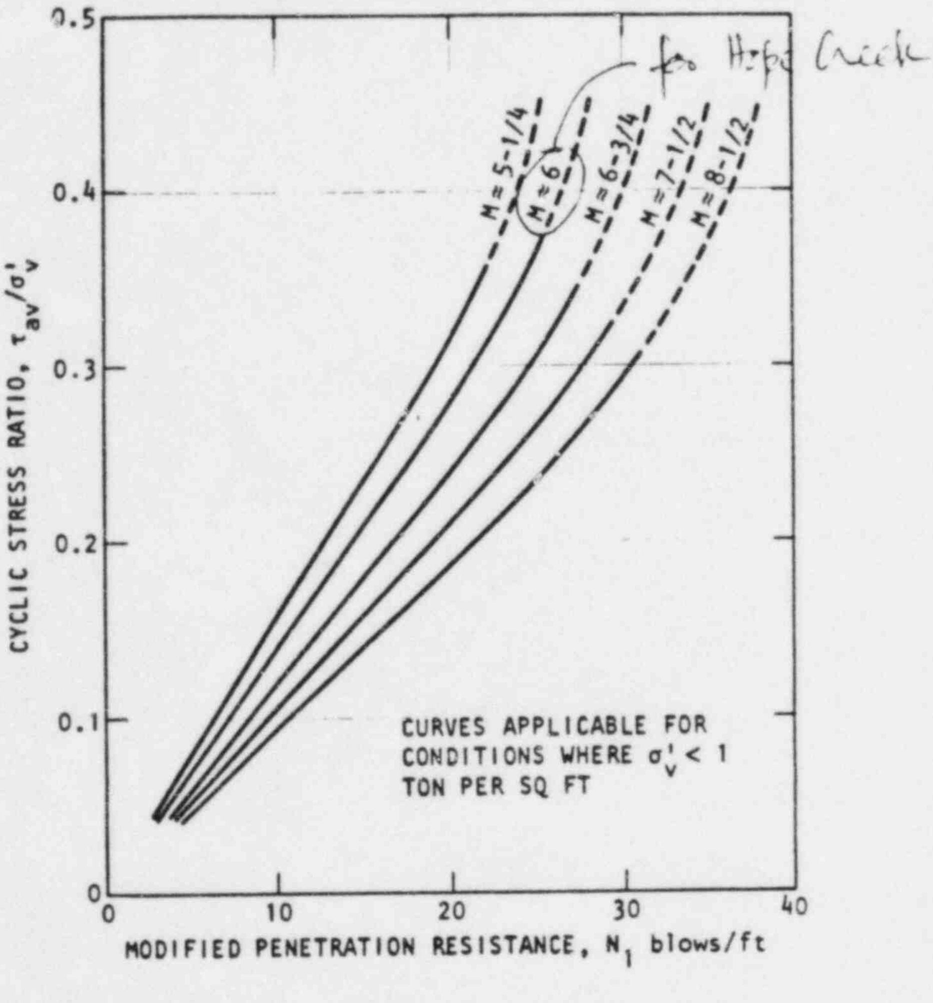

Chart for evaluation of liquefaction potential for sands f n different magnitude earthquakes.

Response to NRC Audit

Meeting Date: January 10, 1984

Question No.: A.16

QUESTION: Provide calculations of ductility ratios due to pipe break for key elements.

RESPONSE: FSAR Section 3.8.4.8.2 discusses the allowable ductility ratios used for the design of pipe whi restraints. For flexure in beams, an allowable ductility ratio of 20 is used.

As discussed with Mr. D. Jeng of the NRC Staff, the majority of the pipe whip restraints have ductility ratios less than or equal to 10. However, the ductility ratios for approximately 25% of the pipe whip restraints exceed 10 under the current design basis. These restraints will be reevaluated based on as-built conditions, final pipe break loads and actual hot gap requirements in an attempt to reduce the ductility ratios.

The restraints that remain with ductility ratios in excess of 10 will be identified to the NRC along with a discussion of the consequences. This information will be furnished in June 1984.

Response to NRC Audit

Meeting Date: January 10, 1984

Question No: B-5

Question: Provide example calculation for combination of NS, EW, and vertical responses.

Response: As defined by the Regulatory Guide, the spectral accelerations for three earthquake components were summed at each frequency point using an SRSS-type procedure. As demonstrated by Figures B-216 through B-224, the out-of-plane components do not contribute significantly to the in-plane spectra, and were clearly not required for the development of the floor response spectra.

Similarly, the out-of-plane displacements, accelerations, shears, and moments were found to have no significance to the in-plane response maxima values for the Reactor Building (Tables E-7 and E-8). The element numbers in Tables E-7 and E-8 are referenced in the Reactor Building mathematical model provided on Page 12.

It was found that the rocking motion contributes significantly at certain perimeter locations to the vertical response, and therefore it was incorporated in the vertical response envelopes using the SRSS approach. Sample vertical response spectra with and without the rocking contribution to the vertical response at a given floor of the Reactor Building are provided on pages 13 and 14, respectively. The calculations describing how vertical response spectra with rocking contributions are determined are summarized on pages 15 through 20.

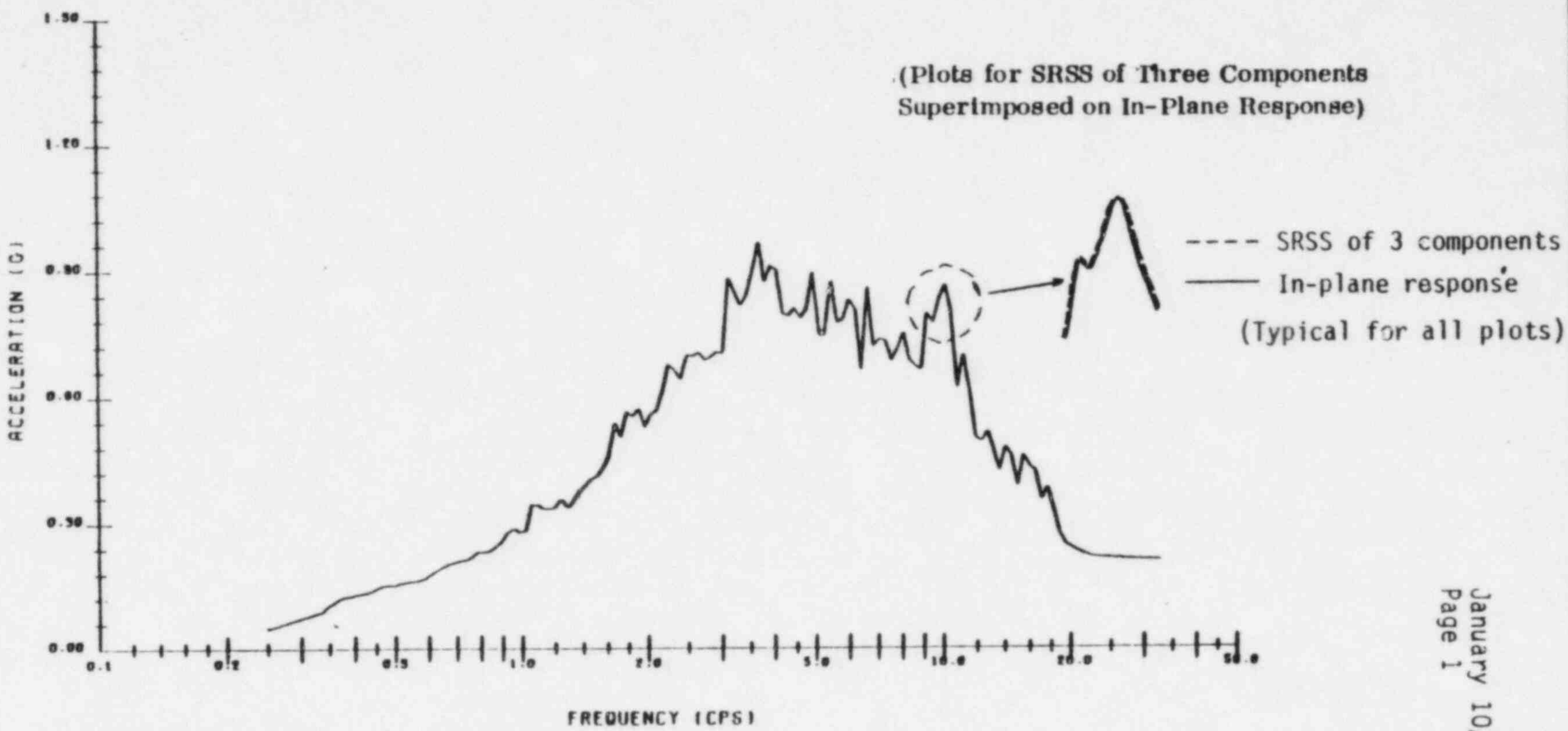

OUT-OF-PLANE RESPONSE STUDY
REACTOR BUILDING, ELEVATION 77.0
VERTICAL RESPONSE

FIGURE B-216

January 10/B-5
Page 1

PUBLIC SERVICE ELECTRIC & GAS CO.	SEISMIC STRUCTURAL ANALYSES
HOPE CREEK PROJECT	

SED-76-017 REVISION 2

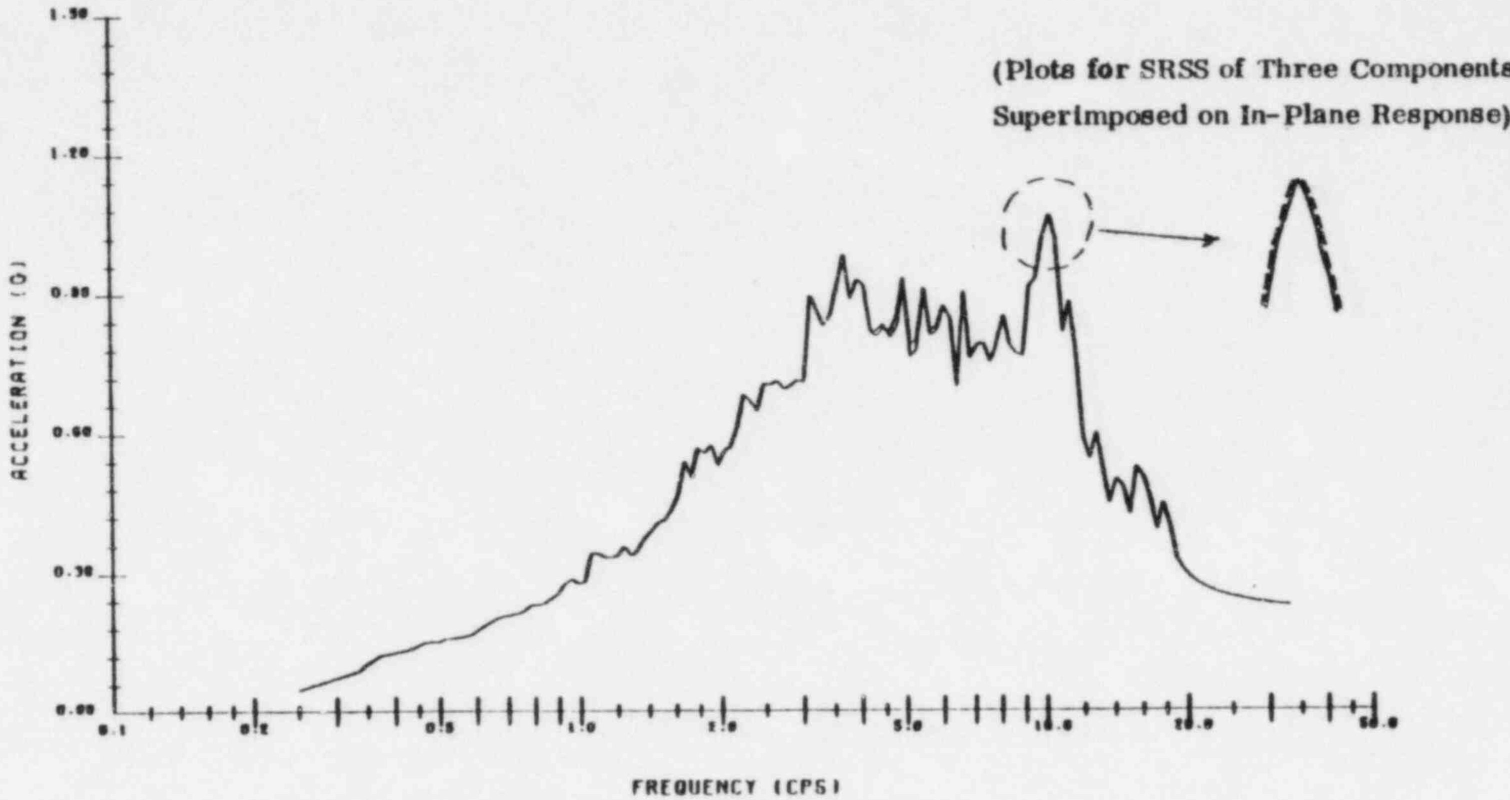

OUT-OF-PLANE RESPONSE STUDY
REACTOR BUILDING, ELEVATION 102.0
VERTICAL RESPONSE

FIGURE B-217

January 10/B-5
Page 2

PUBLIC SERVICE ELECTRIC & GAS CO.

HOPE CREEK PROJECT

SEISMIC STRUCTURAL ANALYSES

SED-76-017 REVISION 2

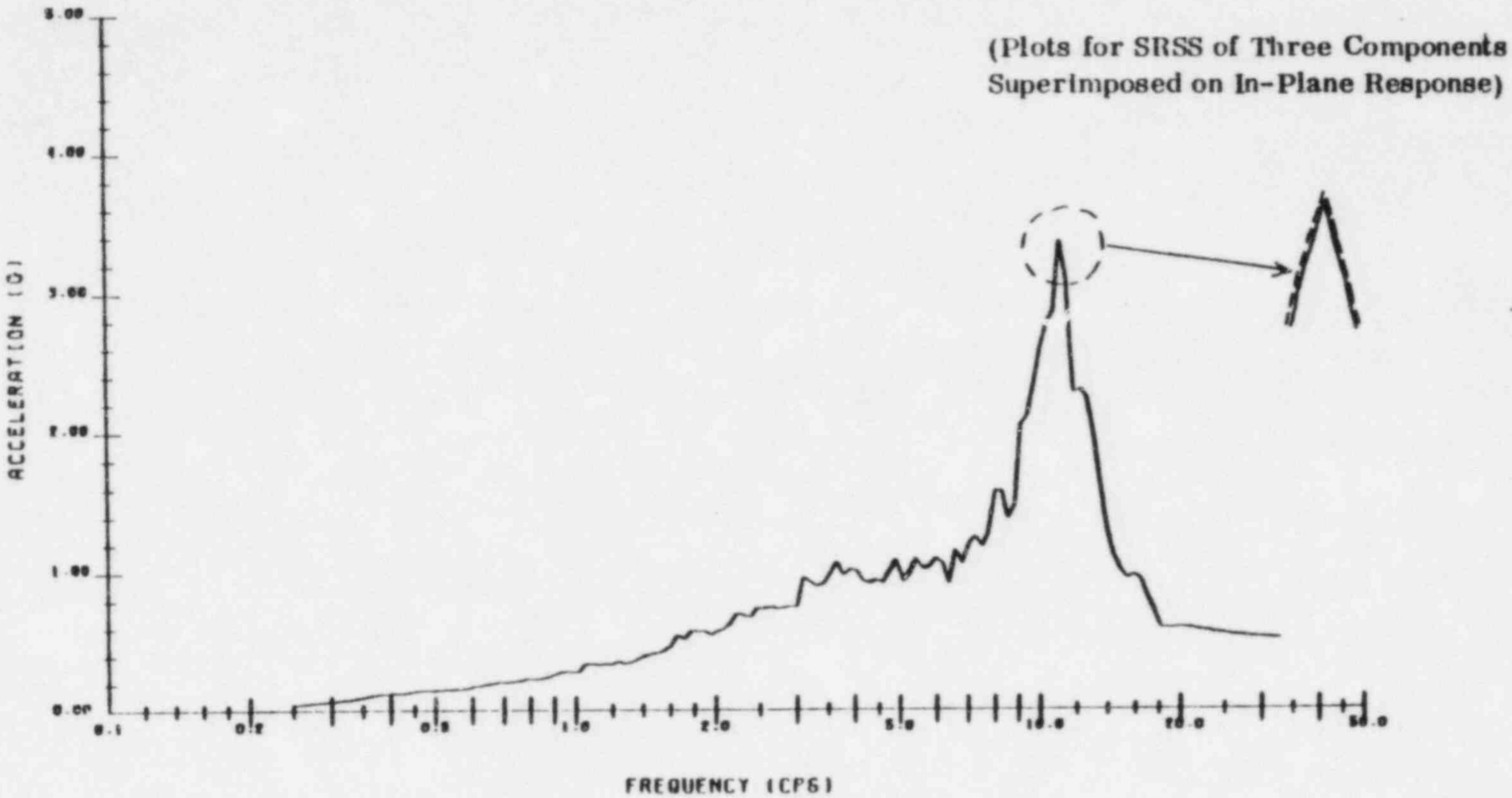

OUT-OF-PLANE RESPONSE STUDY
REACTOR BUILDING, ELEVATION 201.0
VERTICAL RESPONSE

FIGURE B-218

PUBLIC SERVICE ELECTRIC & GAS CO.	SEISMIC STRUCTURAL ANALYSES
HOPE CREEK PROJECT	

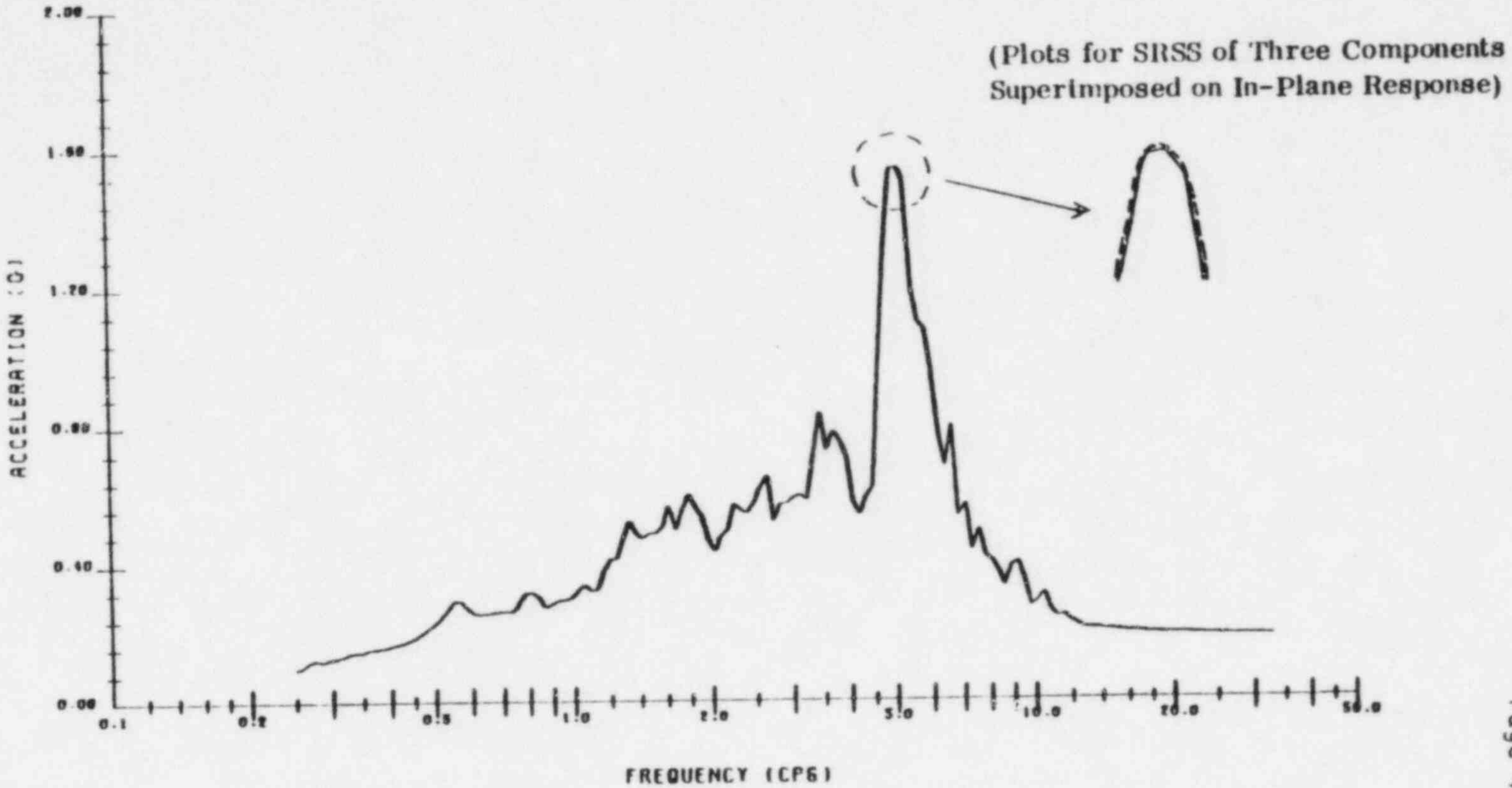

OUT-OF-PLANE RESPONSE STUDY
REACTOR BUILDING, ELEVATION 77.0
N-S RESPONSE

FIGURE B-219

PUBLIC SERVICE ELECTRIC & GAS CO.

HOPE CREEK PROJECT

SEISMIC STRUCTURAL ANALYSES

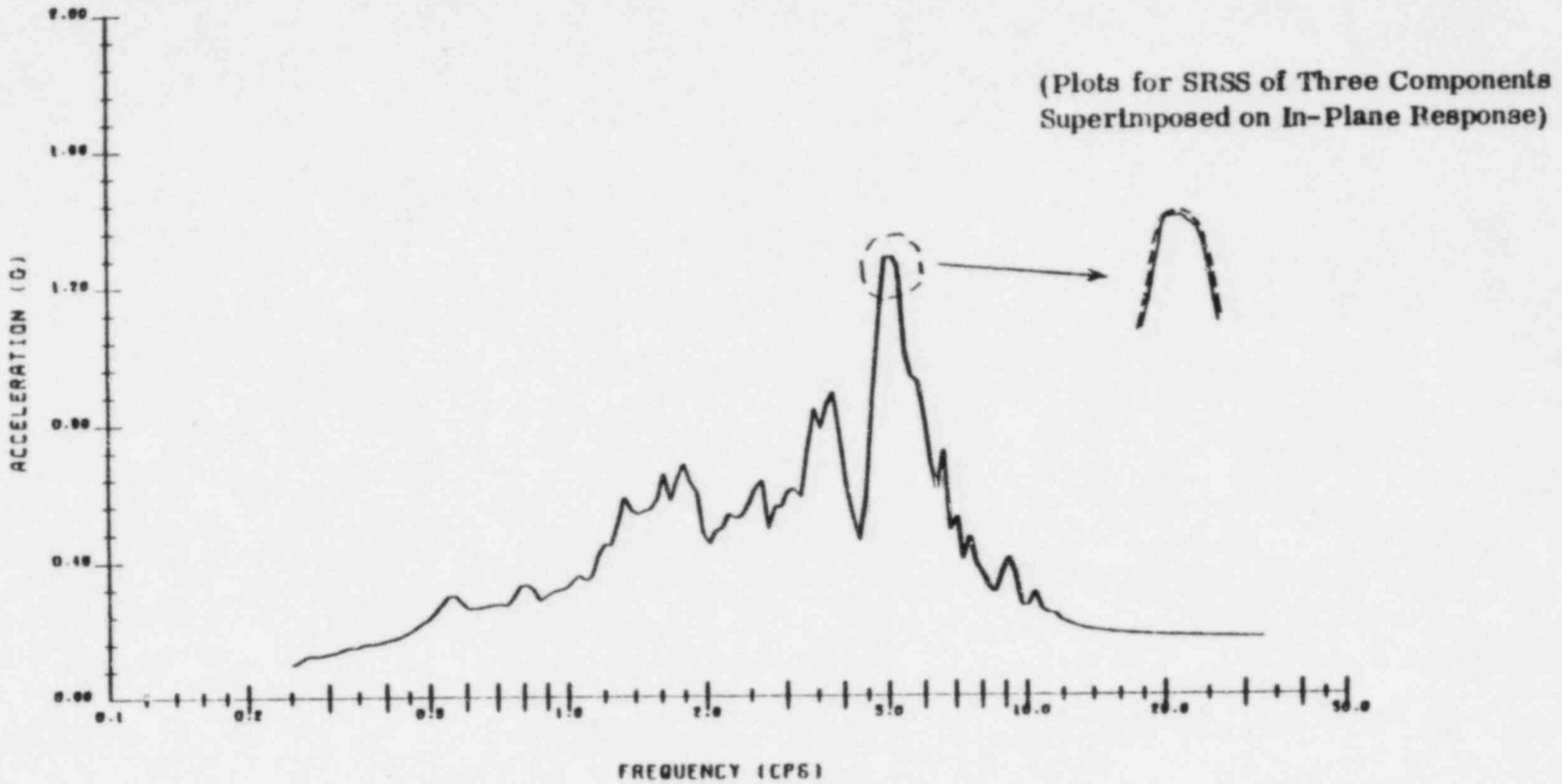

OUT-OF-PLANE RESPONSE STUDY
REACTOR BUILDING, ELEVATION 102.0
N-S RESPONSE

FIGURE B-220

PUBLIC SERVICE ELECTRIC & GAS CO.	SEISMIC STRUCTURAL ANALYSES
HOPE CREEK PROJECT	

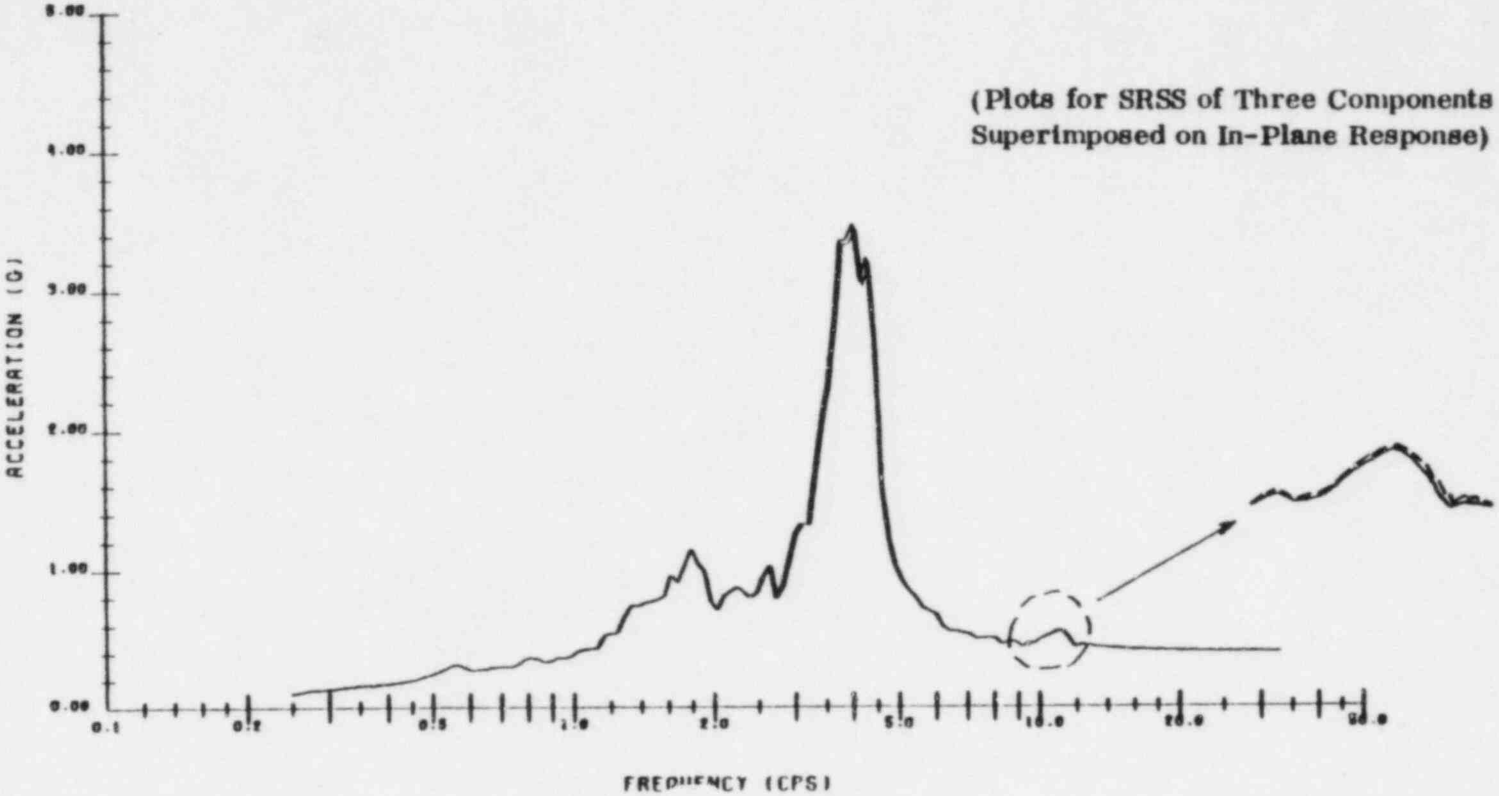

OUT-OF-PLANE RESPONSE STUDY
REACTOR BUILDING, ELEVATION 201.0
N-S RESPONSE

FIGURE B-221

PUBLIC SERVICE ELECTRIC & GAS CO.	SEISMIC STRUCTURAL ANALYSES
HOPE CREEK PROJECT	

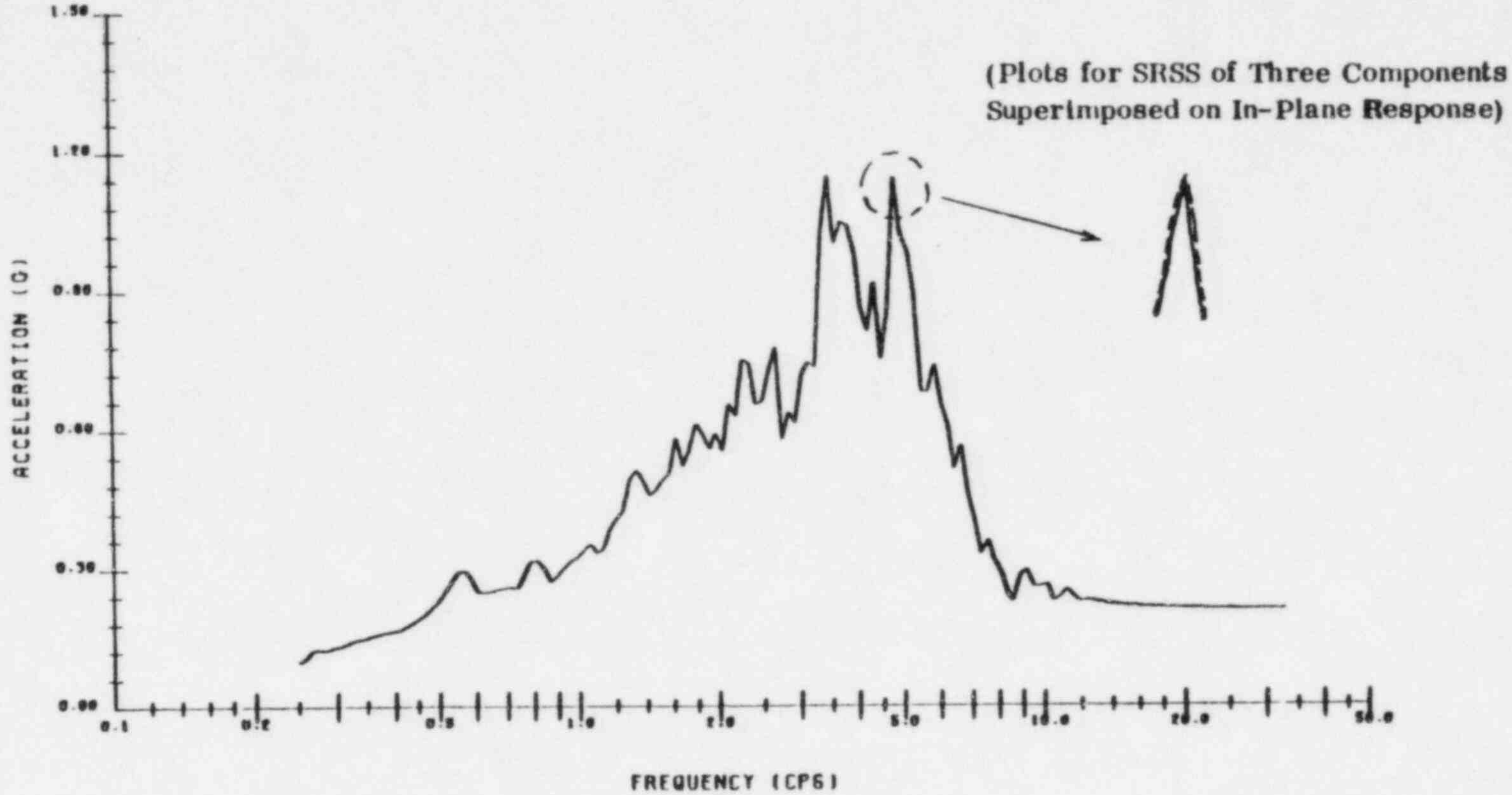

OUT-OF-PLANE RESPONSE STUDY
REACTOR BUILDING, ELEVATION 77.0
E-W RESPONSE
FIGURE B-222

PUBLIC SERVICE ELECTRIC & GAS CO.

HOPE CREEK PROJECT

SEISMIC STRUCTURAL ANALYSES

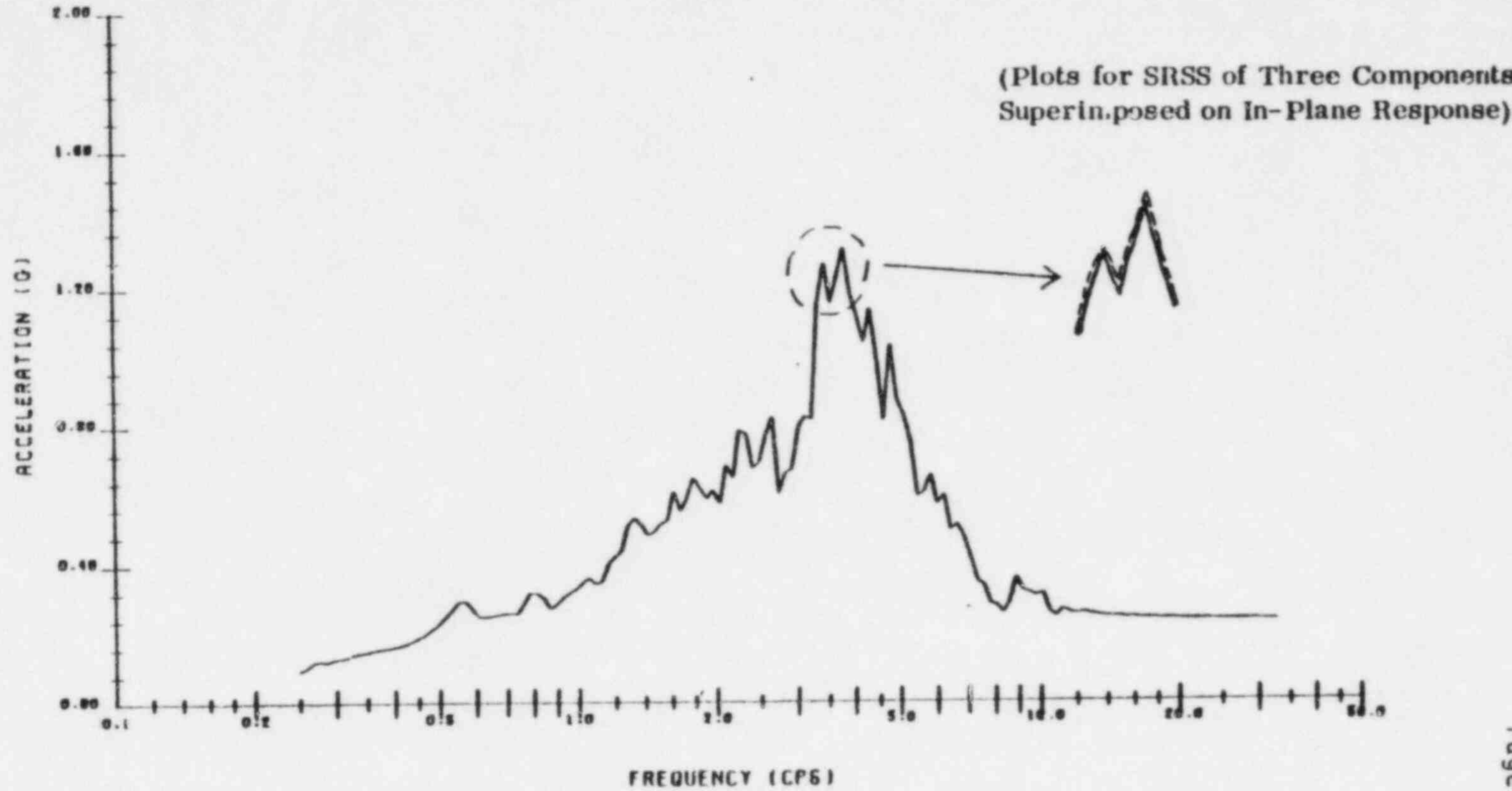

OUT-OF-PLANE RESPONSE STUDY
REACTOR BUILDING, ELEVATION 102.0
E-W RESPONSE
FIGURE B-223

PUBLIC SERVICE ELECTRIC & GAS CO.	SEISMIC STRUCTURAL ANALYSES
HOPE CREEK PROJECT	

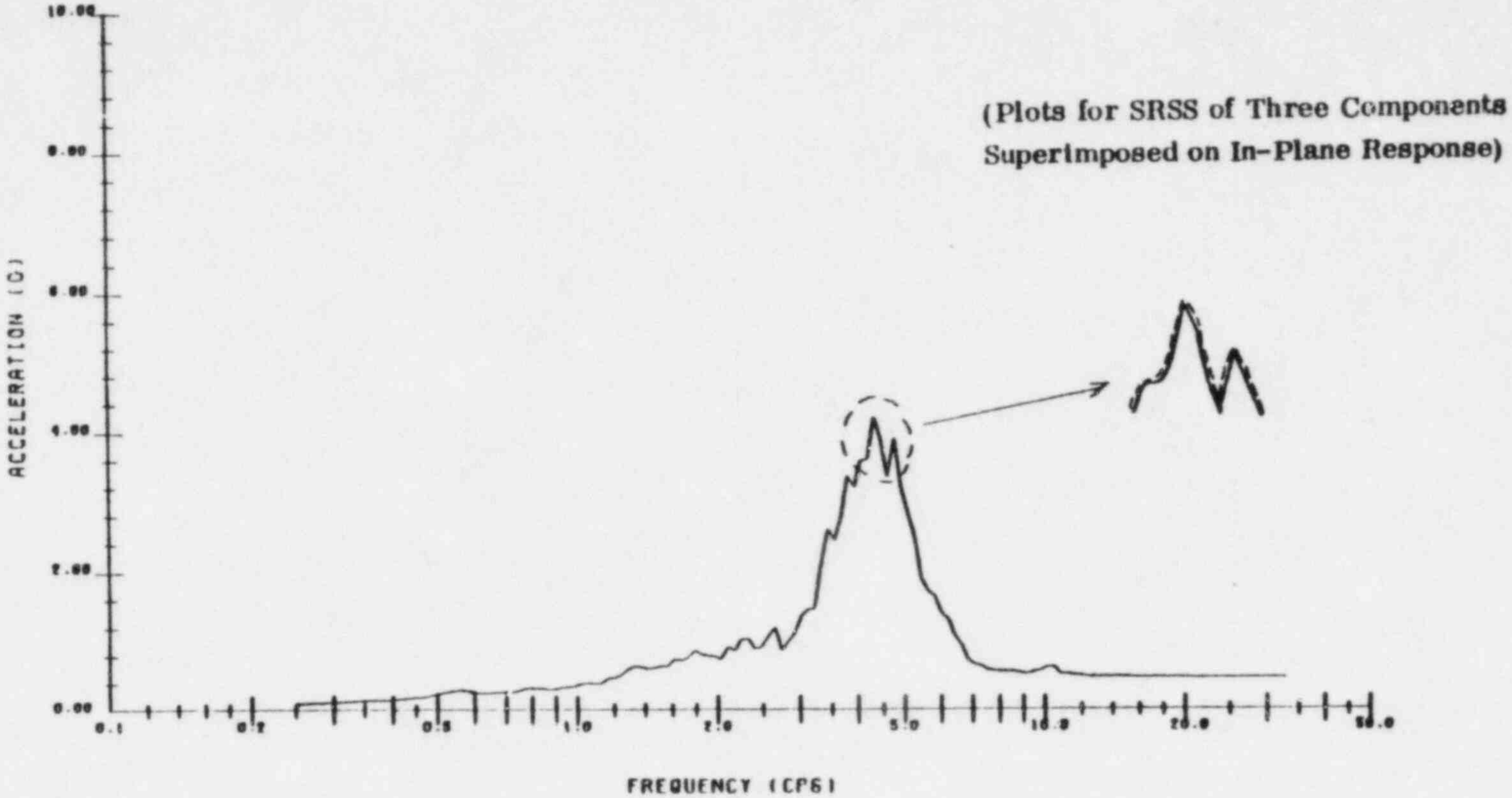

OUT-OF-PLANE RESPONSE STUDY
REACTOR BUILDING, ELEVATION 201.0
E-W RESPONSE

FIGURE B-224

PUBLIC SERVICE ELECTRIC & GAS CO.

HOPE CREEK PROJECT

SEISMIC STRUCTURAL ANALYSES

TABLE E-7

REACTOR BUILDING OUT-OF-PLANE RESPONSE OPERATING BASIS EARTHQUAKE					January 10/B-5 Page 10
		E-W Response			
Element Number	Variable	E-W Base Motion (A)	N-S Base Motion (B)	SRSS (C)	Ratio (C)/(A)
1	Shear Moment	6.049×10^2 5.673×10^2	1.604×10^1 1.571×10^2	6.05×10^2 5.889×10^2	1.00 1.04
7	Shear Moment	----- 5.791×10^5	2.178×10^2 1.391×10^4	---- 5.793×10^5	---- 1.00
11	Shear Moment	9.271×10^3 9.109×10^5	6.722×10^2 1.798×10^5	9.295×10^3 9.285×10^5	1.00 1.02
15	Shear Moment	2.437×10^4 3.842×10^5	6.431×10^2 1.235×10^4	2.438×10^4 3.844×10^3	1.00 1.00
19	Shear Moment	3.187×10^4 8.143×10^5	7.589×10^2 3.060×10^5	3.188×10^4 8.699×10^5	1.00 1.07
21	Shear Moment	---- 2.628×10^6	8.172×10^2 1.406×10^5	---- 2.632×10^6	---- 1.00
33	Shear Moment	7.598×10^2 1.051×10^3	3.297×10^1 9.159×10^2	7.605×10^2 1.394×10^3	1.00(2) 1.33
35	Shear Moment	1.679×10^3 1.816×10^4	5.966×10^1 1.601×10^3	1.680×10^3 1.823×10^4	1.00 1.00
37	Shear Moment	2.920×10^3 7.680×10^4	8.827×10^1 1.183×10^4	2.921×10^3 7.771×10^4	1.00 1.01
39	Shear Moment	7.333×10^3 1.487×10^5	1.910×10^2 8.248×10^3	7.335×10^3 1.489×10^5	1.00 1.00
42	Shear Moment	4.065×10^3 2.373×10^4	1.018×10^2 3.039×10^3	4.066×10^3 2.392×10^4	1.00 1.01
44	Shear Moment	---- 1.045×10^5	1.129×10^2 5.758×10^3	---- 1.047×10^5	---- 1.00

Note: 1. Units: Kip, Ft.

2. This is considered insignificant because the moment for this beam is very small.

PUBLIC SERVICE ELECTRIC & GAS CO.	SEISMIC STRUCTURAL ANALYSES
HOPE CREEK PROJECT	

TABLE E-8

REACTOR BUILDING
OUT-OF-PLANE RESPONSE
SAFE SHUTDOWN EARTHQUAKE

January 10/B-5
Page 11

Element Number	Variable	E-W Response: E-W Base Motion (A)	E-W Response: N-S Base Motion (B)	SRSS (C)	Ratio (C)/(A)
1	Shear Moment	8.829×10^2 7.835×10^2	1.164×10^1 1.186×10^2	8.830×10^2 7.924×10^2	1.00 1.01
7	Shear Moment	---- 8.504×10^5	2.203×10^2 1.267×10^4	---- 8.505×10^5	---- 1.00
11	Shear Moment	1.698×10^4 1.430×10^6	4.092×10^2 2.653×10^5	1.698×10^4 1.454×10^6	1.00 1.02
15	Shear Moment	4.918×10^4 5.688×10^5	5.880×10^2 1.138×10^4	4.918×10^4 5.689×10^5	1.00 1.00
19	Shear Moment	6.499×10^4 1.477×10^6	6.400×10^2 4.853×10^5	6.499×10^4 1.555×10^6	1.00 1.05
21	Shear Moment	----- 5.337×10^6	6.283×10^2 1.837×10^5	---- 5.340×10^6	---- 1.00
33	Shear Moment	1.601×10^3 1.524×10^3	5.216×10^1 2.022×10^3	1.602×10^3 2.532×10^3	1.00 (2) 1.66
35	Shear Moment	3.491×10^3 3.649×10^4	8.271×10^1 4.509×10^3	3.492×10^3 3.677×10^4	1.00 1.01
37	Shear Moment	5.981×10^3 1.099×10^5	1.188×10^2 9.354×10^3	5.982×10^3 1.103×10^5	1.00 1.00
39	Shear Moment	1.482×10^4 2.070×10^5	1.707×10^2 1.200×10^4	1.482×10^4 2.073×10^5	1.00 1.00
42	Shear Moment	8.162×10^3 4.795×10^4	1.084×10^2 6.000×10^3	8.163×10^3 4.832×10^4	1.00 1.01
44	Shear Moment	---- 2.138×10^5	1.284×10^2 6.323×10^3	---- 2.139×10^5	---- 1.00

Note: 1. Units: Kip, Ft.
2. This is considered insignificant because the moment for this beam is very small.

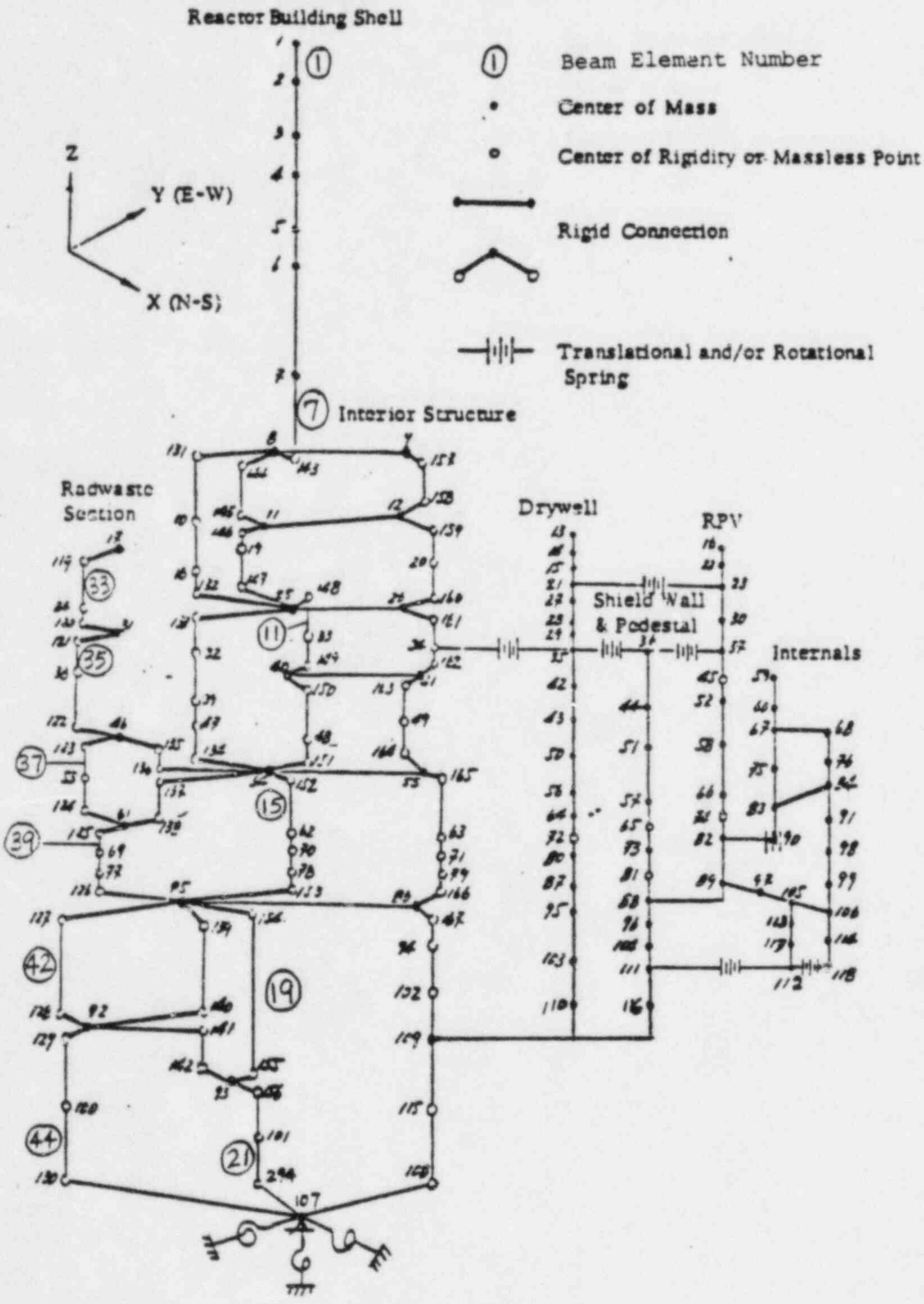

REACTOR BUILDING MATHEMATICAL MODEL

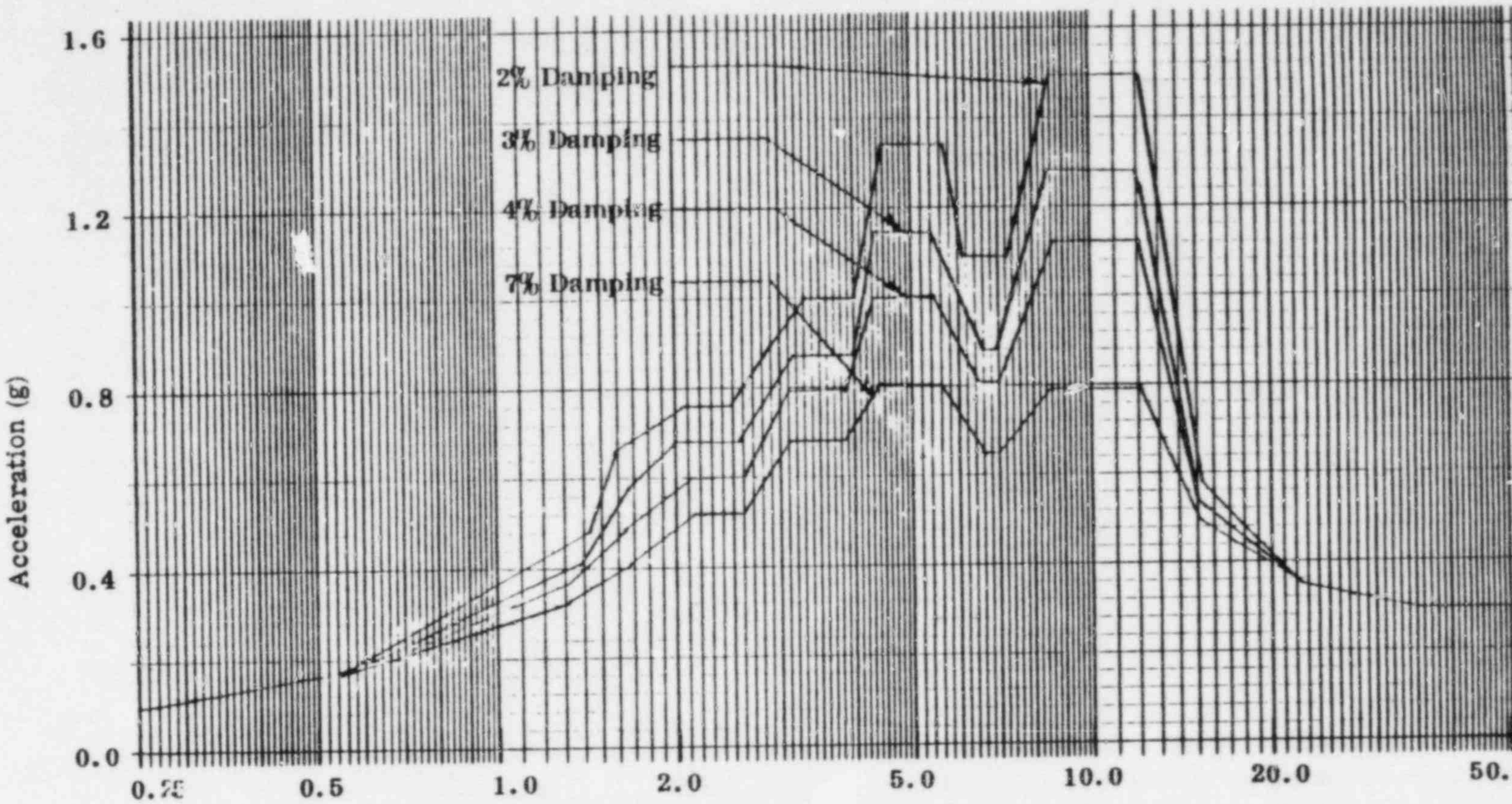

REQUIRED RESPONSE SPECTRA (WITH ROCKING CONTRIBUTION)
VERTICAL SAFE SHUTDOWN EARTHQUAKE
REACTOR BUILDING
FLOOR ELEVATION 145'-0"

FIGURE F-27

HOPE CREEK UNITS 1 & 2
1400012-329Z, Revision 1
4/3/79

PUBLIC SERVICE ELECTRIC & GAS CO.	SEISMIC STRUCTURAL ANALYSES
HOPE CREEK PROJECT	

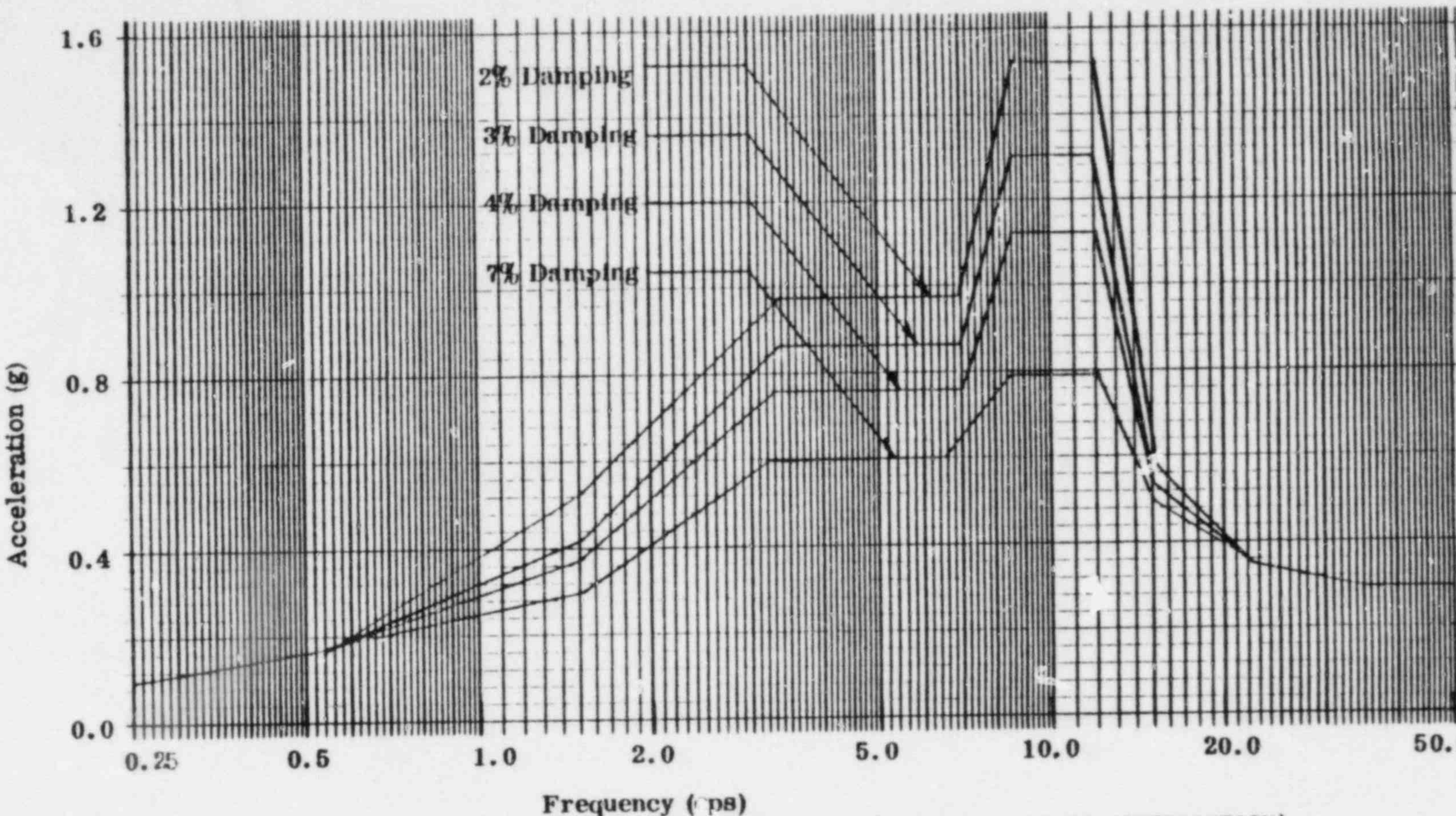

REQUIRED RESPONSE SPECTRA (WITHOUT ROCKING CONTRIBUTION)
VERTICAL SAFE SHUTDOWN EARTHQUAKE
REACTOR BUILDING
FLOOR ELEVATION 145'-0"

PURPOSE:

THE PURPOSE OF THE ANALYSIS IS TO EVALUATE THE VERTICAL COMPONENT OF ACCELERATION AT THE PERIPHERAL WALLS OF THE REACTOR BUILDING AND AUXILIARY BUILDING, DUE TO A ROCKING BASE MOTION.

PROCEDURE:

SINCE THE VERTICAL ACCELERATION DUE TO ROCKING IS SIMPLY A CONSTANT MULTIPLIER OF THE ROCKING MOTION, COMPUTATION OF THE VERTICAL SPECTRA WILL BE PERFORMED BY SIMPLY MANIPULATING THE BASE ROCKING SPECTRA.

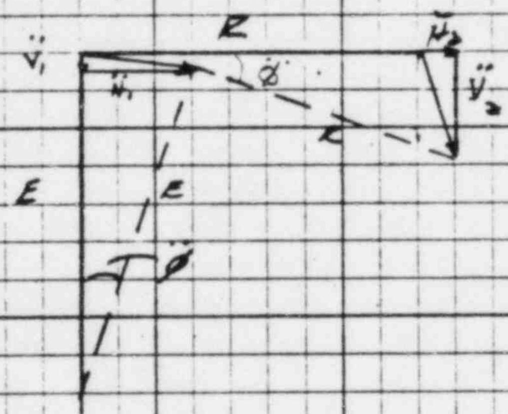

$\ddot{H}_1 = E \sin\ddot{\phi} = E\ddot{\phi}$ (SMALL ANGLE ASSUMPTION)

$\ddot{V}_1 = E(1-\cos\ddot{\phi}) \approx 0$ (" " ")

$\ddot{V}_2 \approx R\sin\ddot{\phi} = R\ddot{\phi}$ " " "

ITEM VERTICAL RESPONSE DUE TO ROCKING MOTION	CLIENT PSE&G PROJECT HOPE CREEK
	JOB NO. 0140-012
BY JBM DATE 3/20/79 CKD. JMC DATE 3/23/79	ITEM NO. 001ECK SHT 1 OF

THEREFORE THE PROCEDURE WILL BE TO MULTI-
PLY THE BASE ROCKING RESPONSE SPECTRA
BY THE DISTANCE FROM THE POINT OF INPUT
ROTATION TO THE PERIPHERAL WALL. ✓

TO ACCOUNT FOR THE RESPONSE AT WALL
CORNERS, AN SRSS OF THE RESPONSE
DUE TO ORTHOGONAL ROTATIONAL MOTIONS
WILL BE USED. THE FINAL RESULTANT
VERTICAL MOTION WILL BE COMBINED WITH
THE VERTICAL DUE TO VERTICAL BY SRSS. ✓

COMPUTE VERTICAL RESPONSE AT INSIDE FACE
OF WALLS

- ASSUME ROCKING MOTION WILL PIVOT ABOUT THE
CENTER OF THE REACTOR BUILDING BASE
MAT ✓

- CENTER OF COORDINATE SYTEM IS AT ℄
OF RPV. x = N-S
y = E-W
z = VERTICAL

ITEM VERTICAL RESPONSE	CLIENT PSE&G
	PROJECT HOPE CREEK
	JOB NO. 0140-012
BY JDM DATE 3/23/79 CKD. [illegible] DATE 3/23/79	ITEM NO. 001ECK SHT. 2 OF

REACTOR BUILDING

ELEV.	N-S PNT OF ROT (FT)	E-W PNT OF ROT (FT)	N-S COOR OF FDTN WALL (FT)	E-W COOR OF RX WALL (FT)	N (FT)	E (FT)
54.0	0.0	27.0	-94.5	-126.0	94.5	153.0
77.0	↓	↓	-94.5	-126.0	94.5	153.0
102.0	↓	↓	-94.5	-126.0	94.5	153.0
132.0	↓	↓	-94.5	-126.0	94.5	153.0
145.0	↓	↓	82.5	-82.5	82.5	109.5
162.0	↓	↓	82.5	-82.5	82.5	109.5
201.08	↓	↓	82.5	-82.5	82.5	109.5
250.0	↓	↓	82.5	-82.5	82.5	109.5

RADWASTE BUILDING

ELEV.	N-S PNT OF ROT (FT)	E-W PNT OF ROT (FT)	N-S COOR OF FDTN WALL (FT)	E-W COOR OF RX WALL (FT)	N (FT)	E (FT)
54.0	0.0	27.0	-94.5	180.0	94.5	153.0
87.0	↓	↓	-94.5	180.0	94.5	153.0
102.0	↓	↓	-94.5	180.0	94.5	153.0
124.0	↓	↓	-94.5	180.0	94.5	153.0
137.0	↓	↓	92.5	180.0	92.5	153.0
153.0	↓	↓	93.0	181.0	93.0	154.0
171.0	↓	↓	93.0	181.0	93.0	154.0

ITEM: VERTICAL RESPONSE
CLIENT: PSE&G
PROJECT: HOPE CREEK
JOB NO.: 0140-012
BY: JDM DATE: 3/23/79 CKD.: [illegible] DATE: 3/26/79
ITEM NO.: 001ECA SHT. 3 OF

PROCEDURE FOR COMBINING RESPONSE:

1) COMPUTE INDIVIDUAL RESPONSE SPECTRA ✓

(3) ~~2)~~ BROADEN INDIVIDUAL SPECTRA USING ENVEL

(2) ~~3)~~ COMBINE BY SRSS WITH VERTICAL RESPONSE SPECTRA.

Procedure: do 1 (compute R.S)
do 2 (SRSS)
do 3 (broaden)

✓ NOTED JDM 4/17/79

ITEM VERTICAL RESPONSE	CLIENT PG&E
	PROJECT HOPE CREEK
	JOB NO. 0140-012
BY JDM DATE 3/23/79 CKD. JMC DATE 4/17/79	ITEM NO. 001RCK SHT. 4 OF

- ASSUME AUXILIARY BUILDING ROTATES ABOUT CENTER OF BASE MAT.

$\Rightarrow$ N-S = 0.0

E-W = $\frac{312.0}{2}$ = 156.0 − 143.0 = 13.0

REF: BECHTEL DRAWING SK-C-637 REV A

- CENTER OF COORDINATE SYSTEM = INTERSECTION OF R LINE AND LINE 29

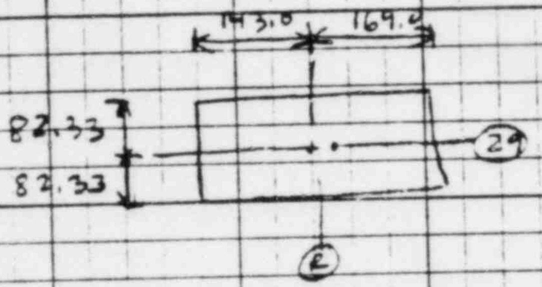

ITEM: VERTICAL RESPONSE	CLIENT: PSE&G
	PROJECT: HOPE CREEK
	JOB NO. 0140-012
BY: [illegible] DATE: 3/26/79 CKD.: JMC DATE: 3/28/79	ITEM NO. 001ECK SHT. 5 OF

Auxiliary Building Control Area

ELEV. (FT)	N-S Dist. of Rot (FT)	E-W Dist. of Rot (FT)	N-S Coor of Extr Wall (FT)	E-W Coor of Extr Wall (FT)	N (FT)	E (FT)
54.0	0.0	13.0	82.3	166.0	82.3	153.0
77.0			82.3	166.0	82.3	153.0
87.0			82.3	166.0	82.3	153.0
102.0			82.3	166.0	82.3	153.0
117.0			82.3	95.5	82.3	82.5
124.0			82.3	166.0	82.3	153.0
137.0			82.3	166.0	82.3	153.0
155.25			82.3	166.0	82.3	153.0
172.0			82.3	166.0	82.3	153.0

Auxiliary Building Diesel Area

ELEV. (FT)	N-S Dist. of Rot (FT)	E-W Dist. of Rot (FT)	N-S Coor of Extr Wall (FT)	E-W Coor of Extr Wall (FT)	N (FT)	E (FT)
54.0	0.0	13.0	82.3	-140.0	82.3	153.0
77.0			82.3	-140.0	82.3	153.0
102.0			82.3	-140.0	82.3	153.0
130.0			82.3	140.0	82.3	153.0
146.0			82.3	-140.0	82.3	153.0
150.0			82.3	-140.0	82.3	153.0
160.0			63.0	-140.0	63.0	153.0
177.0			63.0	-140.0	63.0	153.0

ITEM: Vertical Response
CLIENT: PSE&G
PROJECT: Hope Creek
JOB NO. 0140-012
BY: JDM DATE: 3/22/79 CKD.: [illegible] DATE: 3/28/79 ITEM NO. 801 RCK SHT. 6 OF

EDS NUCLEAR: 220 MONTGOMERY ST. • SAN FRANCISCO, CALIFORNIA 94104

Response to NRC Audit

Meeting Date: January 10, 1984

Question No.: B-10

Question: Provide calculations to show that rotational time history input $\phi(t)$ to detailed structural model is same as rotational time history R(t) from SSI model.

Response: Page 1 of the attachment shows the finite element representation of the model used for SSI analyses in the N-S direction. Node 1202 of this model corresponds to the rotational node at the base-mat elevation of the reactor building. Page 2 shows the maximum value of the rotational acceleration time history output for node 1202. Page 3 of the attachment shows the detailed model of the reactor building. The rotational response at node 107 (node at base-mat elevation) is shown on page 4 of the attachment. Comparison of the maximum value, and time at which it occurs, of the rotational time history response between nodes 1202 of SSI model and 107 of detailed structural model, shows that the response from the SSI model is the same as input to the detailed building model.

Page 5 of the attachment shows the reactor building floor plan at elevation 54-0". It shows the number of walls at this elevation (including the containment) which act as stiffeners to the base-mat. (These walls extend all the way from this elevation to the floor slab at the next higher elevation.) This justifies the assumption of using a rigid building base-mat in the analyses.

The base-mat is a 14' thick layer of concrete with shear modulus of approximately 2 orders of magnitude higher than the underlaying soil (2.35×10^5 ksf for concrete vs. 2×10^3 ksf for soil). Therefore locally in the region of mat/soil interface, the base-mat exhibits much higher stiffness than the soil.

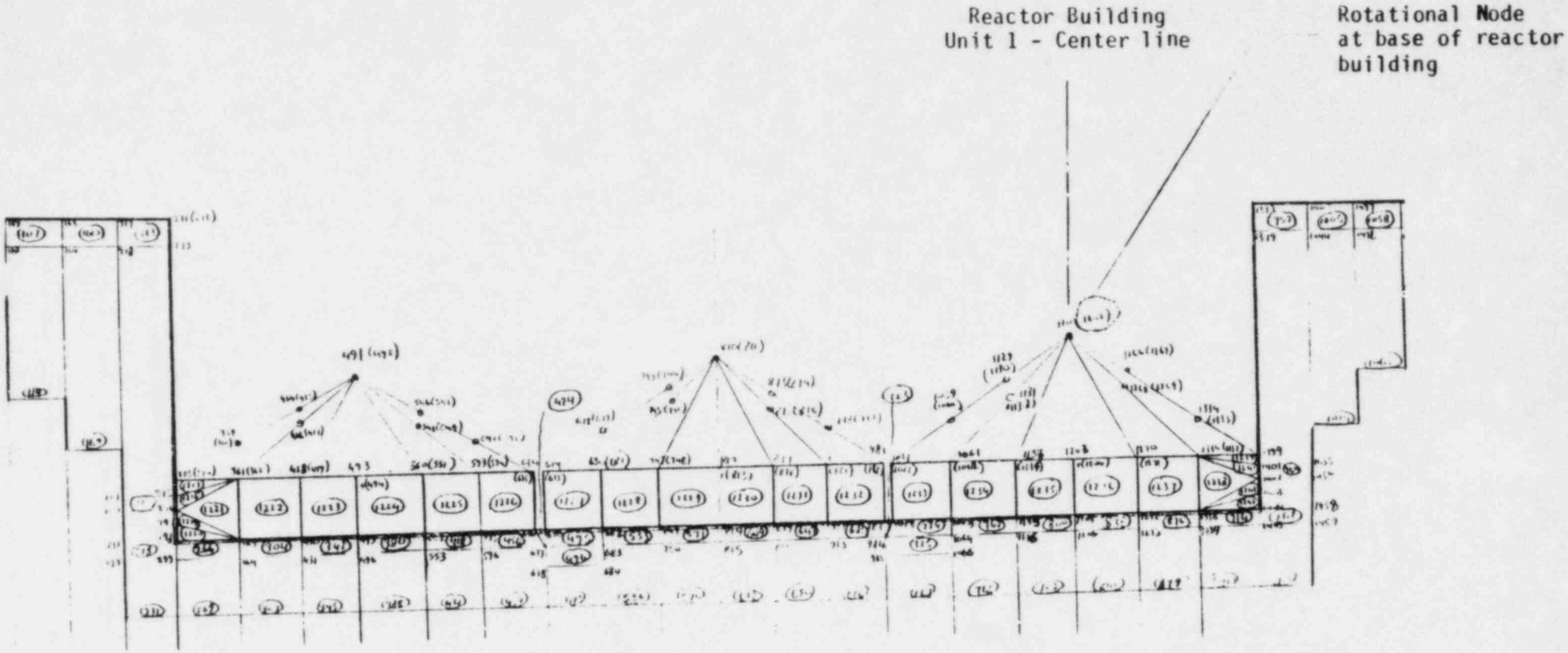

Portion of the SSI Model Representing
the Base-Mat Area

ATTACHMENT TO RESPONSE B-10

MAXIMUM ABSOLUTE ACCELERATIONS(G)

ITERATION NO. 2 MAX. BASE ACC. = 0.4590 (G) IN HORZ. DIRECTION
MAX. BASE ACC. = 0.0000 (G) IN VERT. DIRECTION

N.P.	XORD	YORD	X-ACC	AT TIME	Y-ACC	AT TIME
1201	177.90	54.00	0.2226	10.2300	0.0275	10.4100
1202	177.90	54.00	0.0434	10.3400	* ROTATIONAL NODE *	
965	177.90	252.90	0.5603	10.3200	0.0415	10.4150
810	0.00	54.00	0.2142	10.2250	0.0248	10.4350
811	0.00	54.00	0.0828	10.4550	* ROTATIONAL NODE *	
721	0.00	198.00	0.5647	10.4500	0.0370	10.4430
491	-177.90	54.00	0.2523	10.2600	0.0160	10.3900
492	-177.90	54.00	0.0146	10.3450	* ROTATIONAL NODE *	

X-ACC VALUES FOR ROTATIONAL NODES ARE ROTATIONAL ACCEL. IN RAD/SEC/SEC

TIME REQUIRED FOR COMPUTATION AND OUTPUT OF 13 MOTION(S) = 14.246 SEC

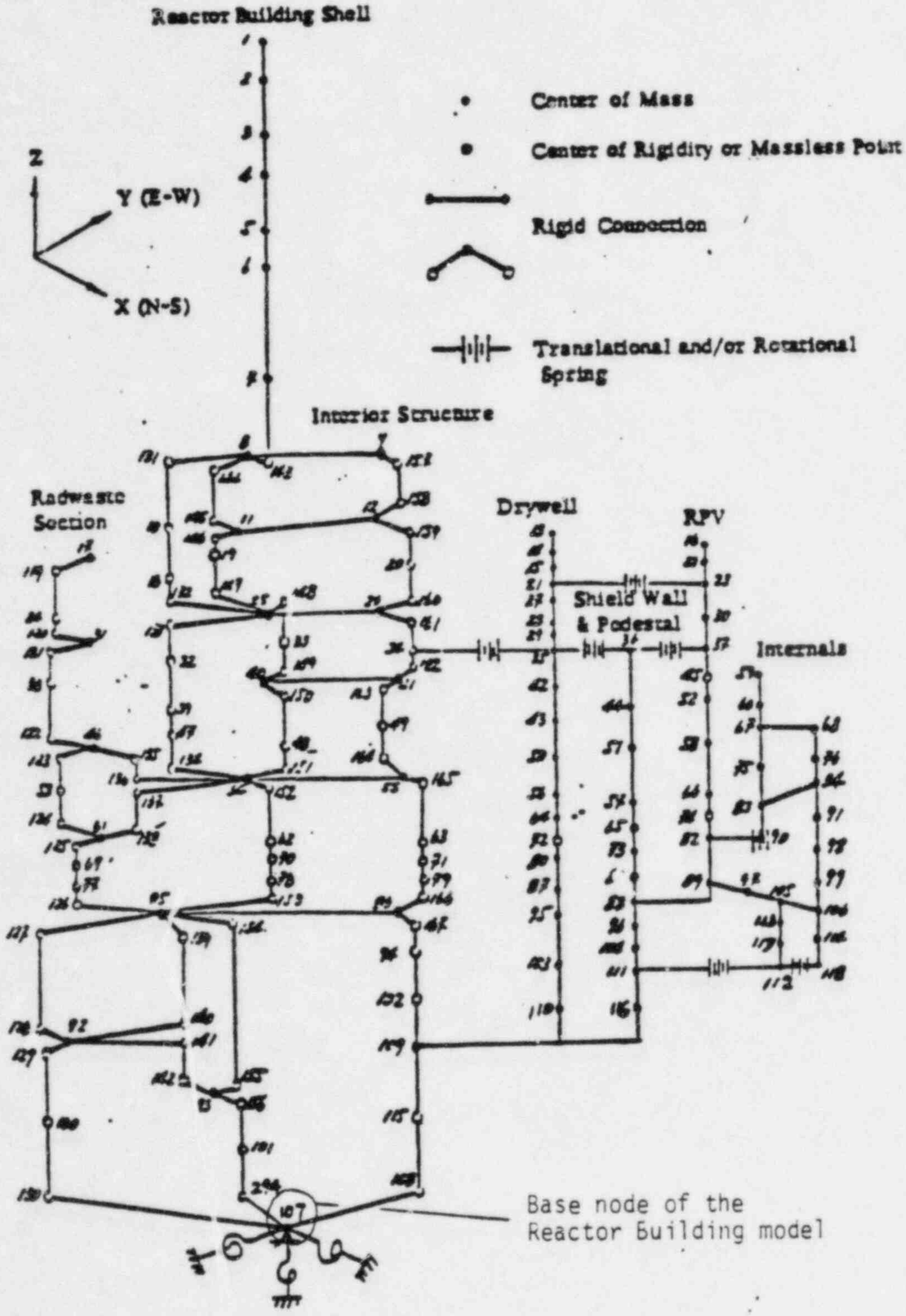

REACTOR BUILDING MATHEMATICAL MODEL

OUTPUT TO TAPE 19

4.327E-02 rad/sec/sec

1.035E+01 sec

ACCE NUMBER	ACCELERATION COMPONENT	MAXIMUM VALUE	TIME AT MAXIMUM
116	1	6.607E+00	1.032E+01
115	1	6.514E+00	1.034E+01
111	1	6.982E+00	1.035E+01
110	1	6.921E+00	1.032E+01
109	1	6.019E+00	1.025E+01
107	2	4.327E-02	1.035E+01
104	1	7.086E+00	1.036E+01
102	1	6.984E+00	1.036E+01
96	1	7.157E+00	1.026E+01
95	1	7.[illegible]E+00	1.036E+01
93	1	6.872E+00	1.034E+01
92	1	7.372E+00	1.036E+01
89	1	7.794E+00	1.027E+01
86	1	7.316E+00	1.036E+01
87	1	7.138E+00	1.036E+01
86	1	6.850E+00	1.035E+01
85	1	6.911E+00	1.025E+01
83	1	8.017E+00	1.037E+01
81	1	7.291E+00	1.026E+01
80	1	7.267E+00	1.037E+01
74	1	8.402E+00	1.027E+01
73	1	7.665E+00	1.037E+01
72	1	7.296E+00	1.037E+01
66	1	8.511E+00	1.036E+01
65	1	7.802E+00	1.037E+01
64	1	7.170E+00	1.036E+01
61	1	7.896E+00	1.031E+01
58	1	9.320E+00	1.030E+01
57	1	8.102E+00	1.028E+01
56	1	8.226E+00	1.028E+01
55	1	7.457E+00	1.027E+01
54	1	7.281E+00	1.037E+01
52	1	9.971E+00	1.036E+01
51	1	4.603E+00	1.029E+01
50	1	8.451E+00	1.028E+01
46	1	8.168E+00	1.028E+01
45	1	1.025E+01	1.029E+01
44	1	9.514E+00	1.030E+01
43	1	8.796E+00	1.029E+01
42	1	9.296E+00	1.029E+01
41	1	8.277E+00	1.028E+01
40	1	8.360E+00	1.028E+01
37	1	1.097E+01	1.031E+01
36	1	1.035E+01	1.030E+01
35	1	9.505E+00	1.025E+01
34	1	9.654E+00	1.029E+01
31	1	8.441E+00	1.028E+01
30	1	1.249E+01	1.031E+01
29	1	1.082E+01	1.029E+01
28	1	1.043E+01	1.030E+01
27	1	1.106E+01	1.026E+01
26	1	9.916E+00	1.025E+01
25	1	9.912E+00	1.035E+01
23	1	1.609E+01	1.031E+01
22	1	1.316E+01	1.031E+01
21	1	1.137E+01	1.029E+01
17	1	8.872E+00	1.025E+01
16	1	1.918E+01	1.031E+01
15	1	1.108E+01	1.039E+01
13	1	1.[illegible]E+01	1.[illegible]E+01
12	1	1.26[illegible]E+01	1.[illegible]E+01
1[illegible]	1	1.182E+01	1.036E+01
11	1	1.213E+01	1.030E+01
9	1	1.482E+01	1.028E+01
8	1	1.402E+01	1.026E+01
7	1	1.622E+01	1.031E+01
6	1	1.630E+01	1.031E+01
4	1	1.915E+01	1.032E+01
3	1	2.072E+01	1.032E+01
2	1	2.176E+01	1.032E+01
1	1	2.233E+01	1.032E+01

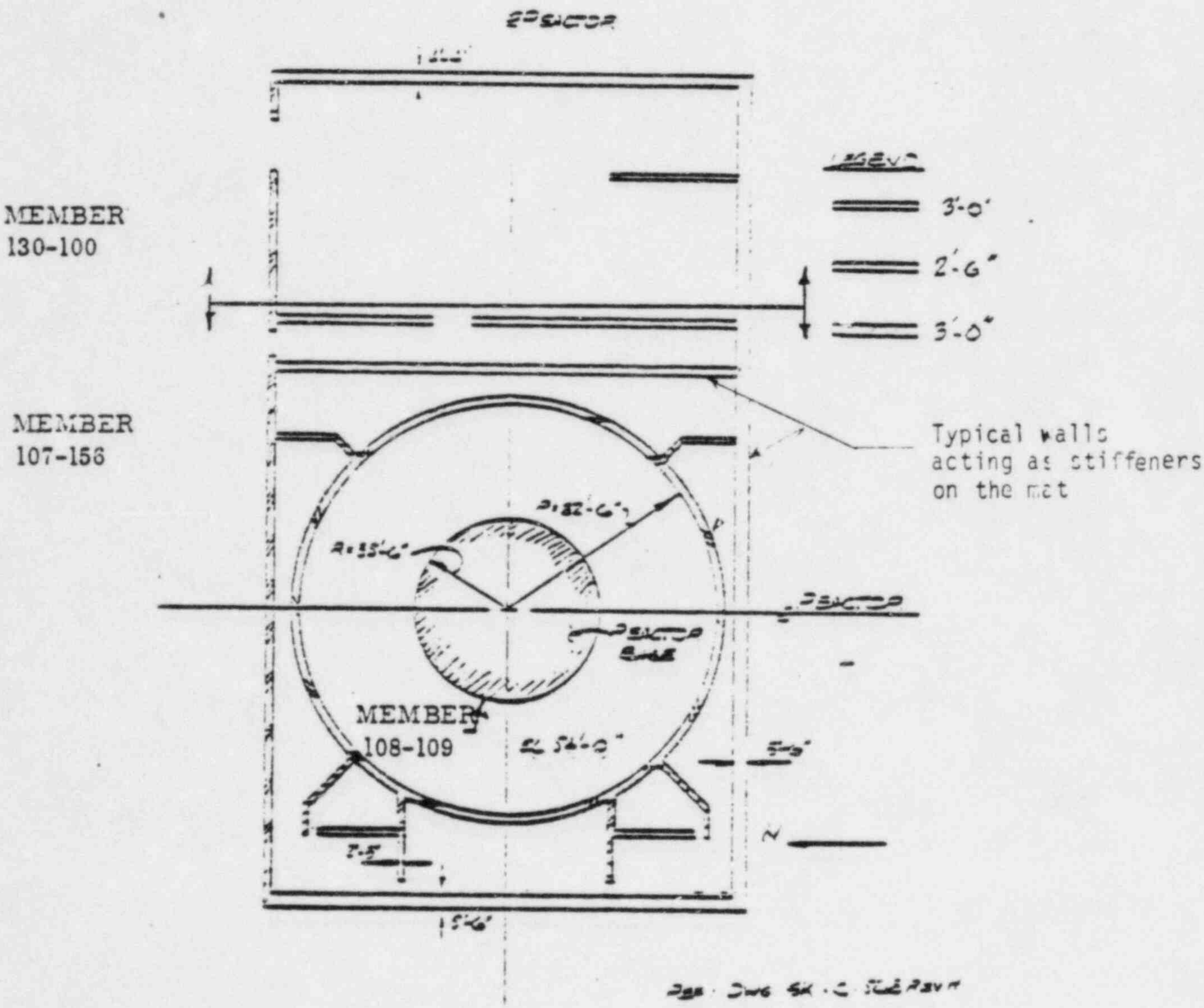

REACTOR BUILDING PLAN AT ELEVATION 54' - 0"

<u>FIGURE C-1</u>

Response to NRC Audit

Meeting Date: January 10, 1984

Question No.: B.12

QUESTION: Summary of events, including dates, concerning the drying and wetting effect on Vincentown.

RESPONSE: The construction sequence for the excavation to the Vincentown formation and the protection of the Vincentown are as follows:

- Hydraulic dredging between March 23, 1976 and October 29, 1976.
- Dewatering of excavation complete January 11, 1977.
- Dental work to remove dredge spoils complete April 7, 1977.
- Immediately following the dental work, the competent Vincentown formation was inspected and accepted by soil engineer. The surface was surveyed and covered with backfill material to protect the Vincentown from freezing.
- Thickness of backfill was monitored for frost penetration during winter.
- Mud mat was placed between April 1977 and August 1977.

The above operations protected the Vincentown formation against wetting and drying conditions.

The response to Question 241.15 will be revised to include the above information.

Response to NRC Audit

Meeting Date: January 10, 1984

Question No.: B.13

QUESTION:

Provide detailed information on power block settlement monitoring including reference points and settlement monuments.

RESPONSE:

The Hope Creek settlement bench mark monuments were installed in the early months of 1974, prior to the start of construction at the HCGS. The monuments are 12-3/4 in. diameter steel pipe piles driven into Vincentown formation at elevation 35 feet (PSD) and filled with concrete. The bench mark monuments are shown in the attached Figure 1.

The line and level for these monuments was established from the master bench at the adjoining Salem Generating Station. A level check was performed in 1979 between the HCGS master bench (BM-A) and the master bench at Salem. The elevation was within 0.004 feet or less than 1/16-in. Subsequently, the master bench at Salem was destroyed.

Since 1979, bench marks BM-B, D and F have been used to verify the elevation of the HCGS master bench BM-A. These bench marks are close enough to detect a small movement in the master bench.

The master bench has been used to determine the elevation of the settlement markers which have been installed in the power block. The settlement readings have been obtained periodically during the construction of the power block. A plot of these level readings are shown in the response to FSAR Question 241.25. All level readings are obtained running level circuits using optical survey equipment.

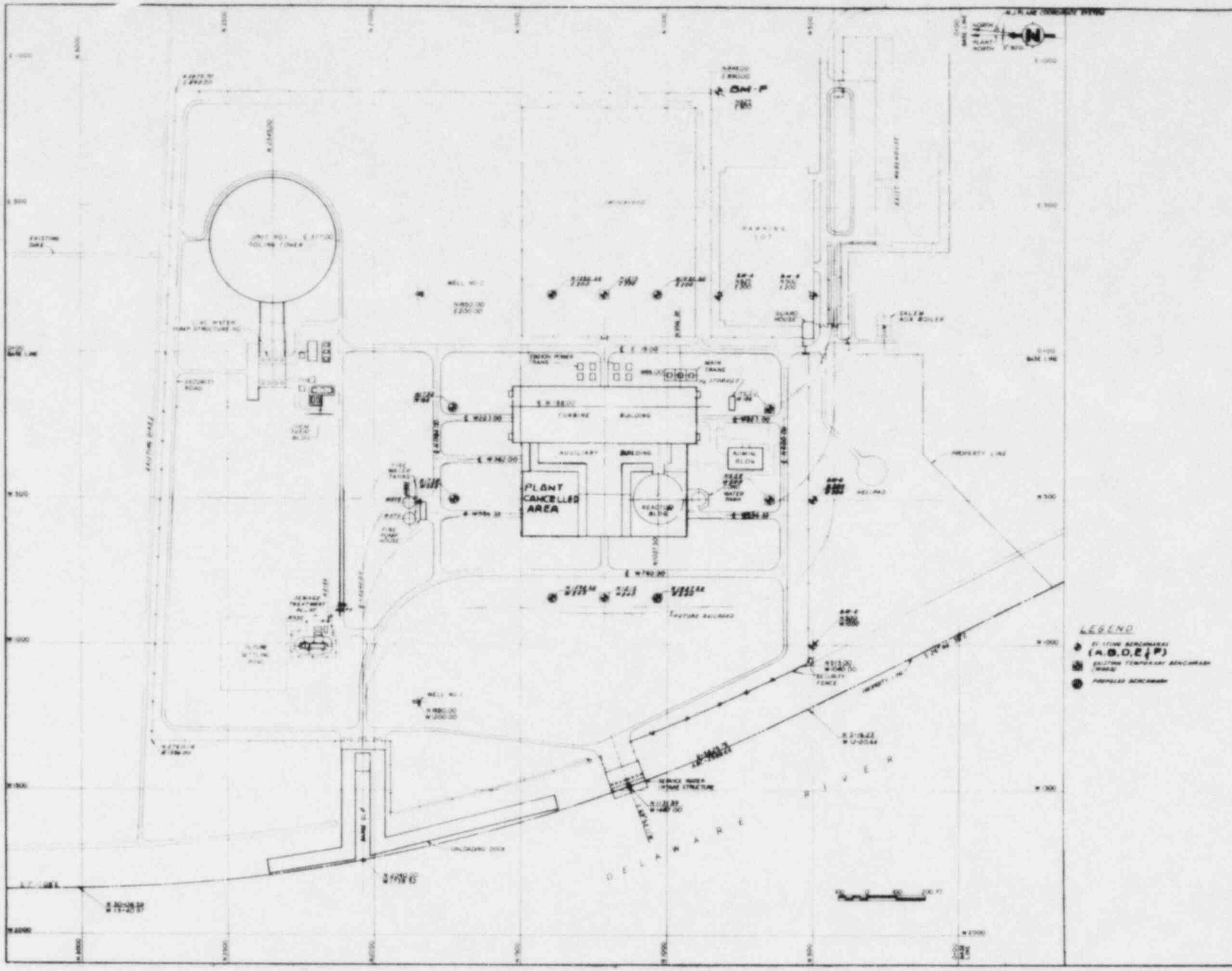

FIGURE 1 BENCH MARK MONUMENTS

Response to NRC Audit

Meeting Date: January 11, 1984

Question No.: A.2

QUESTION:

Review the liquefaction analysis for service water pipeline to check factor of safety of river bottom sands and basal sands. Also, check pore pressure buildup in hydraulic fill.

RESPONSE:

As discussed in the response to Item A-15 of the January 10, 1984 meeting, based on various methods of analyses (Ref. 2.5-79 and 2.5-114), the factor of safety against liquefaction of the river bottom sands is generally well above unity. The hydraulic fill materials are primarily cohesive, highly plastic, and will not be susceptible to liquefaction. (FSAR Section 2.5.4.8.3). As a result of the dynamic loading during an SSE, however, the pore pressure in the hydraulic fill will rise above the initial hydrostatic conditions. The maximum pore pressure increase in the river bottom sands and the hydraulic fill is equal to the corresponding effective vertical stress. Since the effective vertical stress in the hydraulic fill is less than that in the river bottom sands, it is unlikely that the excess pore pressure in the hydraulic fill would be large enough to cause liquefaction of the river bottom sand. Therefore, the pore pressure buildup in the hydraulic fill will not affect the previous conclusions regarding the liquefaction potential of the river bottom sands.

FILE 2443.132.10 (3554)
SUBJECT PSE&G Hope Creek
Jan. 11 meeting - Item A.2 SHEET 1 OF 1

Liquefaction Potential of River Bottom Sands:

Explanation of Factor of Safety Calculation from Finite Element analyses:

Refer to Additional Site Stability Evaluation report, December 1976, Reference 2.5-79, Vol. I, Part I.

Table 4-2 provides the information regarding Liquefaction Potential Evaluation from 2-D analyses.
Page 53 of the report is attached.

Element 156 of the Finite Element model on Figure 4.2 represents a typical element of the River Bottom sand layer in "Free Field".

Due to approximately "Free Field" conditions, the σ_{fc} value (effective normal stress on the potential failure plane - in this case near-horizontal) is 1820 psf. This corresponds well with the estimated effective vertical stress as shown on the attached sheet

Based on Figure A-19A of Reference 2.5-96, the average stress ratio causing ±2.5 % axial strain in 5 cycles for the river bottom sands is 0.55

Therefore the average shear strength (cyclic)

$$= \left(\frac{\tau_{av}}{\sigma_0'}\right)_{\substack{lab\\triaxial}} \times C_r \times \sigma_0' \qquad \text{where } C_r = 0.57 \text{ correction factor}$$

$$= 0.55 \times 0.57 \times 1820 \text{ psf} = 571 \text{ psf}$$

which is comparable to $\tau_{cyclic} = 580.9$ psf in Table 4-2

$\tau_{eq} = 0.65\ \tau_{max} = 178.6$ psf (induced seismic average shear stress is computed from the finite element analysis which is comparable to that from 1-D analysis.

The Factor of safety against liquefaction is computed as

$$F.S. = \frac{\tau_{av.\ cyclic}}{\tau_{eq}} = \frac{580.9}{178.6} = \underline{3.25} \text{ as shown in Table 4.2}$$

F.S. of basal sands computed in the same manner

REVISIONS
BY ____ DATE ____ TO EO ____
BY ____ DATE ____ TO EO ____

BY UKP DATE 2/2/84
CHECKED BY HSG 2/6/84
COPY TO EO ____

DAMES & MOORE

945.1 (3-72) PRINTED IN U.S.A.

TABLE 4-2 (Continued)

Element No.	Soil Type	σ_{fc} (psf)	τ_h (psf)	$\alpha = \frac{\tau_h}{\sigma_{fc}}$	τ_{cyclic} (psf)	τ_{max} (psf)	$\tau_{eq} = 0.65\,\tau_{max}$ (psf)	F.S.	Seismic-Induced Strain(%)
111,132	H.F.	1273.	4.7	0.004	293.9	269.1	174.9	1.68	± .23
112,131	H.F.	1246.	5.6	0.004	287.6	190.6	123.9	2.32	± .12
113,130	H.F.	1330.	9.2	0.007	307.0	128.9	83.5	3.66	± .07
114,129	H.F.	1446.	27.0	0.019	333.8	136.0	88.4	3.78	± .07
115,128	H.F.	1750.	19.5	0.011	404.0	104.1	67.7	5.97	± .04
116,127	H.F.	1601.	25.2	0.016	369.6	73.2	47.6	7.77	± .03
117,126	B.F.	2203.	65.8	0.030	923.4	495.7	322.2	2.87	± .15
118,125	B.F.	2009.	9.4	0.005	779.9	668.2	434.3	1.80	± .50
119,124	B.F.	2045.	39.2	0.019	829.3	670.0	435.5	1.90	± .44
120,123	B.F.	2058.	8.4	0.004	796.4	590.3	383.7	2.08	± .33
121,122	B.F.	2055.	5.8	0.003	792.6	560.3	364.2	2.18	± .31
133,154	H.F.	1508.	6.3	0.004	348.1	293.0	190.5	1.83	± .18
134,153	H.F.	1496.	3.5	0.002	345.4	241.6	157.0	2.20	± .13
135,152	H.F.	1540.	31.3	0.020	355.5	211.9	137.7	2.58	± .11
136,151	H.F.	1762.	55.4	0.031	406.8	198.2	128.8	3.16	± .08
137,150	H.F.	1821.	14.3	0.008	420.4	176.2	114.5	3.67	± .07
138,149	H.F.	2119.	50.6	0.024	489.2	148.0	96.2	5.08	± .05
139,148	H.F.	2181.	60.3	0.028	503.5	126.9	82.5	6.10	± .04
140,147	B.F.	3670.	117.9	0.047	1165.5	1121.9	729.2	1.60	± .74
141,146	B.F.	2418.	18.8	0.008	947.6	748.5	486.5	1.95	± .40
142,145	B.F.	2519.	20.9	0.008	987.2	704.2	457.7	2.16	± .31
143,144	B.F.	2988.	5.9	0.002	956.6	662.8	430.8	2.22	± .29
155,176	R.S.	1822.	1.3	0.001	581.6	320.3	208.2	2.79	± .07
156,175	R.S.	1820.	8.6	0.002	580.9	274.8	178.6	3.25	± .05
157,174	R.S.	1891.	47.5	0.025	603.6	272.8	177.3	3.40	± .04
158,173	R.S.	2027.	63.5	0.031	647.0	273.6	177.8	3.64	± .04
159,172	R.S.	2182.	31.4	0.014	696.5	274.6	178.5	3.90	± .03
160,171	R.S.	2344.	7.9	0.003	748.2	306.9	195.6	3.83	± .04
161,170	R.S.	2693.	95.1	0.035	859.6	500.5	325.3	2.64	± .08

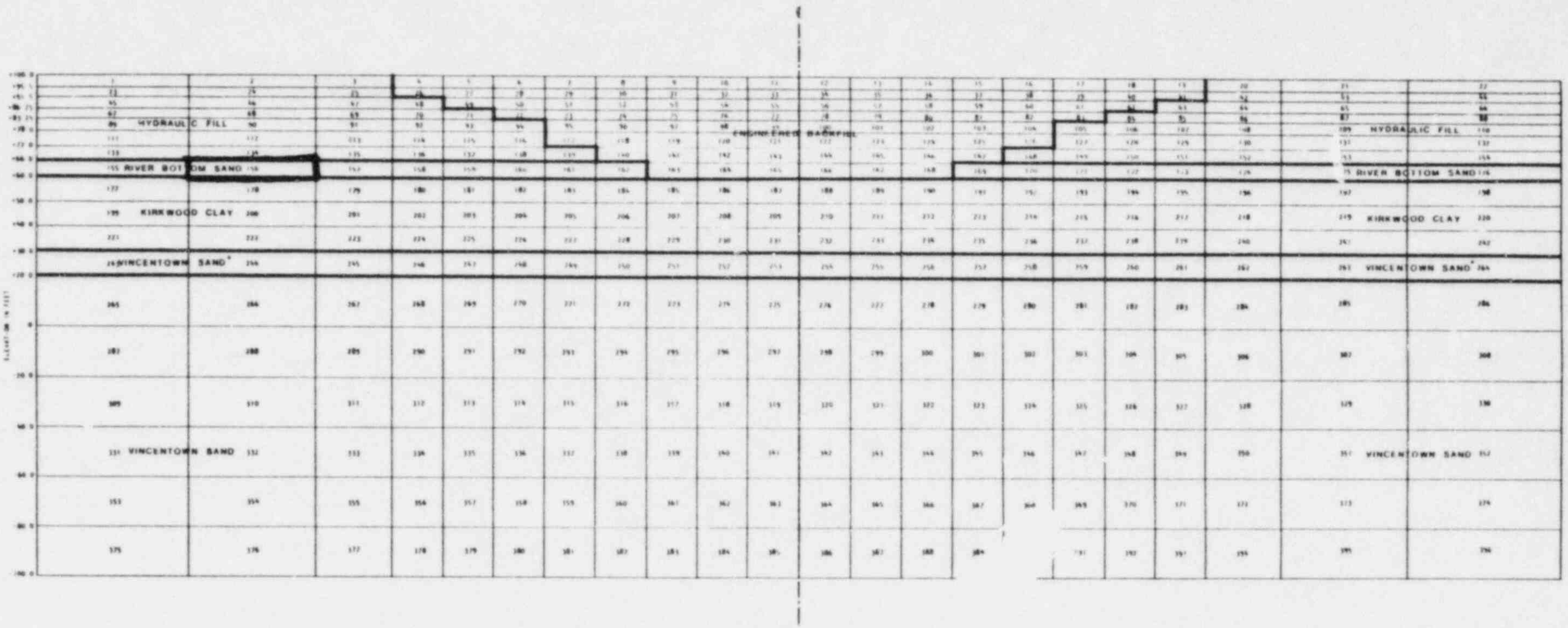

FINITE ELEMENT MESH FOR PROFILE B-B

NOTE

* THE MAJOR PORTION OF THIS LAYER IS VINCENTOWN SAND. THEREFORE, FOR EASE OF MODELLING, THE SOIL PROPERTIES OF THE VINCENTOWN SAND HAVE BEEN ADOPTED FOR THE ELEMENTS IN THIS LAYER.

KEY: ELEMENT NUMBER

DAMES & MOORE

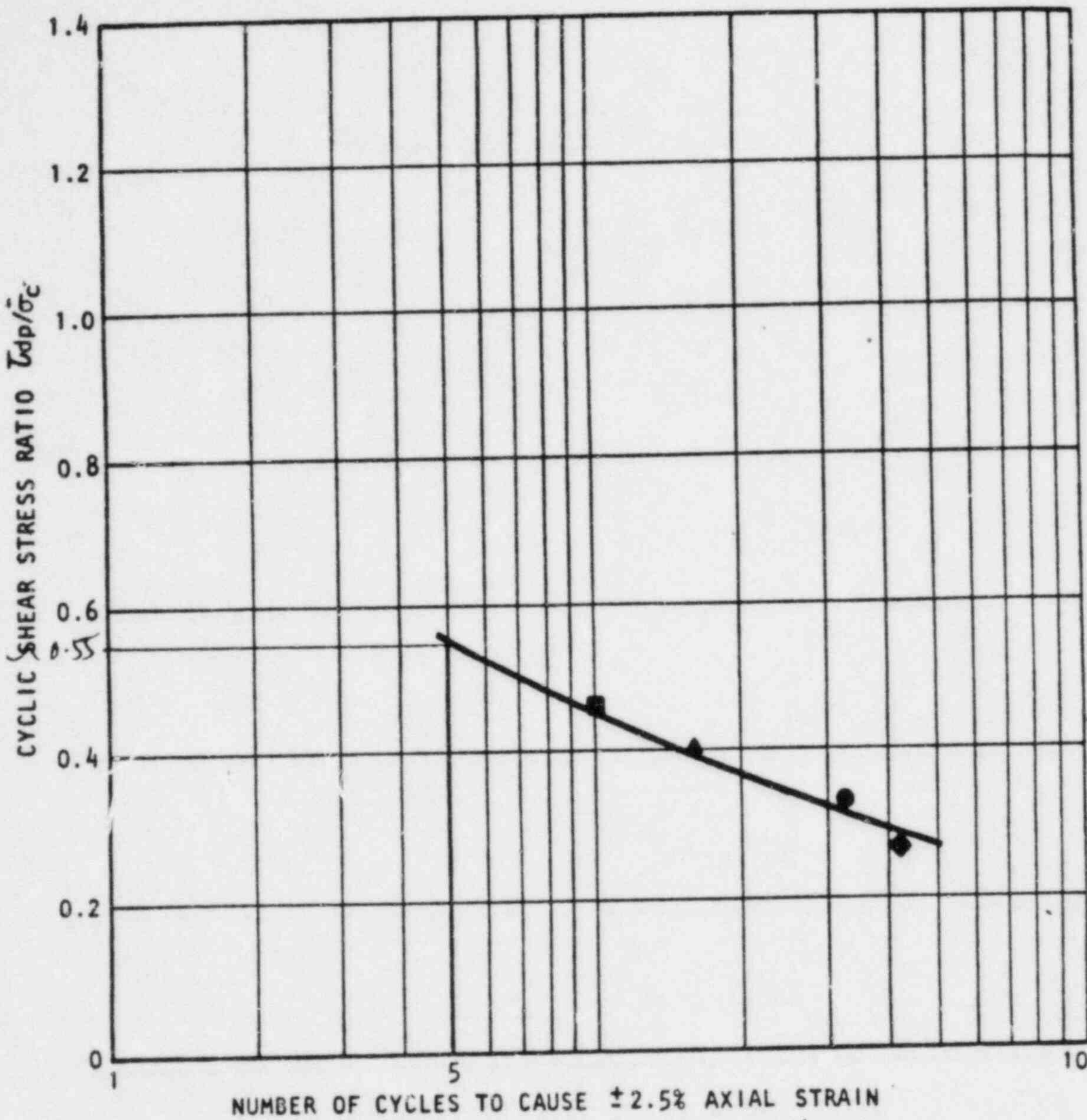

SYMBOL ±2.5% AXIAL STRAIN	BORING NO.	SAMPLE NO.	DEPTH (FT)	$\bar{\sigma}_c$** (P.S.I.)	Blowcounts DRM	SPT
●	AB-1	12	35	11	14	24
▲	AB-1A	11	~~34~~ 35'	11	21	
■	AB-1A	12	38	11	18	
◆*	AB-1	12	35	11	same	

* RECONSTITUTED SAMPLE

** $\bar{\sigma}_c$ = EFFECTIVE CONFINING STRESS

DYNAMIC STRENGTHS - RIVER BOTTOM SANDS

DAMES & MOORE

FIGURE A-19A

Response to NRC Audit

Meeting Date: January 11, 1984

Question No.: A.3

QUESTION:

Review the power block settlement records in terms of loads and soil properties to explain observed settlements in the power block area.

RESPONSE:

INTRODUCTION

The response to Question 241.25 contains plots of load and settlement vs. time. This information has been reviewed using revised data which includes a reduction in the load resulting from the rise in the water table. The mat supporting the power block is divided into five sections and an average load versus time has been plotted for each section. The settlement data for each marker are plotted on a curve beneath the load versus time curve corresponding to the portion of the mat in which the marker is located. All of the markers are located at the edge of the individual mats. The readings are referred to permanent remote benches established on concrete-filled pipe piles driven into the Vincentown Formation. The settlement markers, originally established on the mats have been transferred as construction progressed to other points higher on the structure.

APPROACH

The approach taken to review the data was to plot the marker locations on one plan and redisplay the load curves separated from the marker curves (there are really only five different load curves). The data for each settlement marker was then evaluated against the load curves for the mat in which it is located plus the adjacent mats. These mats are separated by a 2-in. seismic gap in the upper 10 feet of the mat. The bottom four feet is solid concrete throughout the entire mat. Each marker was categorized as to location (i.e., corner, edge, and center). The net settlement of each marker was then displayed in a graph with settlement vs. location. It would be expected that the larger settlements would occur in the center with the small settlement at the corner and intermediate settlements along the edge. In addition, markers located on separate mats but in very close proximity (e.g., 15 and 4 were compared).

The soil properties for the Vincentown were reviewed to confirm that there are no trends distinguishable in a horizontal direction (Ref. 2.5-57, -58, -59).

DISCUSSION

Accuracy of Data

A review of the settlement data indicates many instances of reverse movement on the order of 1/8 to 1/4 inch over a period of three months. There is no indication that the load has undergone a similar reversal and to the contrary, except for sudden changes in ground water level this could not be possible. Therefore, these reversals in settlement suggest an error in the survey or some form of bias. This is very likely given the conditions under which the surveys were made. Because of this and the complete lack of response of the extensometer after times ranging from July 1977 to June 1979 we conclude that the extensometer data is not reliable and the optic survey has an error band of $\pm 1/4$ in. Therefore, one is limited to evaluating general trends in these data. In spite of these shortcomings we believe certain observations can be made and conclusions can be drawn.

Settlement Versus Load

With the exception of markers 16, 18, and 19, all markers were found to respond relatively well in comparison with the applied load. Settlements usually occur as the load is applied. In the cases of 16, 18, and 19, there appears to be an over response to a load on the base mat. However, when surrounding backfill loads are taken into account the settlements seem reasonable.

Comparison of Adjacent Settlment Markers

Five pairs of settlement markers located at the edge of the large mat were compared. In all cases they respond very similarly to the loads applied and net settlement is very close. A pair of markers located near the center of the slab were also compared and were very similar in response to the loads applied. A group of four markers in very close proximity but located on four different mats were also compared and responses were similar to the loads applied and generally were directly proportional to the load versus the settlement.

Settlement Versus Location Within the Mat

As expected there is a rough general trend in magnitude of settlement with the lower settlements being observed in the corner markers and the higher settlements at the center. There is a greater range of settlement along the edge because of the great variation in load on the individual mats.

CONCLUSIONS

In general, the settlement markers are behaving as expected and respond to the applied loads. All of the settlements recorded are well within those predicted including 16, 18, and 19. Settlement markers will continue to be monitored to evaluate the observed trend and to evaluate any heave that might result from raising the water table.

Response to NRC Audit

Meeting Date: January 11, 1984

Question No.: A.4

QUESTION: Current settlement calculations for the service water pipe are based on average soil properties. Provide additional settlement estimates using actual soil properties at various sections along length of service water pipe line.

RESPONSE: A response to the above question will be provided in April 1984.

Response to NRC Audit

Meeting Date: January 11, 1984

Question No.: A.6

QUESTION: Concerning FSAR Tables 2.5-13 and 2.5-14, clarify for Boring 206, Samples 10A through 10C, the shear modulus and shear strain values indicated in these tables.

RESPONSE: Sample 10 of Boring 206 spans the contact between the Kirkwood clays and basal sands. Tables 2.5-13 and 2.5-14 will be revised to delete sample 10A from Table 2.5-13, and to delete Samples 10B and 10C from Table 2.5-14. The response to question 241.9 will be revised to include this information.

Response to NRC Audit

Meeting Date: January 11, 1984

Question No.: A.8

QUESTION:

Are BSAP element size limitations satisfied for the foundation mat model and the drywell shield wall model.

RESPONSE:

The foundation mat model and the drywell shield wall model were analyzed using computer program BSAP. The isoparametric brick element was used in these models. The accuracy of the analysis results for these models depends on the element mesh size or the number of elements used in the high stress areas. Based on a preliminary analysis of the foundation mat, areas of high soil pressure were determined and the final foundation mat model used a finer mesh in these areas of higher stress to ensure better accuracy of the analysis results.

Response to NRC Audit Meeting

Date: January 11, 1984

Question No.: A-9

<u>QUESTION</u>: Describe the seismic modeling of the drywell shield wall.

<u>RESPONSE</u>: The seismic modeling of the drywell shield wall follows the general procedure used in modeling the Reactor Building. This procedure is described in detail in Pages 1, 2 and 3 of the attachment (Reference: Hope Creek Seismic Structural Report No. SED-76-017, Revision 5).

In modeling the active structural walls and columns between any two floor levels, openings in the walls are not modelled and a continuous system is assumed. The effect of these openings is local and has negligible impact on the overall structural behavior. To illustrate this, the large equipment hatch openings at elevation 107' of the Reactor Building have been selected. There are two hatch openings, each with a diameter of 13 feet, at this elevation. As observed from the attached calculation, the effect of ignoring these two large openings on the beam stiffness is only 7%. In fact, this effect could be further reduced if the following conservatisms are excluded from the attached calculation:

a) These openings are reinforced by reinforcing steels and sleeves. Stiffness contributions from these reinforcements have not been included.

b) The maximum reduction in shear area due to the openings is conservatively assumed for the full length of the diameter (13 feet) of the openings. In fact, the average shear area reduction for the full length of the diameter is considerably less.

Based on the above discussion, it is determined that the effect of openings on the structral properties is negligible.

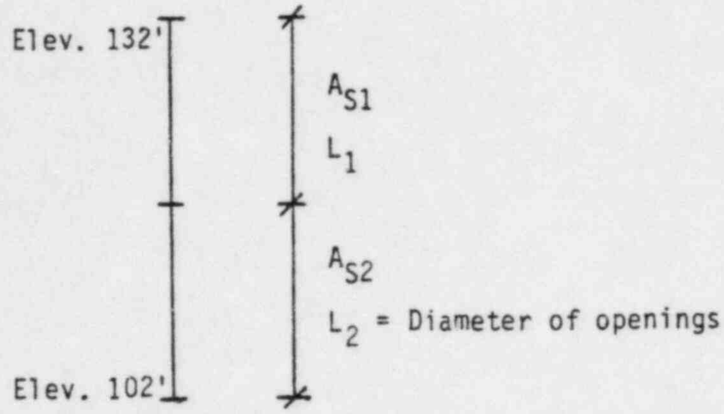

ΔA = Reduction in shear area due to openings = 138.0 ft^2

A_{S1} = 862.3 ft^2

L_1 = 30' - L_2 = 17'

A_{S2} = $A_{S1} - \Delta A$ = 724.3 ft^2

L_2 = 13'

K = Stiffness ignoring openings = $\dfrac{A_{S1}\ G}{L_1 + L_2}$ = 28.7 G

K' = Stiffness considering openings = $G/\left(\dfrac{L_1}{A_{S1}} + \dfrac{L_2}{A_{S2}}\right)$ = 26.6 G

K'/K = 0.93

ATTACHMENT TO RESPONSE A-9

Horizontal and Vertical Lumped Mass Model

The mathematical model used to compute horizontal response and vertical wall response consists of lumped masses connected by massless elastic structural elements. The structural elements connecting two adjacent floors were located at the center of rigidity of the cross-section, and the lumped masses were located at the center of mass of each floor level. To compute element flexibility representing walls between two floor levels, the structural walls and steel columns were assumed to deform in shear and bending, with the concrete floor slabs acting as rigid diaphragms. However, in the case of certain frame structures, such as the Turbine Building superstructures, actual flexibility of the floor was considered in the calculation of properties. Each vertical member between two floors provided stiffness contributions corresponding to an axial area, two shear areas, two area moments of inertia, and a torsional inertia representing the actual structural member between the elevations of the two nodes.

Masses were computed at each mass point by considering the weights of the floor, the equipment located on the floor, the structural component attached to the floor, and the tributary weights of walls above and below each floor. Locations of centers of mass were obtained by computing a weighted average (centroid) of the centers of mass of the floor slabs, equipment and tributary masses of the walls above and below the floor. Mass moments of inertia through the center of mass were computed about the north-south, east-west, and vertical axes.

The active structural walls between any two floor levels were represented by a vertical massless elastic structural members with equivalent cross-section properties corresponding to axial, bending, shearing, and torsional deformations. The computational procedures used in determining the equivalent elastic member properties may be summarized as follows:

1. The axial area was computed as the sum of the cross-sectional areas of all active structural walls and steel columns.

2. Area moments of inertia and shear areas were computed based on the assumption that the floor diaphragms are infinitely rigid. The stiffness of each active structural wall and column was summed using the following relationship:

$$K = \frac{12EI}{L^3(1+\emptyset)}$$

$$\emptyset = \frac{12EI}{L^2GA_v}$$

resulting in a combined stiffness of all walls and columns:

$$K_{tot} = \Sigma k_i$$

Shear areas along north-south and east-west axes were obtained for each wall using the assumption that walls perpendicular to the axis under consideration do not contribute to shear stiffness. Based on a finite element study of the Reactor Building perimeter walls, where unit displacements were applied at the floor elevations, it was found that for walls parallel to the seismic motion, an area factor of 1.0 should be used. A shear factor of 0.5 is used for circullar walls. Total area moments of inertia and shear areas were then computed such that the total stiffness (K_{tot}) was reproduced. This was achieved by computing an area moment of inertia, including cross walls, for the entire system and then back-substituting to compute total shear area:

$$K_{tot} = \frac{12EI_{tot}}{L^3(1+\emptyset_{tot})}$$

$$\emptyset_{tot} = \frac{12EI_{tot}}{L^2G\,A_{v,tot}}$$

3. The center of rigidity for each cross-section was obtained either by calculating the centroid of the effective shear areas in the north-south and east-west directions, or by the procedures described in Reference 1 and 2, as appropriate.

4. The torsion constant was obtained by calculating the torque acting at the center of rigidity due to the forces generated in individual structural elements when a unit rotation is applied at the center of rigidity. The torsion is applied at the center of rigidity. The torsion constant was obtained as the ratio of the torque multiplied by the height between the floor levels to the shear modulus.

References:

1. Peery, D.J., Aircraft Structures, McGraw-Hill, New York, 1950.

2. Przemieniecki, J.S., Theory of Matrix Structural Analysis, McGraw-Hill, New York, 1968.

Response to NRC Audit

Meeting Date: January 11, 1984

Question No.: A-12

<u>QUESTION</u>: Justify the 12 Hz. cut-off frequency for SSI analysis.

<u>RESPONSE</u>: Two independent studies have been performed to justify the 12 Hz. cut-off frequency: a design base evaluation performed by Impell and a confirmatory evaluation by Bechtel. These studies are described separately below.

A. <u>DESIGN BASE ANALYSIS</u>

The selection of a cut-off frequency value was based on two primary considerations:

1. For the particular Hope Creek site, the evaluation of the highest shear wave frequency that can realistically be transmitted through the soil medium.

2. The contribution of the high frequency components of the input free-field (control) motion on the resultant structural response.

<u>DECONVOLUTION ANALYSIS</u>

Two cut-off frequency values were selected for consideration and study: 12 and 20 Hz. An operating basis earthquake was selected for the study, due to its lower peak acceleration level. Because of the nonlinear characteristics of the soil, the lower excitation level will result in stiffer soil properties than for the SSE level excitation, with the soil thus capable of transmitting higher frequency waves. This case will then be more critical for establishing a cut-off frequency value than the SSE.

A soil column, representing the Hope Creek free-field soil properties, was first constructed. The mesh refinement was selected such that a wave frequency of 20 Hz. could be transmitted without loss of numerical accuracy. A schematic representation of the soil column model is presented in Figure 1.

The free-field soil column is composed of a series of two-dimensional plane strain elements of unit width modeling the soil properties. The dimensions of the soil column extend between elevations 102.0 feet, corresponding to the elevation at finished grade for the Hope Creek site, down to elevation -300.0 feet, a depth found to be sufficiently deep to include all significant soil-structure interaction effects.

Using the above free-field soil column, a deconvolution analysis of the OBE Regulatory Guide 1.60 synthetic time-history was performed for both 12 and 20 Hz. cut-off frequency values. This Regulatory Guide control motion was input at elevation 40.0 feet, corresponding to the elevation of the bottom of the foundation base mats for the power block area. Deconvoluted time-history response was obtained at the base of the soil column model, corresponding to elevation -300.0 feet.

SOIL-STRUCTURE INTERACTION ANALYSIS

A simplified soil-structure model was developed for the cut-off frequency study. The model consists of a single soil column, attached to a series of single-degree-of-freedom oscillators representing the Reactor Building structure. A sketch of the model, with the corresponding soil and structural properties, can be seen in Figures 2 and 3.

As in the case of the deconvolution analysis, the soil properties were modeled by a series of two-dimensional plane strain elements of unit width. The soil elements extend from elevation -300.0 feet to elevation 40.0 feet, corresponding to the elevation at the bottom of the foundation base mat. One additional plane strain element was placed between elevations 40.0 feet and 54.0 feet, to simulate the base mat properties. The Reactor Building dynamic properties for the N-S modes with frequencies up to 20 Hz. were duplicated by a series of single-degree-of-freedom oscillators. The mass properties of these oscillators are drawn from the modal effective mass calculation of the detailed model.

A soil-structure interaction analysis was performed for both a 12 and 20 Hz. cut-off frequency value. The input motions obtained from the deconvolution analyses, were input at elevation -300.0 feet of the simplified interaction model. Using a system direct integration technique, a time-history analysis of the soil-structure system was performed, with time-histories of acceleration being obtained at the base mat level. An evaluation of the influence of the cut-off frequency was obtained by comparison of the derived base mat response spectra for each of the cut-off frequencies.

As demonstrated by Figure 4, the base mat response for the two cut-off frequencies are essentially identical for the frequency range below 12 Hz. For the frequency range of 12 to 20 Hz., however, the response at the base mat does diverge somewhat between the two cut-off frequencies. The 20 Hz. cut-off response exhibits a number of minor peaks, as a result of high frequency components of the bedrock motion. The 12 Hz. cut-off analysis, on the other hand, exhibits a non-amplified response beyond 12 Hz., resulting in a constant spectral acceleration.

In order to verify the adequacy of the simplified model, a comparison with a detailed interaction model was made. A comparison of Figures 4 and 5 reveals that the motion at the base mat for the detailed and simplified models exhibit very similar trends, both with regard to the spectral peak and overall shape of the curves.

SEISMIC STRUCTURAL ANALYSIS

In order to identify the significance of the difference in base mat motion for the cut-off frequencies on the structural response of the Reactor Building, a seismic structural analysis of the Reactor Building was performed using the detailed three-dimensional model.

Using the basemat motions derived from the simplified interaction analyses for a 12 and 20 Hz. cut-off frequency, a modal time-history analysis of the Reactor Building was performed. Response spectra at selected elevations were computed from the resultant floor excitations, and a comparison of the results derived from the two cut-off frequencies was performed.

Figures 6 through 8 present response maxima for shear, moment and torque in the drywell of the Reactor Building, when subjected to each of the base mat excitations. The drywell was selected for comparison of cut-off frequency effects because it is a portion of the reactor pressure boundary, and the design of this structure is particularly critical. The comparison of results for the drywell is representative of other portions of the structure as well. As can be seen from these plots, the response maxima of the structure are virtually independent of the high frequency acceleration components of the base mat motion. Clearly the shear, moment and torque response values for the structure are essentially identical for the two different cut-off frequencies, indicating a dependance only on the low and mid frequency range of the base mat motions.

Response spectra plots at various elevations of the Reactor Building are presented in Figures 9 through 12. As can be seen from these figures, the spectral accelerations in the low and mid frequency range are essentially identical for the two cut-off frequencies. In the frequency range above 12 Hz., there are minor differences at the lower elevations of the Reactor Building, but almost no variation in the upper elevations. For all elevations, the overall trend of the curves is identical, duplicating peak response values and shape of the spectral curves.

B. CONFIRMATORY ANALYSIS

Bechtel also performed a confirmatory independent analysis to evaluate the effect of cut-off frequency on the soil structure interaction analysis results. The North-South soil-structure model was analyzed for the SSE case. The soil model was discretized to have elements which are capable of transmitting frequencies of at least 18 Hz. Two soil-structure interaction analyses, with cut-off frequencies of 12 Hz and 18 Hz, were performed using computer code FLUSH. As shown in the response spectrum comparison plots (Figures 13 to 15), there is practically no effect in increasing the cut-off frequency from 12 Hz to 18 Hz on the response of the soil structure system.

CONCLUSIONS

A study has been performed to evaluate the influence of the cut-off frequency value on the soil-structure interaction analysis and subsequent seismic structural analysis for the Hope Creek site. A comparison of response results for a 12 and 20 Hz. cut-off frequency was made for all facets of the analysis.

Comparison of structural response results indicates only minor dependence on the high frequency acceleration components of the input motion, both in the generation of building response maxima and floor response spectra. It would thus be reasonable to assume that an intermediate cut-off frequency between 12 and 20 Hz. would produce only minor deviation from the response results of the 12 Hz cut-off frequency analysis.

Based on the above considerations, it was found that a cut-off frequency of 12 Hz. for the soil-structure interaction analysis was both physically realistic for the Hope Creek site and, in addition, maintains adequate conservatism with regard to structural response. The use of a 12 Hz. cut-off frequency was thus selected for the Hope Creek analysis.

Furthermore, the adequacy of the 12 Hz cut-off frequency for SSI analysis has been verified by an independent study performed by Bechtel.

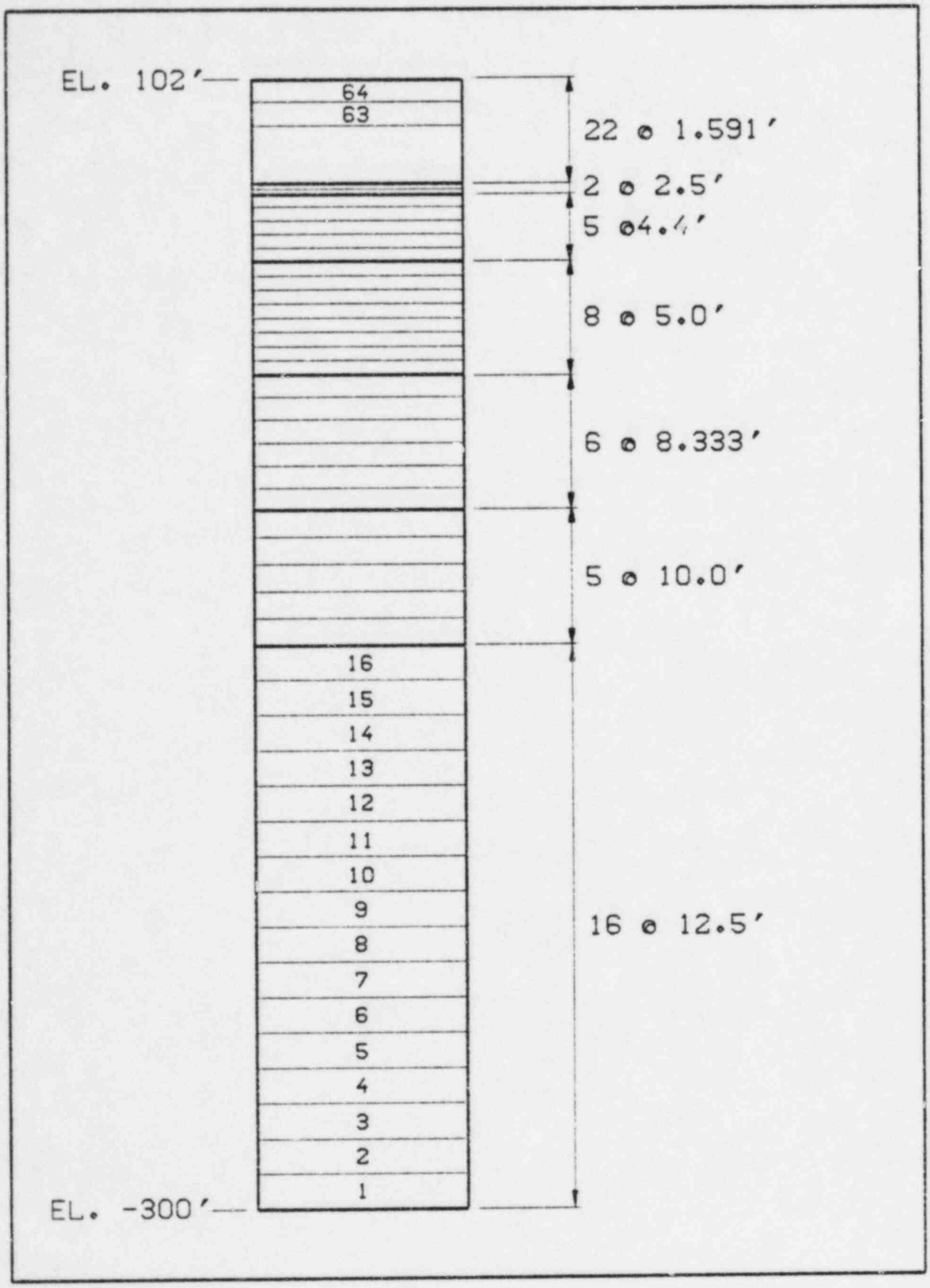

MATHEMATICAL MODEL OF FREE FIELD SOIL COLUMN
FOR DECONVOLUTION ANALYSIS

FIGURE 1

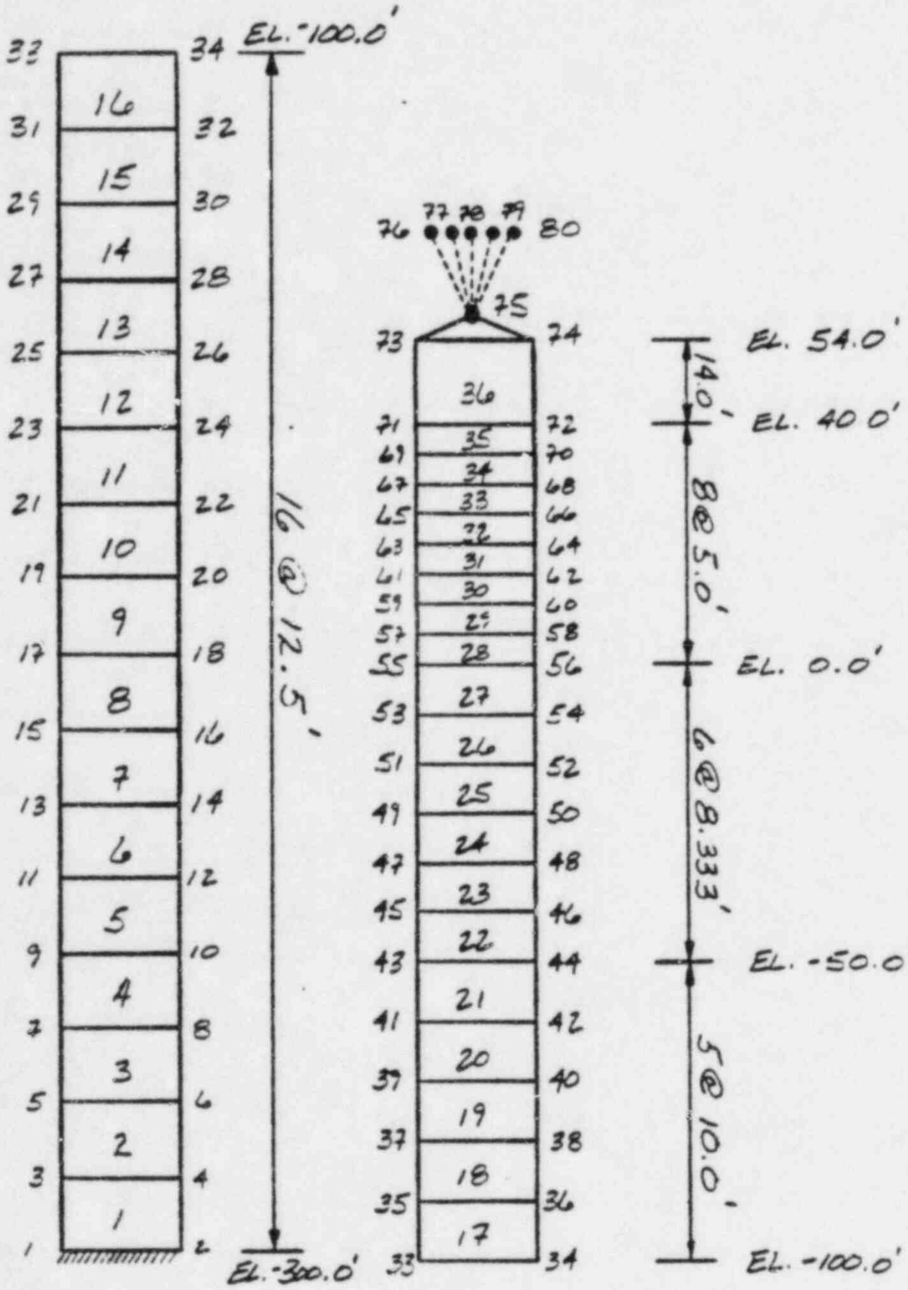

MATHEMATICAL MODEL FOR SOIL-STRUCTURE
INTERACTION ANALYSIS

FIGURE 2

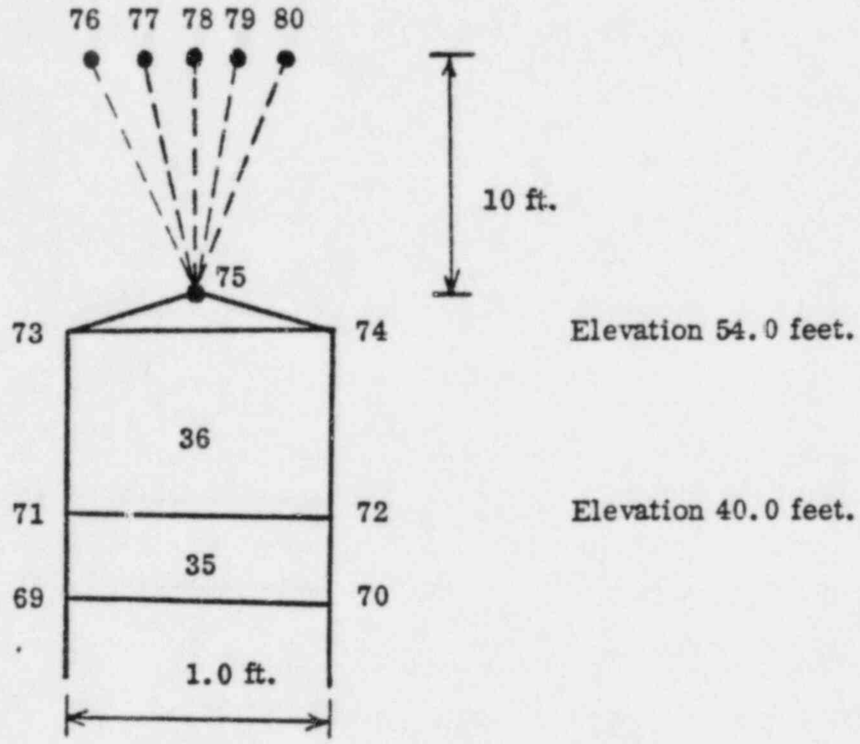

FREQUENCY	MASS PARTICIPATION FACTORS
f_1 = 4.11 Hz.	M_1 = 21.07
f_2 = 9.07 Hz.	M_2 = 10.43
f_3 = 12.08 Hz.	M_3 = 4.75
f_4 = 17.65 Hz.	M_4 = 0.65
f_5 = 19.76 Hz.	M_5 = 2.17

MATHEMATICAL REPRESENTATION OF REACTOR BUILDING
FOR SOIL-STRUCTURE INTERACTION ANALYSIS

FIGURE 3

SIMPLIFIED INTERACTION ANAL.- N-6 OBE BASE MAT RESPONSE SPECTRA
(2% DAMPING)

FIGURE 4

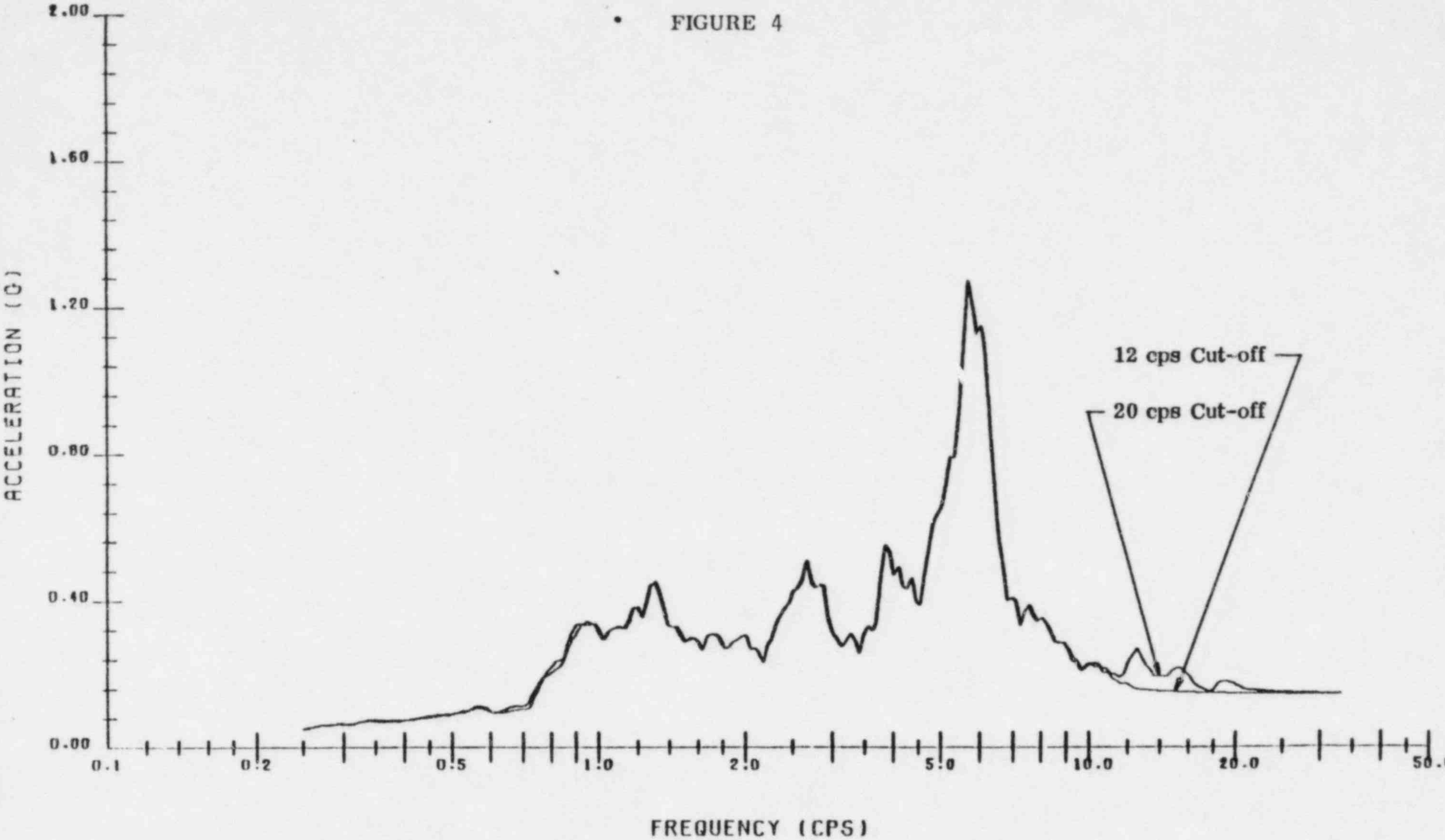

DETAILED INTERACTION ANALYSIS: N-S OBE BASE MAT RESPONSE SPECTRUM
(2% DAMPING)

FIGURE 5

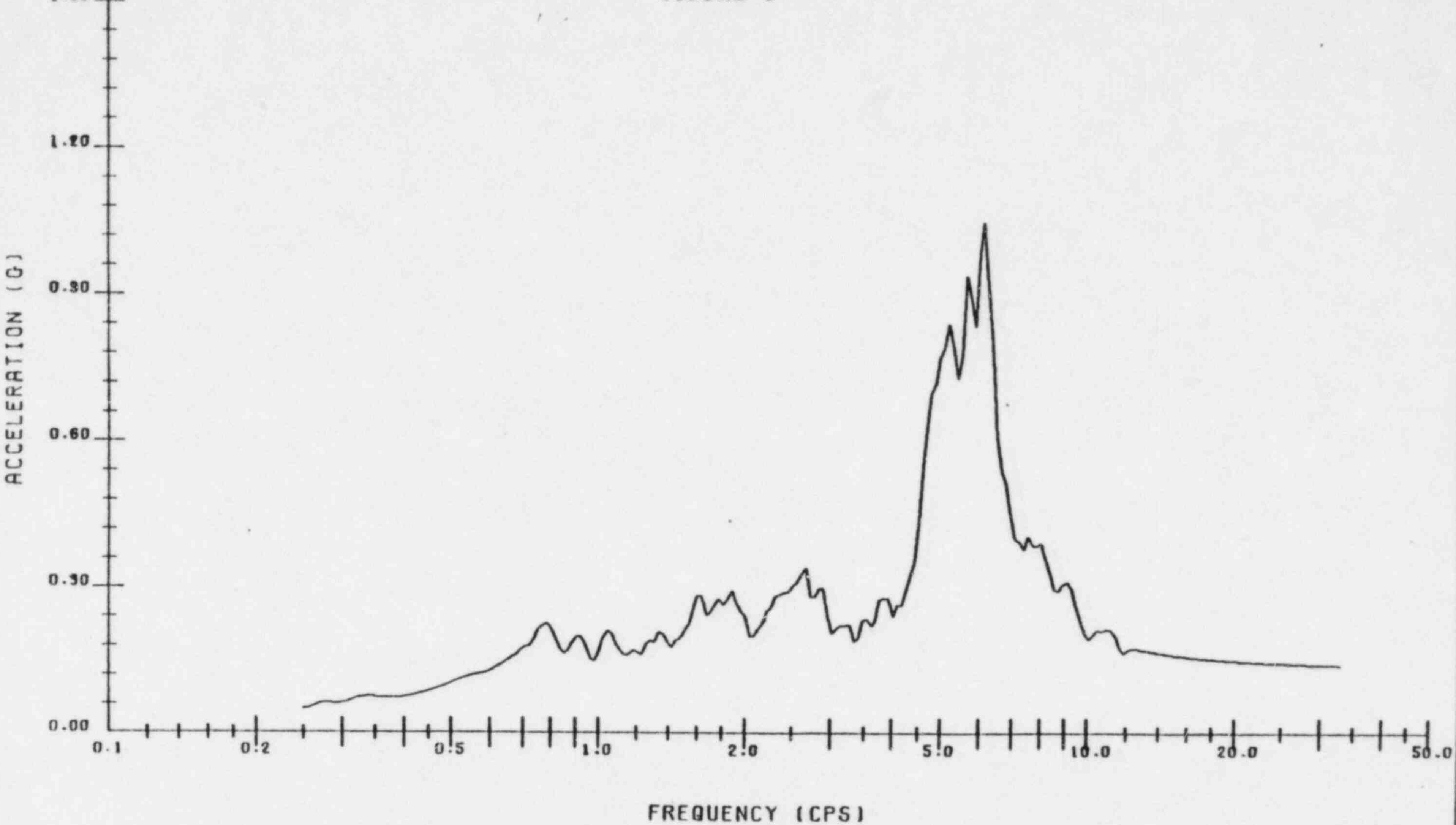

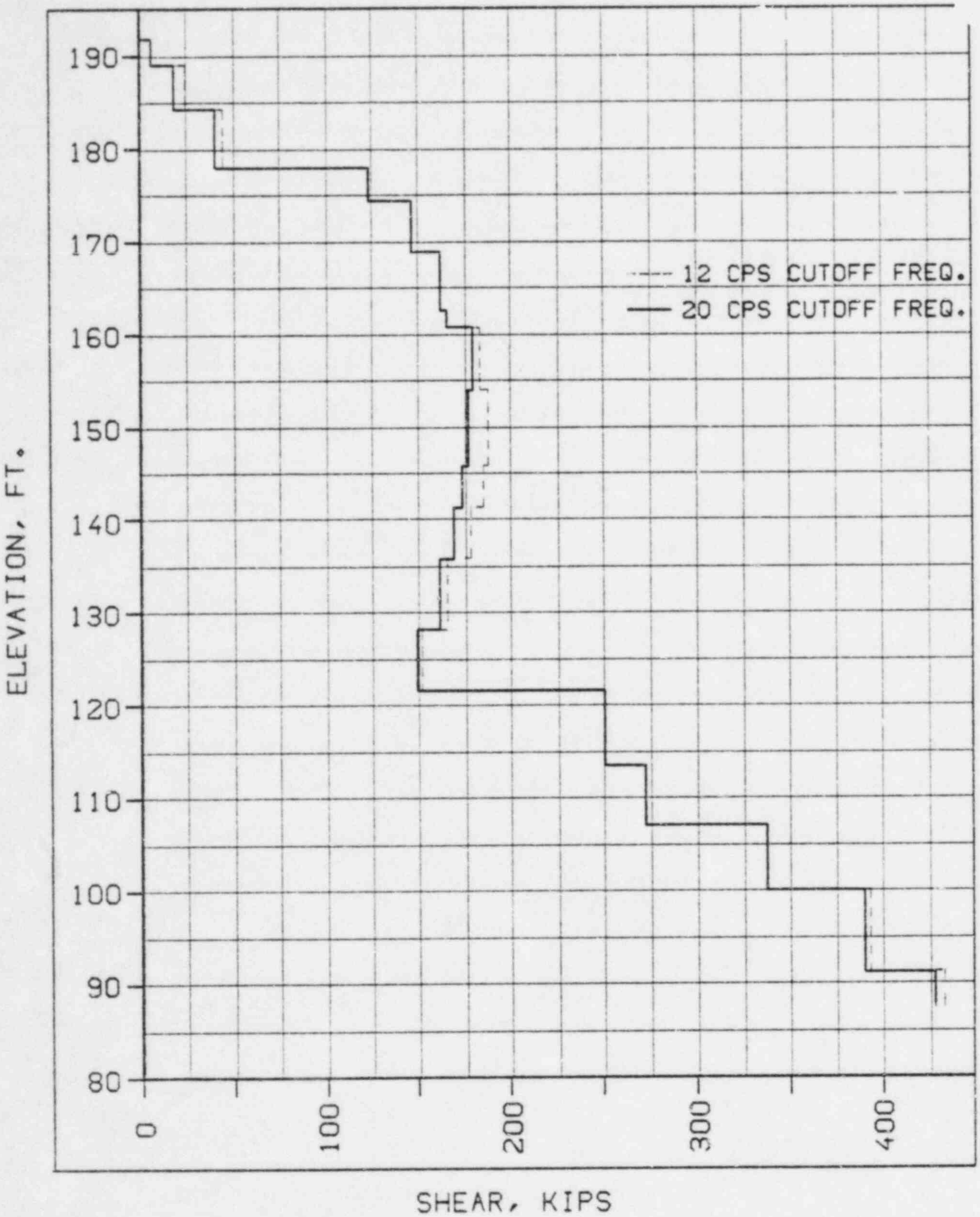

SHEAR RESPONSE MAXIMA FOR DRYWELL

FIGURE 6

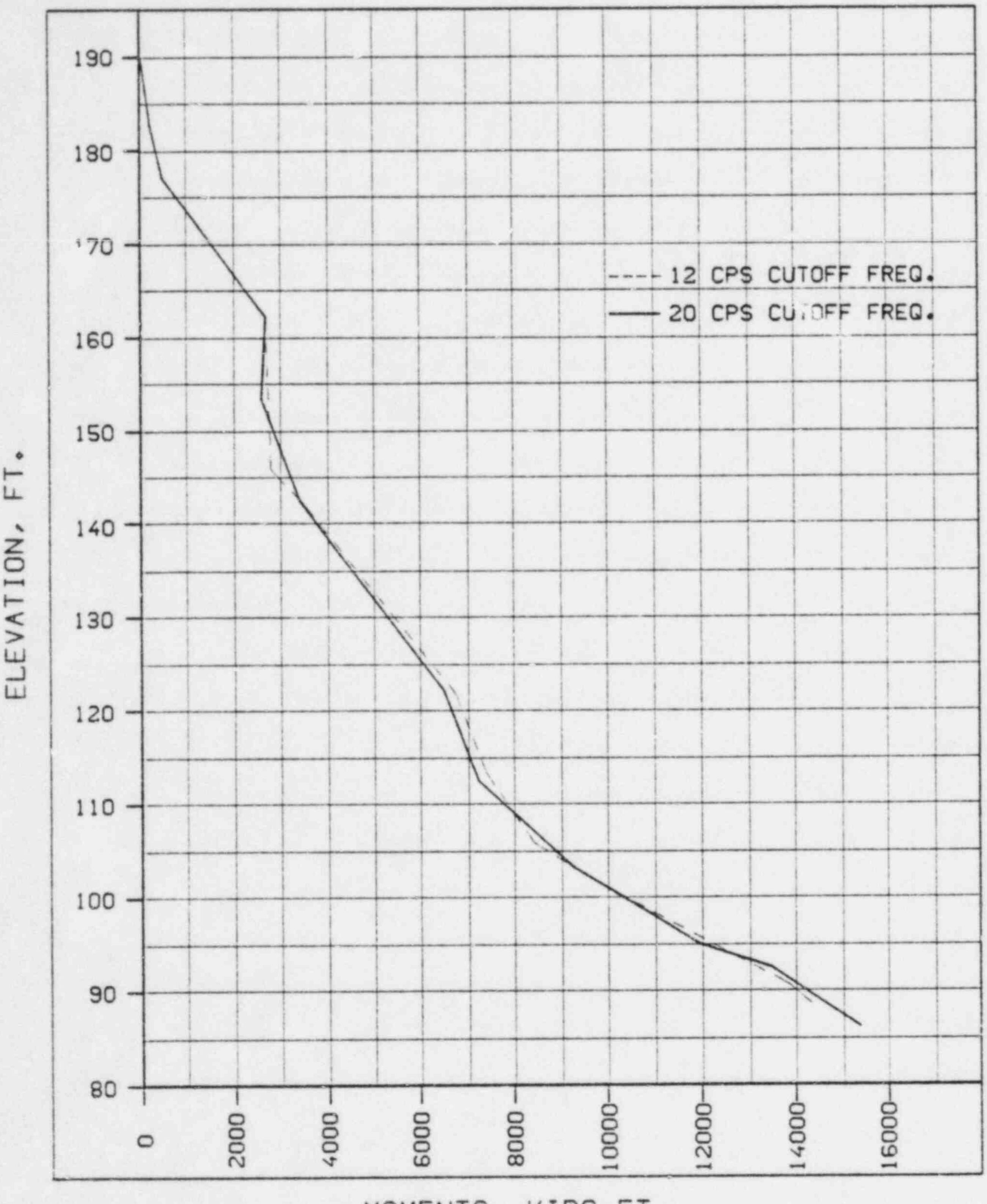

MOMENT RESPONSE MAXIMA FOR DRYWELL

FIGURE 7

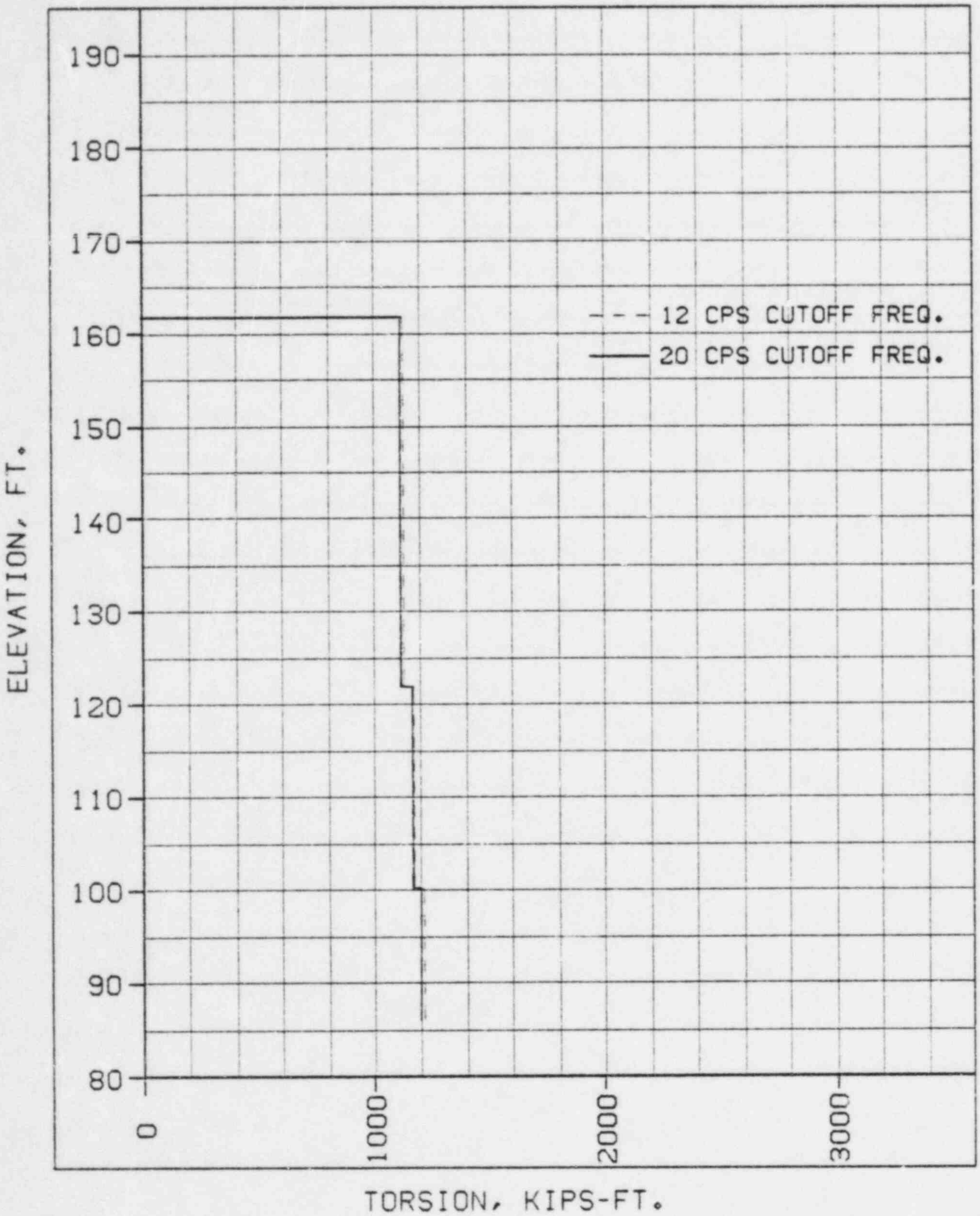

TORSION RESPONSE MAXIMA FOR DRYWELL

FIGURE 8

REACTOR BUILDING ELEV 145 N-S OBE RESPONSE DUE TO SIMPLIED SSIA
(2% DAMPING)

FIGURE 9

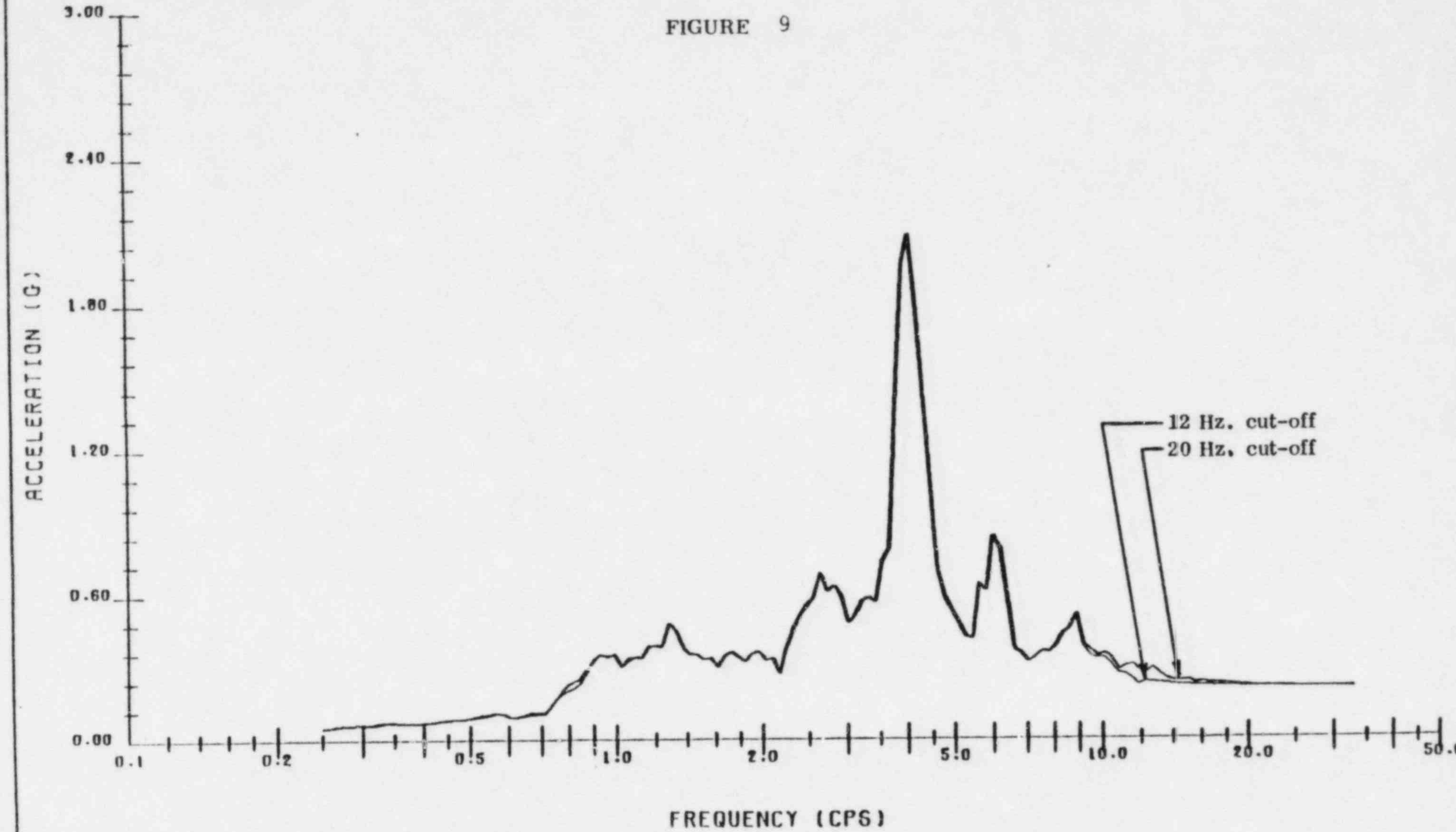

REACTOR BUILDING ELEV 162 N-S OBE RESPONSE DUE TO SIMPLIED SSIA
(2% DAMPING)

FIGURE 10

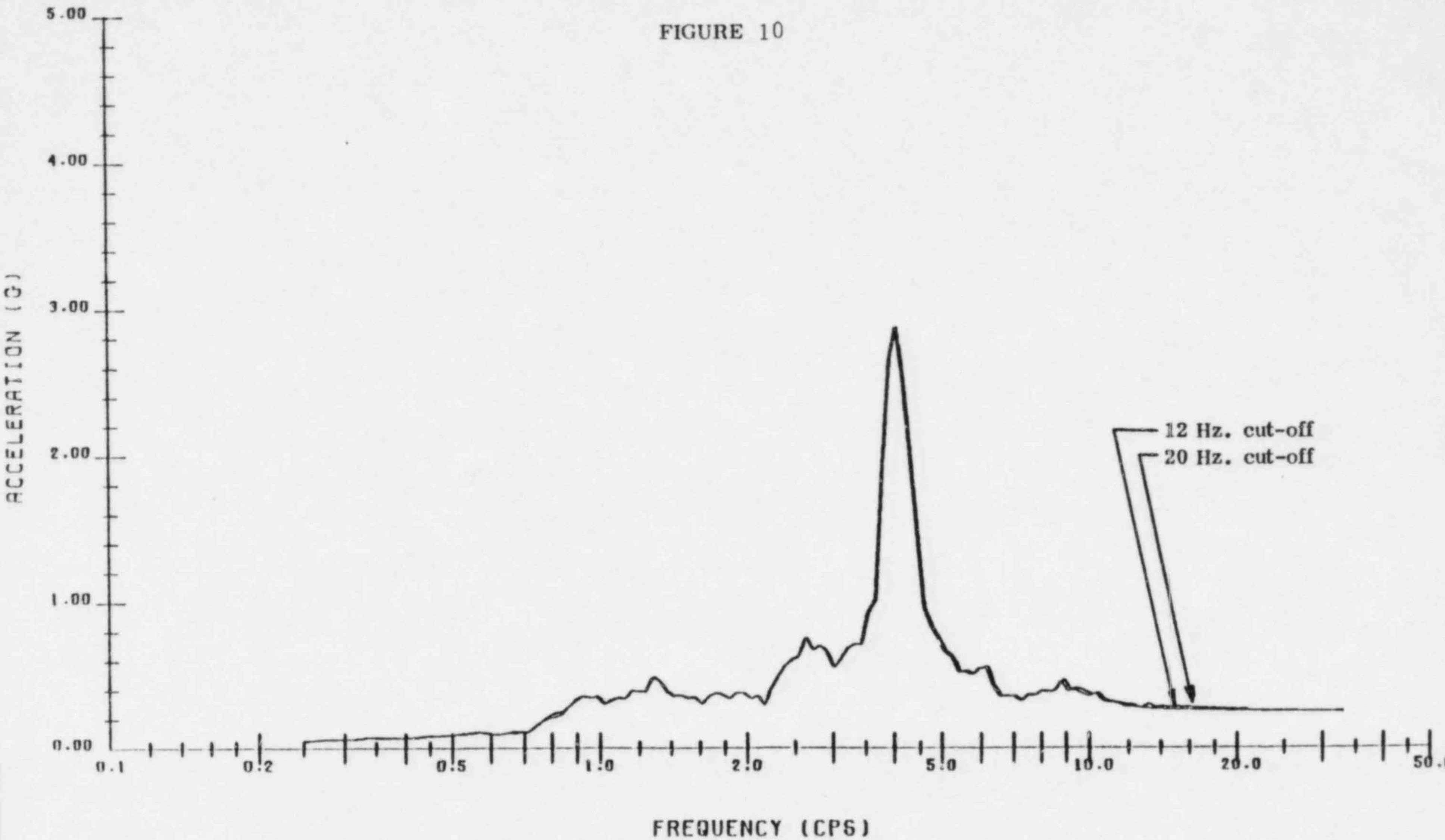

REACTOR BUILDING ELEV. 201 N-S OBE RESPONSE DUE TO SIMPLIFIED SSIA
(2% DAMPING)

FIGURE 11

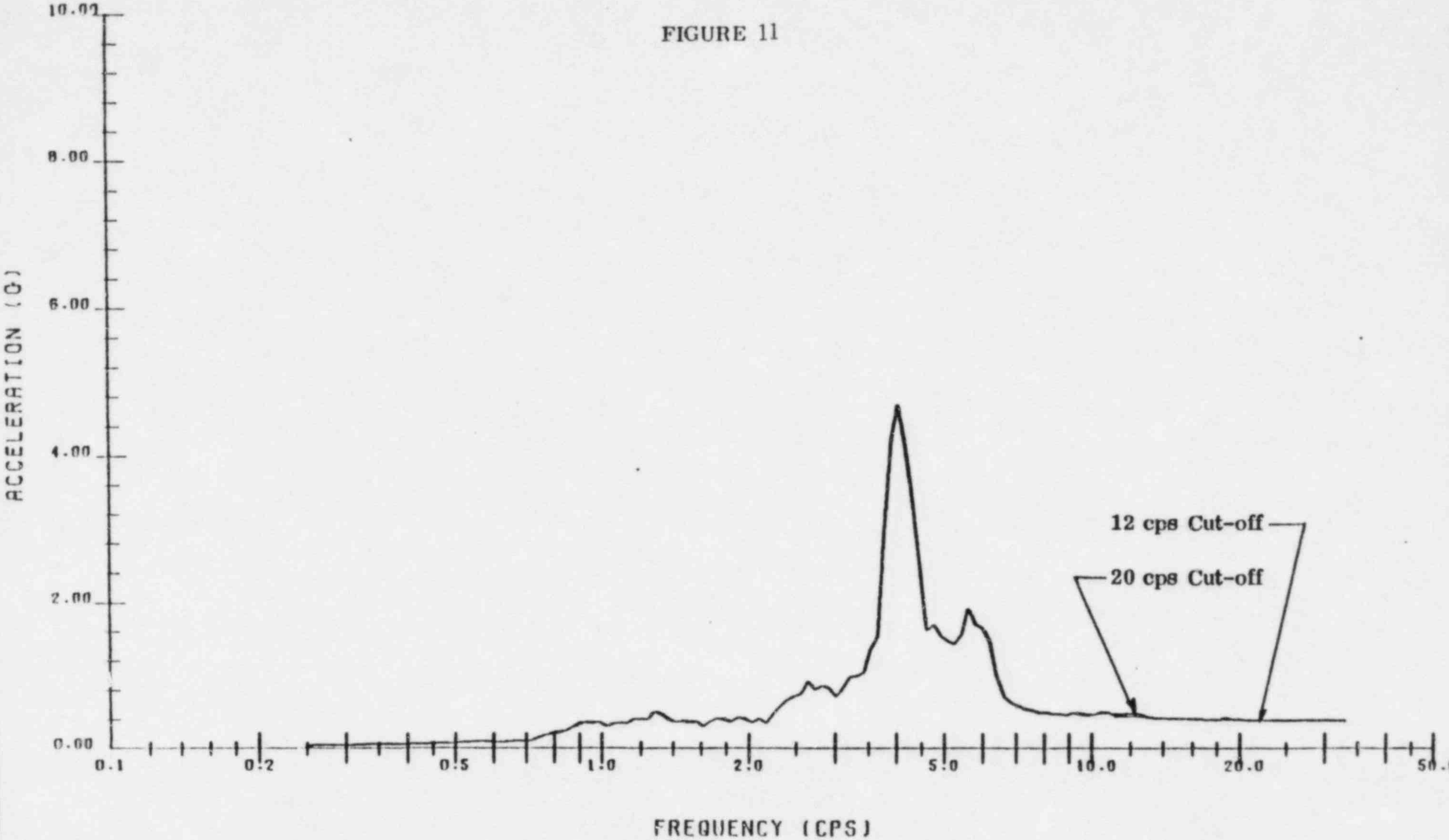

REACTOR BUILDING ELEV 252 N-S OBE RESPONSE DUE TO SIMPLIED SSIA
(2% DAMPING)

FIGURE 12

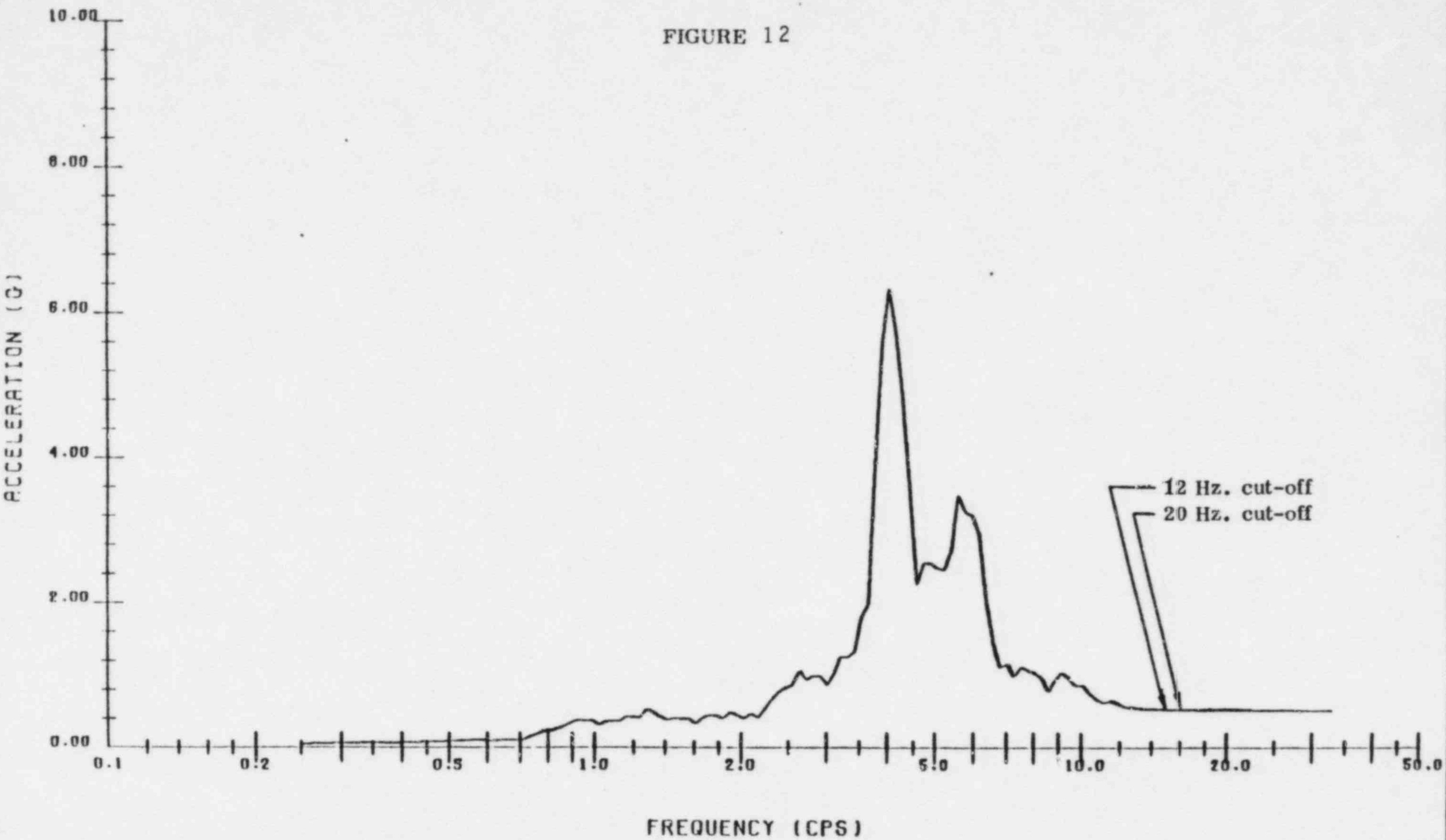

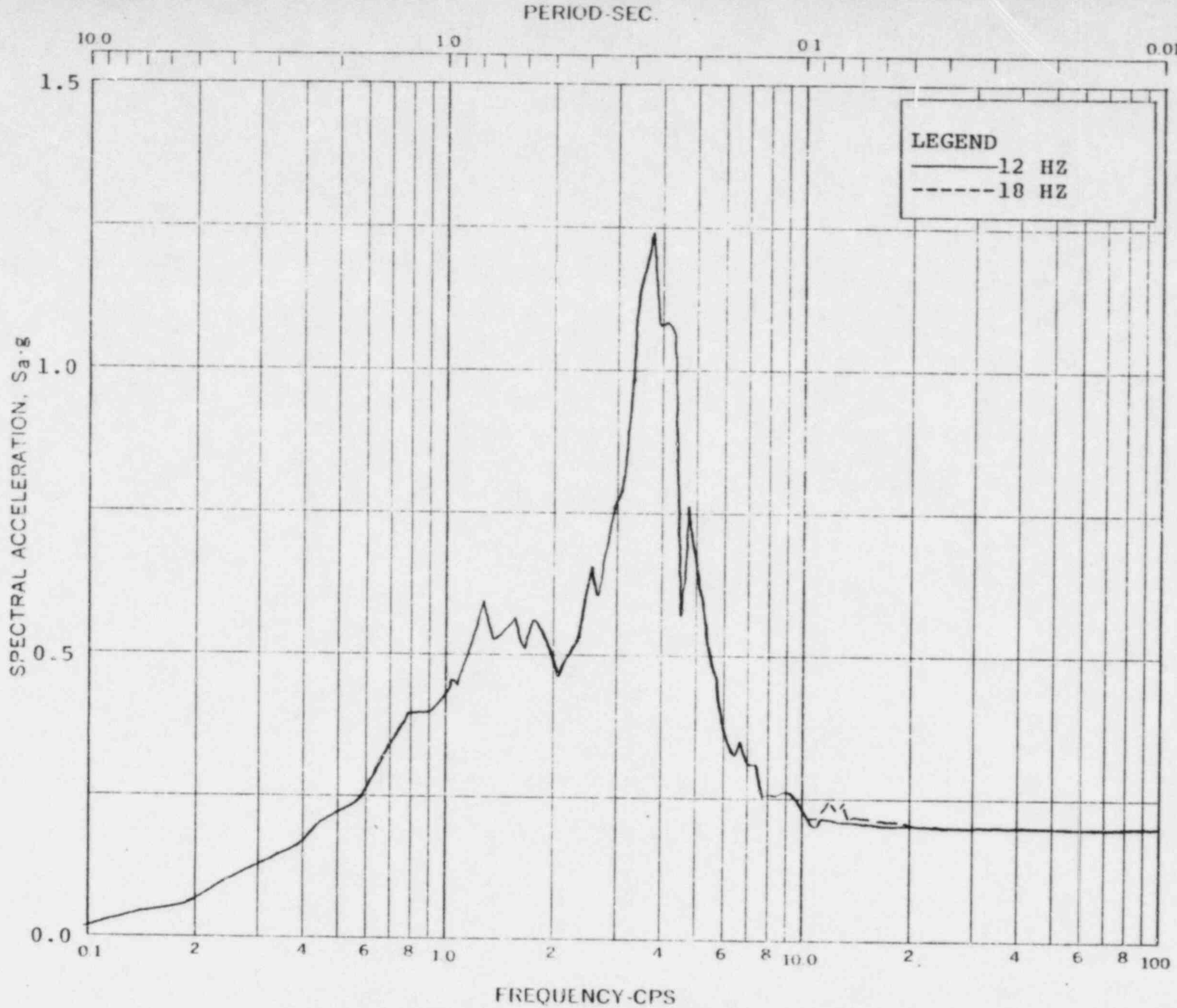

FREQUENCY CUT-OFF STUDY
12 HZ VS. 18 HZ
REACTOR BUILDING AT EL. 54'-0"
N-S, SSE, 2% DAMPING

FIGURE 13

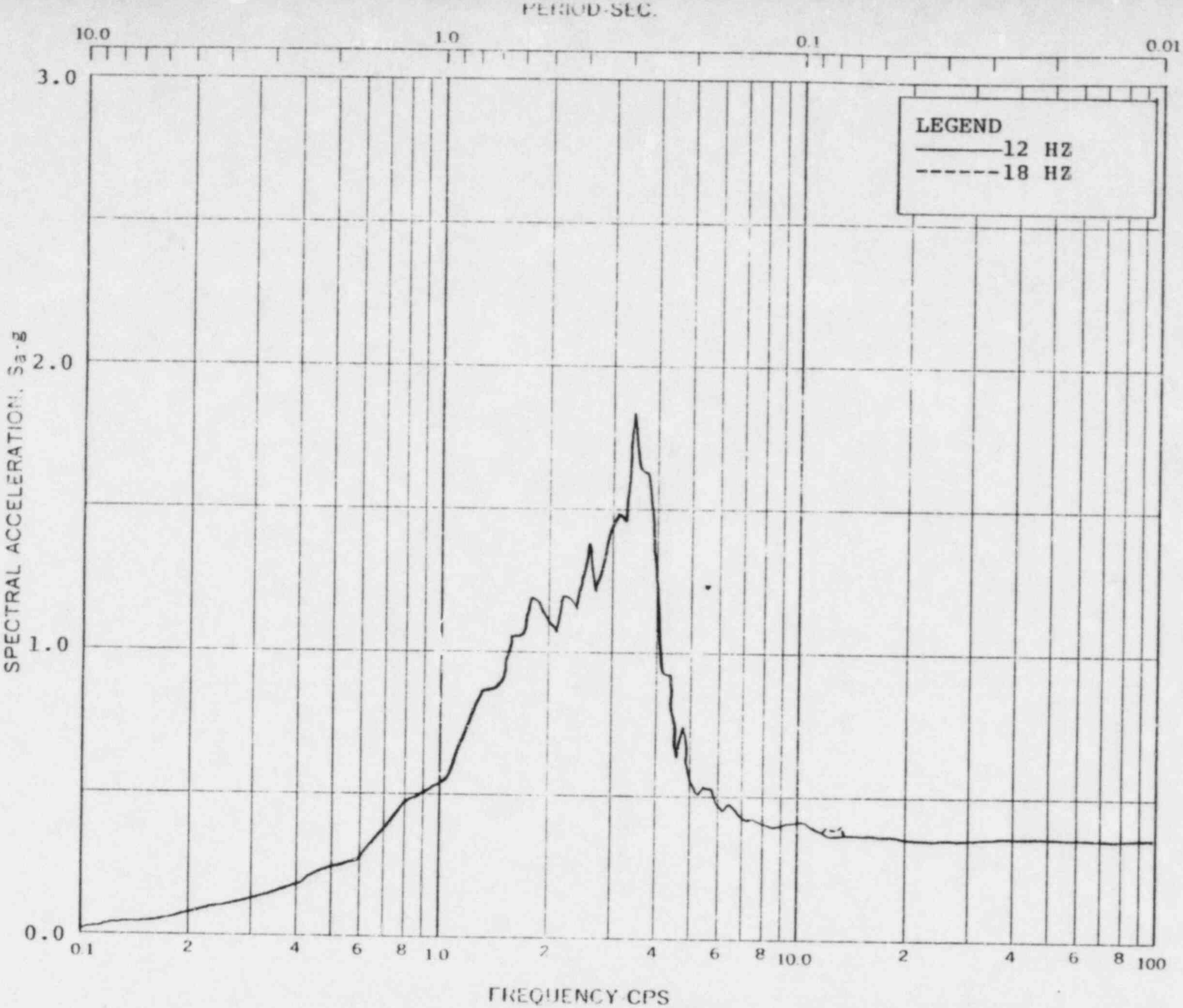

FREQUENCY CUT-OFF STUDY
12 HZ VS. 18 HZ
REACTOR BUILDING AT EL. 201'-0"
N-S, SSE, 2% DAMPING

FIGURE 14

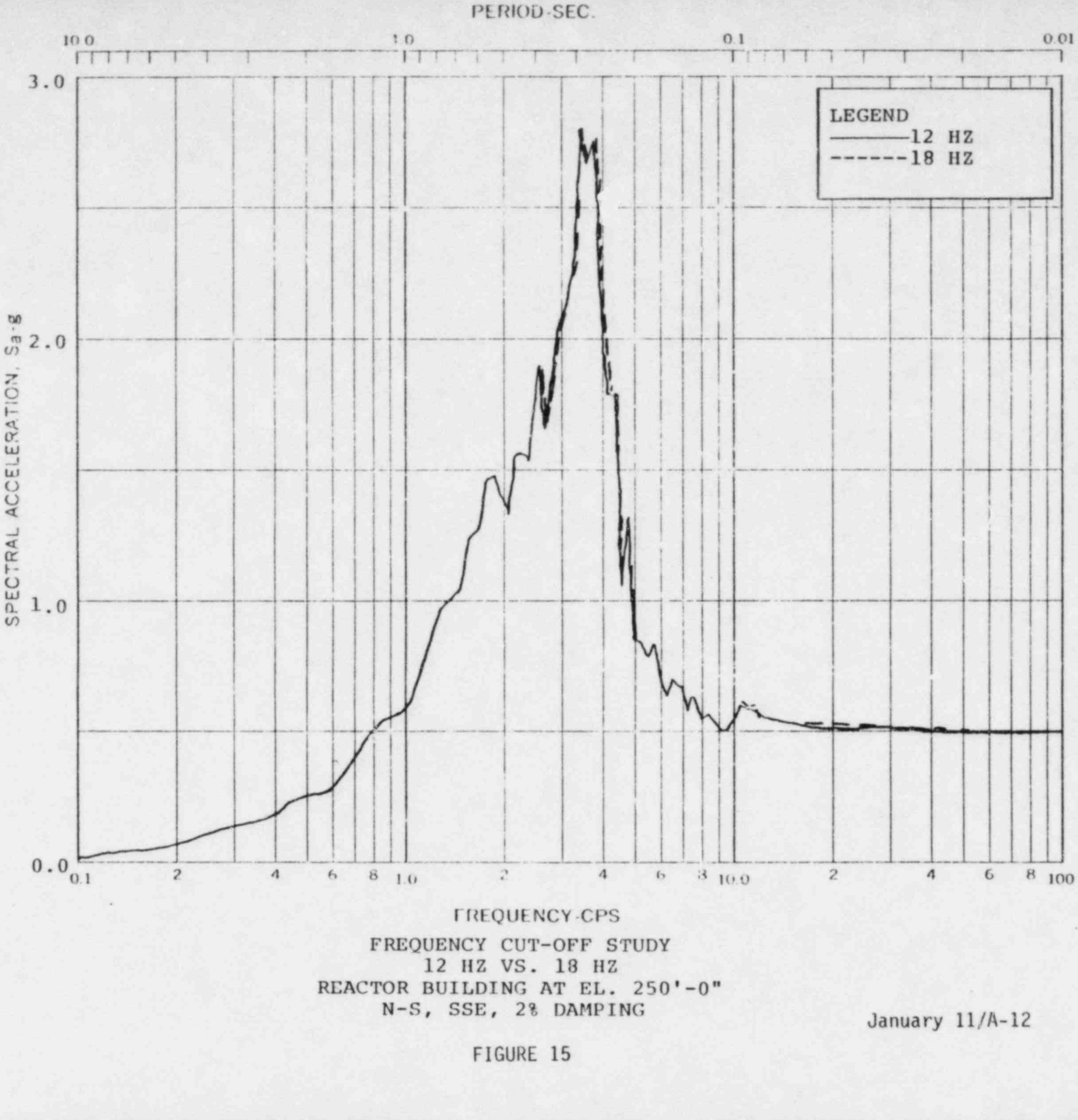

FREQUENCY CUT-OFF STUDY
12 HZ VS. 18 HZ
REACTOR BUILDING AT EL. 250'-0"
N-S, SSE, 2% DAMPING

January 11/A-12

FIGURE 15

Response to NRC Audit

Meeting Date: January 11, 1984

Question No.: A-13

Question: Provide results of three soil depth mouels for intake structure.

Response: Since the intake structure is a considerably smaller structure than the Power Block structures, the depth of significant interaction for the intake structure is expected to be equal or less. To substantiate this, plots of peak shear strain with depth were developed for the following conditions and are shown in page 1 of the attachment:

1. Peak shear strain next to structure.

2. Peak shear strain 20 feet from structure.

3. Peak shear strain in free-field.

The strains converge in the vicinity of elevation - 100 feet (200 foot depth of soil), indicating that no interaction occurs below that depth. Based on this a 300 foot model was used.

It is noted that an independent verification soil-structure interaction analysis for the intake structure is being performed in response to NRC requested action item A-14 from the audit meeting on January 11, 1984. This analysis will provide additional verification to the above response.

ATTACHMENT TO RESPONSE A-13

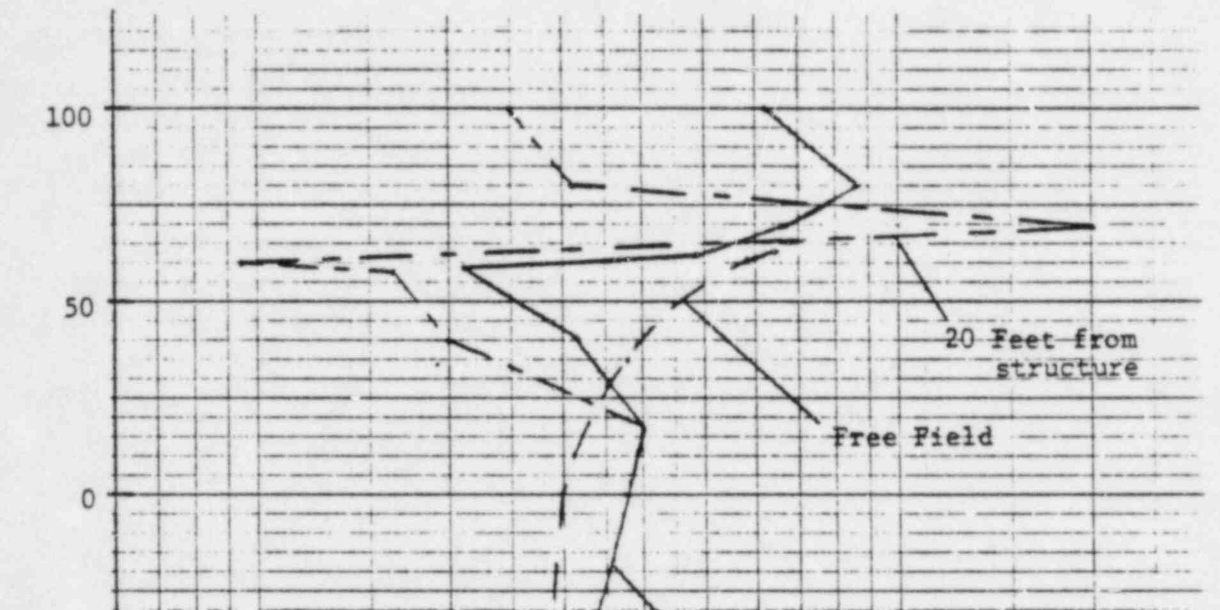

Intake Structure
Comparison of Peak Shear Strain Versus Depth,
Suggested Soil Properties

Response to NRC Audit

Meeting Date: January 12, 1984

Question No.: B.1

QUESTION: Provide the calculated factors of safety for the Code Case N-284 drywell buckling evaluation of the spherical and the cylindrical shells.

RESPONSE: The calculated minimum factors of safety for the Code Case N-284 drywell buckling evaluation are as follows:

Location	Minimum Calculated Factors of Safety	
	Level B Service Limits	Level C Service Limits
Spherical Shell	3.8	2.8
Hatch Area	7.5	7.0
Cylindrical Shell	4.7	4.6

The above values exceed the following allowable factors of safety:

- Level B Service Limits, FS = 3
- Level C Service Limits, FS = 2.5

Response to NRC Audit

Meeting Date: January 12, 1984

Question No.: B.2

QUESTION: With respect to the ultimate capacity of the containment, expand the analysis to include the ultimate capacity of the materials and eliminate seismic considerations.

RESPONSE: The ultimate capacity analysis of the containment has been expanded to include the minimum specified tensile strengths of the materials and to eliminate seismic considerations. The resulting minimum ultimate internal pressure equals 190 psi. Therefore, the safety margin against the design pressure of 62 psi is 3.06.

Appendix 3I will be added to the FSAR to describe the ultimate capacity analysis of the containment.

Response to NRC Audit

Meeting Date: January 12, 1984

Question No.: B.3

<u>QUESTION</u>: Verify the consistency in the load combinations used for the concrete and supporting structural steel for the reactor building slab at el 201 ft-0 in.

<u>RESPONSE</u>: The load combinations used for the design of the reinforced concrete and structural steel portions of the reactor building are listed in FSAR Tables 3.8-8 and 3.8-10 respectively.

For the design of the reactor building slab at el. 201 ft. the controlling load combination for reinforced concrete design is $U = 0.75\ (1.4D + 1.7L_o + 1.9E_o + 1.7T_o + 1.7R_o)$ and the controlling load combination for structural steel floor framing design is $S = D + L$.

The reasons for different load combinations controlling the various designs are as follows:

- Different load factors associated with the various load combinations for concrete and steel design. For concrete design, the relatively large 1.9 load factor for the OBE load results in the OBE load combination controlling.

- The design live load, L, for the reactor building slab at el. 210 ft. is 1000 psf.

  The operating live load, L_o, which is coupled with seismic events is 250 psf. This relatively large difference between design and operating live loads results in the non-seismic load combinations controlling for structural steel design.

Based on the reasons given above, the consistency of the load combinations used for the concrete and supporting structural steel for the reactor building slab at el. 201 ft. is verified.